UNIVERSITÀ DEGLI STUDI DI TRIESTE

XXX CICLO DEL DOTTORATO DI RICERCA IN

Ambiente e Vita

Development of biomonitoring techniques of persistent airborne pollutants using native lichens

Settore scientifico-disciplinare: **BIO/02**

DOTTORANDO / A
NOME COGNOME

Lorenzo Fortuna

COORDINATORE
PROF. NOME COGNOME

Prof. Giorgio Alberti

SUPERVISORE DI TESI
PROF. NOME COGNOME

Prof. Mauro Tretiach

ANNO ACCADEMICO 2016/2017

List of Content

Riassunto

Questo progetto di ricerca vuole contribuire al miglioramento dei protocolli più utilizzati negli studi di biomonitoraggio degli inquinanti aerodiffusi mediante licheni autoctoni. Secondo tali protocolli, il contenuto di inquinanti nei talli epifiti fogliosi deve essere misurato nelle parti più esterne, quelle sviluppatesi nell'anno precedente. Ciò permette di associare il contenuto di inquinanti ad un periodo di esposizione noto. La crescita dei licheni è comunque sensibile alle condizioni ambientali locali e la mancanza di dati per la maggior parte delle specie utilizzate ha determinato una sottostima del problema. Quindi, un primo studio, ha voluto indagare l'influenza dei fattori climatici sito specifici sulla variabilità inter-sito del tasso di crescita radiale (RaGR) di *Xanthoria parietina*, nelle diverse stagioni e a lungo termine. Per 17 mesi RaGR è stato monitorato in 11 siti lungo un transetto altitudinale, misurando la lunghezza dei lobi di 54 talli, mentre le variabili climatiche sito specifiche sono state monitorate con sensori termo-igrometrici. I risultati evidenziano che le differenze sito specifiche in termini di disponibilità idrica atmosferica e frequenza dei venti erano correlate alla variabilità inter-sito osservata di entrambi RaGR. Infatti, talli in siti secchi avevano un RaGR stagionale significativamente più basso di quello di talli in siti umidi. Quindi, è stato concluso che gli studi di biomonitoraggio con i licheni autoctoni dovrebbero essere limitati ad aree climaticamente omogenee, per assicurare periodi di esposizione comparabili.

In un secondo studio, il periodo di esposizione si è rivelato essere un parametro importante se volessimo usare correttamente dataset di licheni per la validazione di modelli di dispersione atmosferica (ADMs). In questo studio, il contenuto elementare di campioni lichenici raccolti nei dintorni di una centrale termoelettrica è stato utilizzato come dataset per la validazione di due diversi ADMs. Questi simulavano la dispersione del Particolato Totale Sospeso emesso dalla centrale durante l'anno 2005, selezionato dalle autorità quale periodo meteorologico di riferimento (ADM1), e, durante i sei mesi precedenti alla raccolta dei licheni (ADM2), periodo corrispondente all'età del materiale lichenico campionato.

Dopo aver normalizzato per il contenuto elementare del suolo, i risultati indicavano che il contenuto di Cr nei licheni era più correlato a ADM2 piuttosto che a ADM1. Questi risultati furono poi confermati da un campionamento del PM_{10} condotto da ARPA FVG, rivelando che le concentrazioni di Cr erano significativamente più basse durante i periodi di inattività della centrale.

Infine, con un terzo studio è stata valutata l'influenza delle melanine licheniche nell'accumulo di elementi in traccia. La maggior parte delle specie di lichene utilizzate come biomonitor appartiene alle Parmeliaceae, una famiglia molto diversificata e caratterizzata da un cortex inferiore fortemente melanizzato. È stato quindi ipotizzato che le melanine possano influenzare il contenuto di elementi selezionati. Il contenuto di macro (Ca, K, S) e micro (Fe, Mn, Zn) nutrienti in pseudo tessuti melanizzati e non melanizzati di nove specie è stato prima valutato mediante analisi micro-XRF nel cortex inferiore, superiore e nella medulla. In seguito, la concentrazione degli stessi elementi è stata misurata mediante ICP-AES, e, un esperimento con tecniche di eluizione sequenziale è stato eseguito su due specie: una fortemente e una debolmente melanizzata. È stato così dimostrato che i licheni autoctoni con superfici fortemente melanizzate hanno un maggiore contenuto di Fe e Zn rispetto a quelle debolmente o non-melanizzate. Quindi per escludere errori associati a un differente grado di melanizzazione si propone che il materiale lichenico destinato alle analisi abbia un grado di melanizzazione omogeneo.

Abstract

This PhD project has been focused on the improvement of the methods commonly used in biomonitoring surveys of persistent airborne pollutants based on native lichens. These protocols recommend to measure the content of pollutants in the outermost parts of foliose epiphytic thalli, which purportedly developed in the last year before sampling. This allows to associate the pollutant content to a known exposure period. Unfortunately, lichens are very sensitive to local environmental conditions, although the lack of data concerning most of the species used in biomonitoring surveys caused an underestimation of the problem. Therefore, in a first study, I investigated the influence of site-specific climatic factors on the inter-site variability of seasonal and long-term Radial Growth Rates (RaGR) of *Xanthoria parietina*, one of the most popular lichen biomonitor. For 17 months RaGR was monitored in 11 sites along an altitudinal transect by measuring the lobe length of 54 thalli, whereas site-specific climatic variables were monitored with thermo-hygrometric sensors. Results highlighted that site-specific climatic differences in terms of air water availability and wind frequency were strongly correlated to the observed inter-site variability of both RaGRs, with thalli of dry sites that had significantly lower seasonal RaGR with respect to those of moist ones. For this reason, it was concluded that biomonitoring surveys with native lichens should be limited to climatically homogeneous areas in order to ensure comparable exposure periods.

In a second study, the correct reference exposure period revealed itself as an important yardstick if we want to correctly use lichen data in the validation of atmospheric dispersion models (ADMs). In this study, I used the element concentrations measured in lichen samples from the surroundings of a coal-fired power plant as the core dataset for the validation of two alternative ADMs. These ADMs simulated the dispersion of Total Suspended Particulate emitted by the plant during the year 2005, selected by the authorities as reference meteorological period (ADM1), and, the six months preceding the lichen sample collection (ADM2), because this was the age of the collected lichen samples, as estimated using the above-mentioned RaGR. After normalization for the element soil content, results showed that the Cr content of lichen samples were more correlated with the outcomes of ADM2 rather than with those of ADM1. These results were confirmed by a PM_{10} survey, carried out by ARPA FVG, which revealed that in two successive periods of activity and inactivity of the putative source, concentration of Cr was significantly higher in the former.

Finally, a third study was aimed at investigating the influence of lichen melanins in trace element retention. Most of the species used as biomonitor of airborne trace elements belong to the Parmeliaceae, a highly differentiated family characterized by a highly melanised lower cortex, whose adaptive value is unknown. Here, I tested the hypothesis that melanins can affect the content of selected elements. Macro- (Ca, K and S) and micro- (Fe, Mn and Zn) nutrients in melanized and non-melanized pseudotissues of nine species was first evaluated by micro-XRF analysis on either the upper and lower cortex, and on the artificially exposed medulla. Afterwards, the total concentration of the same elements was measured by ICP-AES, and a sequential elution experiment was performed on one heavily melanised and one lightly melanised species. In this way, I could demonstrate that native lichens with heavily melanised surfaces are more Fe- and Zn- enriched than lightly or non-melanised lichens, possibly increasing the bioavailability of both elements in favour of the photobionts. Therefore, in order to exclude any bias related to the different degree of melanisation, the proposal is to compose analytical samples with lichen material characterized by a similar degree of melanisation.

Introduction

In the last decades, the increase of air pollutant concentrations in highly populated areas is causing the onset of cardiovascular and pulmonary diseases, cancer and neurodegenerative diseases in adults (Calderón-Garcidueñas et al.2015; Landrigan 2017). Only in the European Union (EU), the high atmospheric concentrations of fine particulate matter ($PM_{2.5}$), nitrogen oxides (NO_x) and ozone (O_3) are said to be responsible for 400 thousands deaths per year (Badyda et al. 2016). On the other hand, an increasing number of studies reports air pollution effects on plants and wildlife from cellular to community level, highlighting adverse effects on biodiversity, ecosystem functions and services (Barker and Tingey 2012; Paoletti et al. 2010). In addition, crop field damages related to high air O_3 concentration (Van Dingenen et al. 2009) and even stone cultural heritage deterioration due to acidification phenomena (Varotsos et al. 2009) have also been correlated to air pollution.

To cope with these problems, the EU Commission issued several directives aimed at limiting the release of harmful substances into the atmosphere, improving the quality of fossil fuels, and introducing environmental protection requirements into the transport and energy sectors (Gemmer and Xiao 2013). In particular, with the transposition of 2008/50/CE directive (Air Quality Directive; AQD), member States adhered to comply with specific thresholds for the most common, generalist pollutants and, at the same time, to cooperate in providing quantitative data of air pollutant concentrations based on their network of air pollution monitoring stations. However, not all air pollution stations provide data for the few air pollutants selected as the most important ones. For instance, trace elements and PAHs are routinely monitored only in 6 and 2 member States, respectively, whereas 25% of national networks did not provide data for the five elements (As, Cd, Hg, Cr, Pb) for which thresholds are available. There is, thus, an ever increasing interest for alternative monitoring techniques, which can remedy to these shortcomings and gaps in the network of automatic recording stations for long term air pollution measurements (Wolterbeek 2002; Wolterbeek 2003).

An example of a less expensive and reliable alternative, which provide spatial and time-integrated information of airborne trace element, is given by use of epiphytic lichens as bioaccumulators of persistent airborne pollutants, from trace elements (Nimis et al. 2000; Bargagli et al. 1997; Demiray et al. 2012), to PAHs (Kodnik et al.2015, Domínguez-Morueco et al. 2017) and dioxins (Augusto et al. 2007). Unlike

vascular plants, lichens lack roots, stomata and a waxy cuticle. They predominantly acquire water and nutrients by wet and dry deposition, without the possibility to actively regulate gas and water exchanges between their thallus and the atmosphere (Petruzzellis et al. 2018). These peculiarities makes the elemental content of lichens correlated with that of the bulk deposition in a given area (Sloof and Walterbeek 1991; Van Dobben et al. 2001).

The protocols currently applied in biomonitoring surveys of trace elements with autochthonous lichens highly recommend to analyse samples as much as possible equal in age (Loppi et al. 1997). This criterion was introduced to make more reliable the comparison of the element content measured in lichen samples from different sites. However, lichens are poikilohydric organisms, which cope with prolonged periods of metabolic inactivity (Crabtree and Ellis et al. 2010). Since both photosynthesis and respiration are strongly constrained by the thallus water status (Lange and Green 2008), also lichen growth is primarily limited by water availability (Renhorn et al. 1997, Tretiach et al. 2012). Unfortunately, we still ignore how much different climatic factors at site-specific scale may influence the inter-site variability of lichen growth on a seasonal or annual scale. Therefore, thalli with similar size but collected in climatically diverse sites might actually differ in age, and thus in exposure time to pollutants. By estimating the variability of the annual growth rate of lichens used as biomonitors, it would be possible to increase the accuracy of biomonitoring surveys by reducing the bias related to the different age of lichen samples. This would allow to extend the application of biomonitoring survey with lichens to another important field of air pollution monitoring and assessment, i.e. the validation of atmospheric dispersion models (ADM).

ADMs are produced by sophisticated software containing specific parameterization schemes for simulating the atmospheric processes that affect the concentration and deposition of atmospheric pollutants on a given area for a defined time period (Holmes and Morawska 2006). The use of ADM simulations has been even introduced in decision-making processes concerning air pollution monitoring and assessment (2008/50/CE; AQD). Their reliability therefore need to be estimated with proper crosscheck evaluation studies (Carnevale et al. 2014; Stohl et al. 1998), aimed at evaluating the degree of correlation between the predicted values of the ADM simulation and the data collected by the national networks of air pollution recording stations. Unfortunately, these studies are rarely carried out because they require technologically advanced equipment (e.g. a sufficiently dense network of air pollution stations) and manpower (Ham 1992).

7

Considering that lichen biomonitoring surveys allow to perform extensive samplings with high spatial resolution over long- and short-term period, they could actually contribute also in the context of crosscheck evaluation studies of ADM simulation of persistent airborne pollutants (Abril et al. 2014).

Currently, in Europe, the major part of lichens used as biomonitor of trace elements [e.g. *Flavoparmelia caperata* (L.) Hale, *Hypogymnia physodes* (L.) Nyl, *Parmelia sulcata* (L.) Taylor, *Pseudevernia furfuracea* (L.) Zopf] belong to the highly diversified group of Parmeliaceae whose species share an extremely conserved morpho-chemical trait: the lower surface is heavily melanised. Melanins are ubiquitous compounds found in most organism since they fulfil several biological functions, from defence against UV radiation, oxidizing agents and microbial stress to metal complexation (Eisenman and Casadevall 2012; Pilas et al. 1988). Since the lower cortex in foliose lichens is not directly exposed to sunlight, this morpho-chemical trait could be involved in metal complexation. Indeed, different studies performed on melanised non-lichenised ascomycete indicate that melanins can bind Cu, Fe, U and Zn (McLean et 1998; Fomina and Gadd 2003; Gadd and Rome 1988), and this was confirmed by the sole study carried out so far on an epilithic lichen, *Trapelia involuta* (Purvis et al. 2004). Therefore, the study of the melanin role(s) in lichens might elucidate in some extent whether they affect the accumulation performance of melanised lichen biomonitors.

The activities of this PhD research have been focused at improving the protocols currently applied in biomonitoring of trace element with foliose lichens. Three main studies were carried out, aimed at investigating the following themes:

- the effects of climatic site-specific factors on the seasonal and annual radial growth rate in 11 populations of the lichen biomonitor *Xanthoria parietina* (L.) Th. Fr. along an altitudinal transect in the Classical Karst (NE Italy) ;

- the feasibility of using *Flavoparmelia caperata* and *X. parietina* as point receptors for the evaluation of ADM simulations modelling the emission of a point source pollution in a highly heterogeneous area (Monfalcone, NE Italy)

- the role of melanins in the intra-thalline compartmentalization of macro- (Ca, K, S) and micro- (Fe, Mn, Zn) nutrient content in 9 lichens.

Reference

Augusto S, Pereira MJ, Soares A, Branquinho C (2007) The contribution of environmental biomonitoring with lichens to assess human exposure to dioxins. Int J Hyg Envir Heal, 210:433-438.

Badyda AJ, Grellier J, Dąbrowiecki P (2016) Ambient $PM_{2.5}$ Exposure and mortality due to lung cancer and cardiopulmonary diseases in Polish cities. In: Pokorski M. (ed.) Respiratory Treatment and Prevention. Adv Exp Med Biol, Springer, Cham

Bargagli R, Nimis PL, (2002) Guidelines for the use of epiphytic lichens as biomonitors of atmospheric deposition of trace elements. In: Nimis, P. L., Scheidegger, C., Wolseley P. A. (eds.), Monitoring with Lichens – Monitoring Lichens. NATO Science Series, IV. Earth and Environmental Sciences, Vol. 7. Kluwer, Dordrecht, pp. 295-299.

Bargagli R, Nimis PL, Monaci F (1997) Lichen biomonitoring of trace element deposition in urban, industrial and reference areas of Italy. J Trace Elem Med Bio, 11:173-175.

Barker JR, Tingey DT (2012) The effects of air pollution on biodiversity. In: Barker JR, Tingey DT (eds.), Air pollution effects on biodiversity. Springer Science & Business Media, New York.

Calderón-Garcidueñas L, Kulesza RJ, Doty R L, D'angiulli A, Torres-Jardón R (2015) Megacities air pollution problems: Mexico City Metropolitan Area critical issues on the central nervous system pediatric impact. Environ Res 137:157-169.

Carnevale C, Finzi G, Pederzoli A, Pisoni E, Thunis P, Turrini E, Volta M (2014) Applying the delta tool to support the Air Quality Directive: evaluation of the TCAM chemical transport model. Air Qual Atmos Health 7:335-346.

Crabtree D, Ellis CJ (2010) Species interaction and response to wind speed alter the impact of projected temperature change in a montane ecosystem. J Veg Sci 21:744-760.

Demiray AD, Yolcubal I, Akyol NH, Çobanoğlu G (2012) Biomonitoring of airborne metals using the lichen *Xanthoria parietina* in Kocaeli Province, Turkey. Ecol Indic, 18:632-643.

Domínguez-Morueco N, Augusto S, Trabalón L, Pocurull E, Borrull F, Schuhmacher M, Domingo JL, Nadal M (2017) Monitoring PAHs in the petrochemical area of Tarragona County, Spain: comparing passive air samplers with lichen transplants. Environ Sci Pollut R, 24:11890-11900.

Eisenman HC, Casadevall A (2012) Synthesis and assembly of fungal melanins. Appl Microbiol Biotechnol 93:931–940

Fomina M, Gadd GM (2003) Metal sorption by biomass of melanin producing fungi grown in clay containing medium. J Chem Technol Biotechnol 78:23–34

Gadd GM, Rome L (1988) Biosorption of copper by fungal melanin. Appl Microbiol Biotechnol 29:610–617

Gauslaa Y, Lie M, Solhaug KA, Ohlson M (2006) Growth and ecophysiological acclimation of the foliose lichen *Lobaria pulmonaria* in forests with contrasting light climates. Oecologia 147:406-416.

Gemmer M, Bo X (2013) Air quality legislation and standards in the European Union: background, status and public participation. Adv Clim Change Res 4:50-59.

Ham J (1992) Discussion about the national model for dispersion of air pollution. Lucht 9:84-85.

Holmes NS, Morawska L (2006) A review of dispersion modelling and its application to the dispersion of particles: an overview of different dispersion models available. Atmos Environ 40:5902-5928.

Kodnik D, Carniel FC, Licen S, Tolloi A, Barbieri P, Tretiach M (2015) Seasonal variations of PAHs content and distribution patterns in a mixed land use area: A case study in NE Italy with the transplanted lichen *Pseudevernia furfuracea*. Atmos Environ, 113:255-263.

Landrigan PJ (2017) Air pollution and health. Lancet Public Health, 2, e4-e5.

Lange OL, Green TA (2008) Diel and seasonal courses of ambient carbon dioxide concentration and their effect on productivity of the epilithic lichen *Lecanora muralis* in a temperate, suburban habitat. Lichenologist 40:449-462.

Loppi S, Nelli L, Ancora S, Bargagli R (1997) Accumulation of trace elements in the peripheral and central parts of a foliose lichen thallus. Bryologist, 100:251-253.

McLean J, Purvis OW, Williamson BJ, Bailey EH (1998) Role for lichen melanins in uranium remediation. Nature 391:649–650

Nimis PL, Lazzarin G, Lazzarin A, Skert N (2000) Biomonitoring of trace elements with lichens in Veneto (NE Italy). Sci Total Environ, 255:97-111.

Paoletti E, Schaub M, Matyssek R, Wieser G, Augustaitis A, Bastrup-Birk AM, Bytnerowicz A, Günthardt-Goerg MS, Müller-Starck G, Sereng Y (2010) Advances of air pollution science: from forest decline to multiple-stress effects on forest ecosystem services. Environ Pollut 158:1986-1989.

Pilas B, Sarna T, Kalyanaraman B, Swartz HM (1988) The effect of melanin on iron associated decomposition of hydrogen peroxide. Free Radical Bio Med 4:285–293

Petruzzellis F, Savi T, Bertuzzi S, Montagner A, Tretiach M, Nardini A (2017) Relationships between water status and photosystem functionality in a chlorolichen and its isolated photobiont. Planta, 1-10.

Purvis OW, Bailey EH, McLean J, Kasama T, Williamson BJ (2004) Uranium biosorption by the lichen *Trapelia involuta* at a uranium mine. Geomicrobiol J 21:159–167

Renhorn KE, Esseen PA, Palmqvist K, Sundberg B (1997) Growth and vitality of epiphytic lichens. Oecologia 109:1-9.

Sloof JE, Wolterbeek HT (1991) National trace-element air pollution monitoring survey using epiphytic lichens. Lichenologist 23:139-165.

Stohl A, Hittenberger M, Wotawa G (1998) Validation of the Lagrangian particle dispersion model FLEXPART against large-scale tracer experiment data. Atmos Environ 32:4245-4264

Tretiach M, Pavanetto S, Pittao E, Di Toppi LS, Piccotto M (2012) Water availability modifies tolerance to photo-oxidative pollutants in transplants of the lichen *Flavoparmelia caperata*. Oecologia, 168:589-599.

Valladares F, Sancho LG, Ascaso C, (1998) Water storage in the lichen family Umbilicariaceae. Plant Biol 111:99-107.

Van Dingenen R, Dentener FJ, Raes, F, Krol MC, Emberson, L, Cofala J (2009) The global impact of ozone on agricultural crop yields under current and future air quality legislation. Atmos Environ 43:604-618.

Van Dobben HF, Wolterbeek HT, Wamelink GWW, Ter Braak CJF (2001) Relationship between epiphytic lichens, trace elements and gaseous atmospheric pollutants. Environ Pollut 112:163-169.

Varotsos C, Tzanis C, Cracknell A (2009) The enhanced deterioration of the cultural heritage monuments due to air pollution. Environ Sci Pollut R, 16, 590-592.

Wolterbeek B (2002) Biomonitoring of trace element air pollution: principles, possibilities and perspectives. Environ Pollut 120:11-21.

Wolterbeek HT, Garty J, Reis MA, Freitas MC (2003) Biomonitors in use: lichens and metal air pollution. In: Markert BA, Breure AM, Zechmeister HG (eds.) Trace metals and other contaminants in the environment, Elsiever, Amsterdam, pp. 377-419.

Radial growth variability in the lichen biomonitor *Xanthoria parietina*:

a field study along an altitudinal transect with data modelling

Fortuna Lorenzo, Tretiach Mauro*

Department of Life Sciences, University of Trieste,

Via L. Giorgieri 10, I-34127 Trieste, Italy

Corresponding author:

Prof. Mauro Tretiach

email: tretiach@units.it

Phone: +39 040 558 8822

Abstract

The protocols commonly applied in biomonitoring surveys with foliose lichens require to analyse samples grown in the same period of time, typically the last year before sampling. Unfortunately, we still ignore the degree of variation of lichen growth as a function of ecological site-specific factors, therefore samples of the same size collected in environmentally and climatically diverse sites might actually differ in age. This work aims at quantifying the influence of climatic conditions on the radial growth rates (RaGR) of *Xanthoria parietina,* one of the most popular lichen biomonitor. RaGR was monitored in 11 populations distributed along an altitudinal transect in the Classical Karst (NE Italy), from 20 to 500 m above sea level. For c. 17 months lobe growth was measured seasonally with a digital caliper, whereas site-specific climatic variables were monitored by means of thermo-hygrometric sensors, and implemented by meteorological data. Results reveal that thalli of relatively dry sites had significantly lower seasonal RaGR with respect to moister ones. Considering that cumulative precipitations were equally distributed along the transect, it was concluded that *X. parietina* RaGR is negatively and positively affected by air temperature and relative humidity, respectively. Finally, the lobe growth of *X. parietina* was modelled as a function of 18 environmental variables.

Key-words: chlorolichens; climate; saturation deficit; transect; water availability.

Highlights

- Radial Growth Rates (RaGRs) of the biomonitor *Xanthoria parietina* are provided (80)

- Seasonal RaGRs have been modelled as a function of 18 environmental variables (80)

- The importance of RaGRs variation for lichen biomonitoring is discussed (74)

1. Introduction

Lichens are a stable, extracellular mutualistic symbiotic association between a fungus (the so-called mycobiont), generally an ascomycete, and one or more populations of unicellular algae and/or cyanobacteria (the so-called photobiont) (Honegger 1998), plus an unknown number of further participants, ranging from parasites to saprotrophs (Muggia et al. 2016). Lacking root, stomata and a waxy cuticle, lichens predominantly derive water and inorganic nutrients from dry and wet atmospheric deposition (Williamson et al. 2004). This fact, along with the proven correlation between pollutant concentration in lichen thalli and atmosphere (Sloof 1995), makes lichens excellent biomonitors of airborne persistent pollutants such as trace elements (Richardson 1988; Bargagli 1998) and polycyclic aromatic hydrocarbons (Kodnik et al.2015, Domínguez-Morueco et al. 2017) .

In foliose lichens, most pollutants are significantly higher in the old (central) than in the juvenile (peripheral) part of the thallus, because the element concentration strongly depends on the exposure time of these parts (Loppi et al. 1997; Nimis et al. 2001). For this reason, in order to compare the elemental composition of lichen samples collected in a given area, these have to be composed by portions as much as possible equal in age (Bargagli and Nimis 2002). Standard protocols recommend the use of the outermost portions of thallus lobes, roughly corresponding to the growth of the last year (Nimis and Bargagli 1998).

Dorsiventrally organized, foliose lichens grow radially by expanding their peripheral lobes a few millimeters per year (Armstrong 2011), thanks to the activity of a pseudomeristematic rim area (Honegger 1993, 1996a), characterized by dense, small mycobiont and photobiont cells and high division rates (Hill 1985, 1989; Fiechter 1990). Lichens are generally slow-growing organisms (Honegger 1998). This is due to their poikilohydric lifestyle, and to the relatively high percentage of time in which they are metabolically inactive (Lange and Green 2008). The growth of chlorolichens in particular is favored by prolonged periods with high air humidity, because the photobionts can recover from dehydration also in absence of liquid water, being able to reach a positive CO_2 income (Büdel and Lange 1991; Palmqvist 2000; Del Prado and Sancho 2007). On the contrary, increasing temperatures can rapidly decrease the thallus water content inducing lichens to a dormant state (Crabtree and Ellis 2010).

Considering that water availability and the evaporative demand are heterogeneous even at small spatial scale, the site-specific climatic conditions can strongly affect the lichen growth (Gauslaa et al. 2007;

Gauslaa and Coxon 2011). This fact becomes of major importance in the context of biomonitoring surveys, since significant differences in radial growth rates (RaGRs) among sites would correspond to differences in exposure times of the sampled materials. In this light, a correct assessment of the natural variability of annual RaGR in a given study area would significantly improve the robustness of the lichen biomonitoring data.

Xanthoria parietina (L.) Fr. Th. is a model species and is also one of the most used biomonitor of airborne trace element, but its growth has been investigated by a few studies only (Richardson 1967; Moxham 1981; Honegger et al. 1996b), and never in relation to site-specific factors. In this study, we tested the effects of different site-specific climatic conditions on both seasonal and long term RaGRs in 11 populations distributed along a 30 km long altitudinal transect on the Classical Karst plateau (NE Italy). A second aim was to provide a methodological framework meant to predict *X. parietina* lobe growth by modelling the observed data as a function of environmental variables.

2. Material and methods

2.1   The species

Xanthoria parietina is a very common foliose lichen, with coccoid green algae belonging to the genus *Trebouxia* as photobionts (Ahmadjian 2001). The thallus is greenish-grey to vivid yellow-orange, more or less orbicular in outline and appressed to the substratum, with marginal lobes, and apothecia (the sexual reproductive structures of the fungus) in the central parts of the thallus (Supplementary Figure 1). *X. parietina* is xerophilous and usually colonizes rather nutrient-rich environments with high solar irradiation (Frati et al. 2007). It has been used as model organisms in several studies concerning desiccation tolerance (e.g. Honegger 2003; Brandt et al. 2015), regenerative capacity (Honegger 1996a-b), photo-oxidative tolerance (Piccotto et al. 2011; Bertuzzi et al.2013, 2017), sexual reproduction (Honegger et al. 2004; Scherrer et al. 2005; Itten and Honegger 2010) and lichen re-synthesis (Bubrick and Galun 1986). Due to its worldwide distribution, *X. parietina* has frequently been used as biomonitor of persistent airborne pollutants (Cuny et al. 2004; Yenisoy-Karakaş and Tuncel 2004; Branquinho et al. 2008; Demiray et al. 2012; Agnan et al. 2013; Augusto et al. 2015) and eutrophication phenomena (Brodo et al. 2007; Olsen et al. 2010; Munzi et al. 2017).

2.2 Study sites

The study was carried out in the Classical Karst, a NW-SE directed anticline near Trieste (NE Italy; Fig. 1).
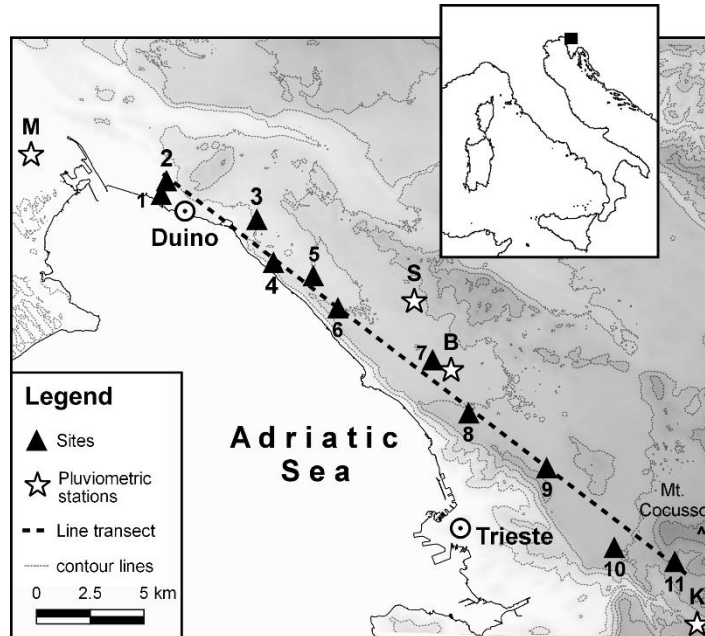

Fig. 1: Geographic location of the sites selected for the growth measurements of the epiphytic lichen *Xanthoria parietina* along a 30 km long transect in the Classical Karst. Variation in grey scale reflects the increasing altitude above sea level (white) to 500 m (dark grey) as calculated by digital elevation modelling (see text). The sites are numbered according to their increasing altitude. Thermo-hygrometric sensors were installed in sites S2, S4, S5 and S7. The pluviometric stations are indicated by a star (B=Borgo Grotta Gigante; K=Kozina M=Monfalcone; S=Sgonico).

Here, 11 sites, similar in terms of land use and epiphytic lichen flora, were selected along a 30 km long altitudinal transect extended from the coast near Duino (16 m a.s.l.; 13°35'23.21"E 45°46'52.10"N) to the base of Mt. Cocusso (500 m a.s.l.; 13°53'59.37"E 45°37'50.27"N). All the sites were selected in rural areas in proximity of *Querco-Ostryetum* forest edges. According to the classification of Koppen-Geiger, the climate of the area is fully humid, warm temperate, with hot summers on the coast and warm ones in the interior, being transitional between sub-Mediterranean and pre-Alpine (Kottek et al. 2006). Average annual temperature and rainfalls are 13°C and 1190 mm, respectively, with marked seasonal changes (Osmer FVG, 1992-2016, weather station of Sgonico, 268 m a.s.l; 13°45'0.00" E 45°44'24.00"N). Cold, dry, intense ENE winds ("Bora") are frequent, especially between October and April, and can reach a speed of 44 – 50 m s^{-1}.

2.3   In-situ measurements

In each site, 4 to 6 thalli of *X. parietina* with an average diameter of 4.5 ± 1.2 cm, growing on one to three sub-vertical trunks of manna ash (*Fraxinus ornus*) trees at 70 - 250 cm above the ground, were selected and individually photographed with a digital device (iPad mini; Apple, California, USA).

At time t_0, a stainless nail was hammered in the centre of each thallus. and eight to ten marginal lobes growing up or downwards were selected. Lateral lobes were excluded *a priori* in order to avoid interference by the radial growth of the lichen-hosting trunk. The radial length of each lobe was measured from the nail to the lobe margin with a digital calliper equipped with a Vernier scale (Maurer, Italy; sensitivity: ± 0.01 mm). The lobe radial measurements were repeated every 100 ± 10 d for six consecutive times (t_0-t_5), so as to define 5 Seasonal Time Intervals (STI_{1-5}) and two Long-Term periods (LT_{1-2}), between February 14, 2015 and June 29, 2016. If snails and arthropods grazed some of the selected lobes, these were discharged and new lobes were selected as explained before.

The measurements of Seasonal Radial Growth Rate (SRaGR) were calculated for each thallus over the jth STI as follows:

[1] $$SRaGR_j = \frac{\sum_i^{N_l} [(L_i^{t_{n+1}} - L_i^{t_n}) / (t_{n+1} - t_n)]}{N_l} \times 1000$$

where $L_i^{t_{n+1}}$ and $L_i^{t_n}$ are the radial measurement of the ith lobe, respectively collected at time t_{n+1} and t_n, and N_l is the number of lobes measured in a single thallus. All the SRaGR were expressed in micrometres per day.

The long-term radial growth (LTRaG) was calculated taking into account only those lobes which had not be grazed. $LTRaG_1$ and $LTRaG_2$ are expressed in millimetres and refer to the average lengthening of the lobes of a single thallus between t_0 and t_4 (Lt_1; 400 d) and between t_0 and t_5 (Lt_2; 504 d), respectively.

2.4   Climatic data

In sites 2, 6, 8 and 11 (the closest to the four pluviometric stations present in the study area) (Fig. 1), air temperature (T), relative humidity (RH) and dew point (DP) were continuously monitored every 30 minutes by thermo-hygrometric sensors (EL-USB-1, Lascar Electronics, UK) fixed on the lower branches of a

lichen-hosting tree. The hourly values of saturation deficit (SD) and air water potential (Ψ_{wv}) were calculated as:

[2] $SD = e_{(s)} \times (1-RH/100)$

[3] $\Psi_{wv} = (R \times T/V_w) \times \ln (RH/100)$

where $e_{(s)}$ is the saturation vapour pressure (kPa), R is the gas constant (J K^{-1} mol^{-1}) and V_w is the partial molar volume of water. Then, the minimum, maximum and average values of T, RH, DP, SD and Ψ_{wv} were calculated for each STI. The cumulative precipitations (cP) in the five STIs were calculated as the sum of the daily precipitation measured by the four pluviometric stations of Fig. 1.

Climatic conditions occurring along the transect were evaluated by performing 80 (16 climatic variables × 5 STI) inverse distance weighed (IDW) interpolations in QGIS environment (QGIS Brighton version 2.6) within a spatial domain of 159 Operational Geographic Units (OGUs) of 1 × 1 km each, at a maximum distance of 2 km from the transect. Moreover, the altitude and the distance from the sea were evaluated in QGIS environment within the spatial domain by digital elevation modelling and "*v.distance*" algorithm, respectively. Overall, each 1×1 km OGUs was characterized as a function of the 16 climatic variables plus altitude and distance from the sea.

2.5   Data analysis

Between two consecutive STIs, the thalli of sites 9 and 7 were entirely grazed or exhibited clear signs of vitality loss (i.e. thallus decolouration), whereas in two other sites, 5 and 4, the steel nails caused bark splitting and thus deep cracks in the thalli (Supplementary Figure 1). The data of these sites were not considered for further statistical analyses, which were thus limited to sites 1, 2, 3, 6, 8, 10 and 11 (Fig. 1). The lobe radial growth data were analysed by Tuckey's test in order to remove the site-specific outliers. Then, SRaGRs, LTRaG$_1$ and LTRaG$_2$ were calculated after exclusion of those lobes whose radial measurements were lower than calliper's sensitivity. The values of SRaGRs, LTRaG$_1$ and LTRaG$_2$ were analysed by factorial ANOVAs using "site" and "time-intervals" (i.e. STI$_{1-5}$ and LT$_{1-2}$) as categorical factors. The "site" × "time interval" interaction term and the LSD post hoc test were used to evaluate the significant inter-site differences in terms of both SRaGR and LTRaG within the respective time intervals.

The Pearson's coefficient (r) was used to evaluate the correlation between SRaGR and the 18 environmental variables measured over the five STIs, limited to those sites (2, 6, 8 and 11) equipped with thermo-hygrometric sensors. Then, the relationship between lichen growth and the site-specific air humidity was explored on the basis of the frequencies of rainless days with an average daily value of (a) RH > 90%, (b) Ψ_{wv} > -14.2 MPa, (c) DP < 0 °C, and (d) SD > 2 kPA.

In order to assess whether the selected 18 environmental variables could be considered as reliable predictors of SRaGR, a Principal Component Regression analysis was performed on a dataset including the 18 environmental variables and the SRaGR values of the thalli occurring in the four sites equipped with thermos-hygrometric sensors. The 16 climatic variables were first analysed by Principal Component Analysis (PCA) and then, the first two Principal Components (PCs) were used together with the altitude and the distance from the sea as independent predictors in a linear mixed model considering the thallus as random effect. The goodness of fit of the linear mixed model (herein named as Growth Rate Distribution Model; GRDM) was assessed by testing for normality the residuals by Shapiro-Wilk test and evaluating the significance of the coefficient of determination (R^2) between estimated and observed SRaGR values in the four sites.

The dataset including the 18 environmental variables, as estimated in the OGUs by IDW interpolations, was used to validate GRDM (validation dataset). Therefore, a further 159 OGUs × 16 climatic variables matrix was submitted to a second PCA, whose first two PCs were used together with altitude and distance from the sea as independent predictors in the equation of GRDM. The reliability of SRaGR estimation provided by GRDM was assessed by testing the significance of R^2 between the estimated and observed SRaGR values collected in those sites (1, 3 and 10), which were not included in the dataset for GRDM fitting.

3. Results

3.1 Site-specific climatic conditions

The data collected by the thermo-hygrometric sensors in sites 2, 6, 8 and 11 over the whole study period revealed a pronounced, relatively stable thermometric gradient along the transect (Supplementary Table 1). In general, the sites closest to the coast were on average warmer (+5 °C) than those at higher altitudes, in

good accordance with the adiabatic lapse rate (1 °C per 100 m altitude). This means that, during summer, the coastal sites were characterised by relatively high evaporative demand (+33.2% of rainless days with an average daily value of $SD_{max} > 2kPa$), especially when compared to site 11. On the contrary, during winter, the frequent occurrence of cold Bora wind gusts characterised site 11 as the driest one, since its average seasonal values of air DP was relatively lower than those recorded at lower altitude.

The average seasonal values of both RH and Ψ_{wv} were quite similar along the transect, but site 8 had the highest air humidity in autumn and winter 2015 and spring 2016. In particular, during the latter STIs, site 8 had on average up to 24% more days with mean daily values of $RH_{max} > 90\%$ and $PSI_{max} > -14.2$ MPa with respect to sites 6 and 11.

Finally, the cumulative precipitations were equally distributed along the transect (Fig. 2).

The cumulative precipitations observed during summer (385 ± 29 mm), autumn (387 ± 52 mm) and spring (359 ± 25 mm) 2016 were quite similar, whereas a significant increase was observed in winter (452 ± 34 mm). Spring 2015 was the driest period, since it was significantly less rainy than the other STIs (158 ± 13 mm) and, at the same time, its seasonal average RH value was relatively more similar to that of summer 2015 than to that of spring 2016.
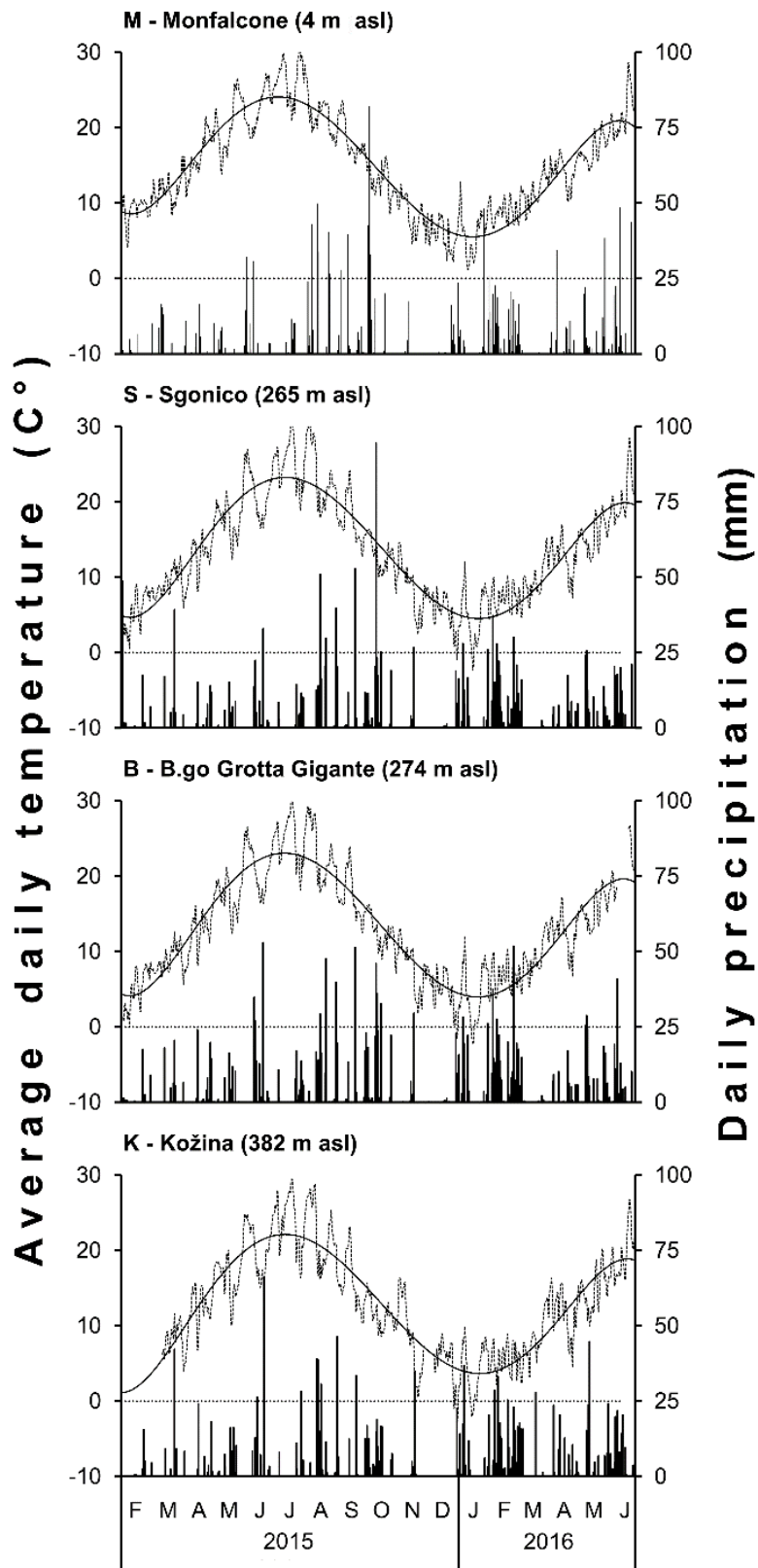
Fig. 2: Average daily temperature (dotted lines) and daily precipitations (black bars) measured in the four pluviometric stations of Fig. 1 in the study period. The continuous lines is an interpolation curve calculated as a function of the average daily temperature.

3.2   Seasonal and long term radial growth

The factorial ANOVA revealed that the radial growth of *X. parietina* was not constant during the study period, the "time period" factor being highly significant (Table 1). SRaGR was lower in the dry, warm seasons (i.e. spring and summer 2015) and higher in the rainy, moist, cold ones (i.e. autumn and winter 2015, and spring 2016) (Fig. 3).

Table 1: Summary of factorial ANOVA analyses performed on seasonal radial growth rate (SRaGR) and long-term radial growth (LTRaG) values. The results of the LSD's post hoc test are given in Supplementary Table 2 and 3 for SRaGR and LTRaG data, respectively. df: degree of freedom; F: F-statistic; P: p-value.

	SRaGR			LTRaG		
	df	*F*	*P*	*df*	*F*	*P*
Time interval (TI)	4	36.96	0.000	1	18.23	0.000
Site (S)	6	19.23	0.000	6	11.64	0.000
TI × S	24	3.82	0.000	6	0.40	0.873
Error	117			46		
Total	151			59		
r^2_{adj}		0.700			0.580	

In agreement with these results, SRaGR measured at sites 2, 6, 8 and 11 were negatively correlated with the seasonal average values of T, DP and SD, and positively correlated with those of P, RH and Ψ_{wv} (Table 2). The highly significant correlations between SRaGR and climatic data coupled with the fact that the outcomes of factorial ANOVA showed significant interaction effect "site × time interval" (Table 1), suggests that the inter-site SRaGR variability was affected by the seasonal climatic conditions at small (site-specific) spatial scale.
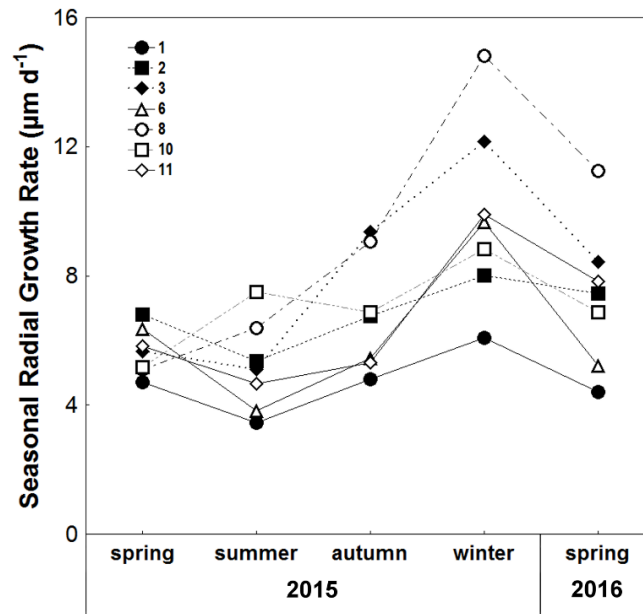
Fig. 3: Average values of site-specific seasonal radial growth rates of the epiphytic lichen *Xanthoria parietina* in five successive seasons in seven sites of Fig. 1. The statistical differences among site-specific average values are given in

Inter-site variability was the lowest in the dry, warm periods of spring and summer 2015 (Fig. 3; Supplementary Table 2). In summer 2015, although the cumulative precipitation doubled along the entire transect with respect to spring 2015, SRaGR slightly decreased in five sites, due to the increased seasonal average values of T and SD. In autumn and winter 2015, inter-site variability increased even though the cumulative precipitations were still equally distributed along the transect. In fact, according to the site-specific water availability (see previous section), thalli at the transect extremes and at site 6 had significant lower SRaGR values than those at site 8 (Supplementary Table 2). During spring 2016, SRaGR sharply decreased in all selected sites in parallel to the average temperature increase. In comparison to spring 2015, the inter-site variability of SRaGR increased during 2016, in line with the seasonal SD gradient between the two transect extremes ($\Delta SD = 0.903$ kPa) (Supplementary Table 1) and the high values of both cumulative precipitations and average seasonal RH.

The factorial ANOVA performed on the LTRaG values revealed a high statistical significance of the factor "site" (Table 1): in particular, the site-specific LTRaG values ranged between 1.27 and 3.19 mm during LT_1, and between 1.79 and 4.44 mm during LT_2. Over both long-term time intervals (i.e. LT_1 and LT_2), the

LTRaGs of thalli at sites 1 and 11 (the transect extremes) were significantly lower than that observed at site 8 (Fig. 4).

Table 2: Pearson's correlation coefficients (r) and their statistical significance (P) between SRaGR values and the seasonal values of the 18 site-specific variables or the frequencies (%) of rainless days with an average daily value of RH >90%; DP <0°C; SD >2kPA and Ψ_{wv} >-14.2MPa. dfs: distance from the sea; cP: cumulative precipitation; T: temperature; RH: relative humidity; DP: dew point; SD: saturation deficit; Ψ: air water potential. min, ave and max: minimum, average and maximum, respectively; -: not calculated.

Site-specific variable	Seasonal values		%	
	r	P	r	P
Altitude	0.07	0.53	-	-
dfs	0.06	0.588	-	-
cP	0.47	< 0.001	-	-
T_{min}	-0.49	< 0.001	-	-
T_{ave}	-0.51	< 0.001	-	-
T_{max}	-0.51	< 0.001	-	-
RH_{min}	0.56	< 0.001	0.46	< 0.001
RH_{ave}	0.63	< 0.001	0.64	< 0.001
RH_{max}	0.67	< 0.001	0.65	< 0.001
DP_{min}	-0.39	< 0.001	0.30	< 0.01
DP_{ave}	-0.40	< 0.001	0.29	< 0.01
DP_{max}	-0.40	< 0.001	0.27	< 0.05
SD_{min}	-0.53	< 0.001	-	-
SD_{ave}	-0.52	< 0.001	-0.32	< 0.01
SD_{max}	-0.49	< 0.001	-0.50	< 0.001
Ψ_{min}	0.56	< 0.001	0.37	< 0.01
Ψ_{ave}	0.63	< 0.001	0.59	< 0.001
Ψ_{max}	0.67	< 0.001	0.66	< 0.001

The site-specific LTRaGs differences are clearly due to the fact that the latter site was characterized by high air humidity in summer, autumn and winter (Supplementary Table 3). Nevertheless, the "site × time interval" interaction term was not significant (Table 1), suggesting that within the same site the LTRaGs were relatively homogeneous. On annual basis, RaGR was similar among thalli placed in inland sites (2.6 ± 0.3 mm y^{-1}; Fig. 5), whereas it was significantly lower (1.65 ± 0.17 mm y^{-1}) for the thalli at site 1.
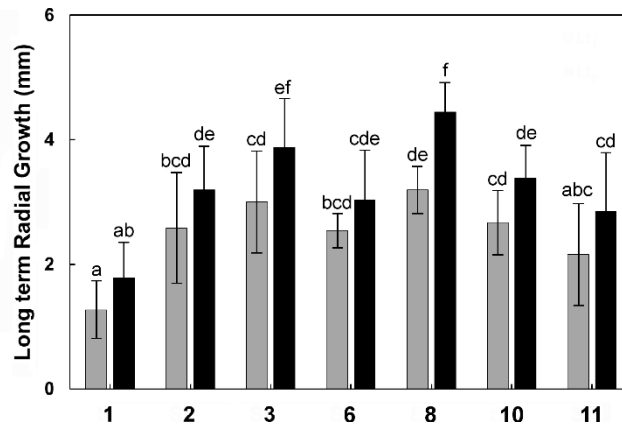
Fig. 4: Site-specific average long term radial growth values of the epiphytic lichen *Xanthoria parietina* in the two long-term periods LT$_1$ (grey bars) and LT$_2$ (black bars). Sites ordered according to their increasing altitude (see Fig. 1). Whiskers indicate standard deviations. Different letters indicates significant statistical differences as evaluated by factorial ANOVA and following LSD's post hoc test.
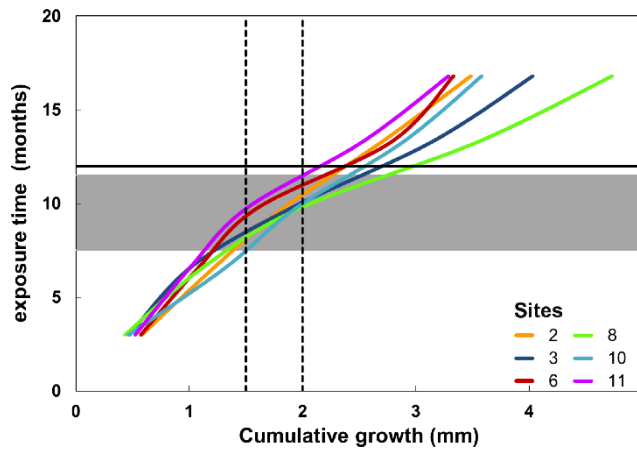

Fig. 5: lobe exposure time as a function of the annual cumulative growth observed in six sites of Fig. 1. Data of sites 1 are not reported. The horizontal grey area represents the exposure time (9.5±2 months) of marginal lobes of the epiphytic lichen *Xanthoria parietina* according to the threshold (1.5 – 2 mm; vertical dashed lines) recommended in the sample preparation for the biomonitoring of trace elements and other airborne persistent pollutants (Nimis and Bargagli 1998). The black horizontal continuous line corresponds to an exposure time of 1 year.

3.3 SRaGR data modelling

The results of PCAs performed on the fitting and validation datasets are reported in Supplementary Fig. 2. The outcomes of PCR analysis revealed that the GRDM satisfactorily fitted the SRaGR values measured *in situ* (Table 3), with normally distributed model residuals, high model statistical significance and multiple correlation coefficient (P < 0.001 and R = 0.80, respectively). Moreover, adjusted R^2 indicates that the predictors explain 63% of the SRaGR-data variance.

Table 3: Summary of linear mixed model predicting SRaGR values in the spatial domain of 159 km^2 as a function of the altitude, distance from the sea (dfs) and the first 2 principal factors (PCs) used as predictors (see section 2.5). β: beta coefficient; SE: standard error of β coefficients; t: t-value of the β coefficient estimation; P: p-value; F(10,73): F: F-statistic on 10 and 73 degree of freedom; R: Multiple regression coefficient: R^2 $_{adj}$: adjusted R^2; W: Shapiro's W-test for residual normality.

	β	SE	*t*	*P*
Intercept	7.31	0.74	9.93	0.000
Altitude	0.01	0.00	2.35	0.039
dfs	0.00	0.00	-2.78	0.018
PC 1	-0.58	0.08	-7.43	0.000
PC 2	-0.59	0.17	-3.47	0.001
Overall statistics	*F*(10,73) = 53.54; *P*<0.001 *R* = 0.80; *R²* = 0.63; *R²* *$_{adj}$*= 0.63 *Residual standard error*: 2.15 µm d^{-1} Residual normality: W=0.98; P=0.193			

The GRDM run with the validation dataset provided a distribution of the predicted SRaGR values within the spatial domain of 159 km^2 over the five STIs (Fig. 6). The model predictions were in good accordance with the ANOVA results, since low SRaGR were estimated for drought and warm seasons and high SRaGR were estimated for cold and moist ones. Moreover, the predicted values in sites 1, 3 and 10 were significantly correlated with their respective *in situ* values (Table 4).

Table 4: Coefficient of determination (R^2) calculated between the predicted and measured values in sites 1, 3 and 10 for GRDM validation. F: F-statistic; P: p-value.

Site	**R^2**	**F**	**P**
1, 3, 10	0.330	32.82	0.000
1	0.250	5.88	0.030
3	0.760	70.57	0.000
10	0.360	12.25	0.002

Although the GRDM was validated, its residual standard error was too high (2.15 µm d^{-1}) to correctly predict RaGR over the whole study domain. For example, the relative error of predictions for site 1 was extremely high (61%), whereas it sharply decreased to 19.3% and 18.7% when the model was implemented to predict SRaGR in site 8 and 10, respectively.
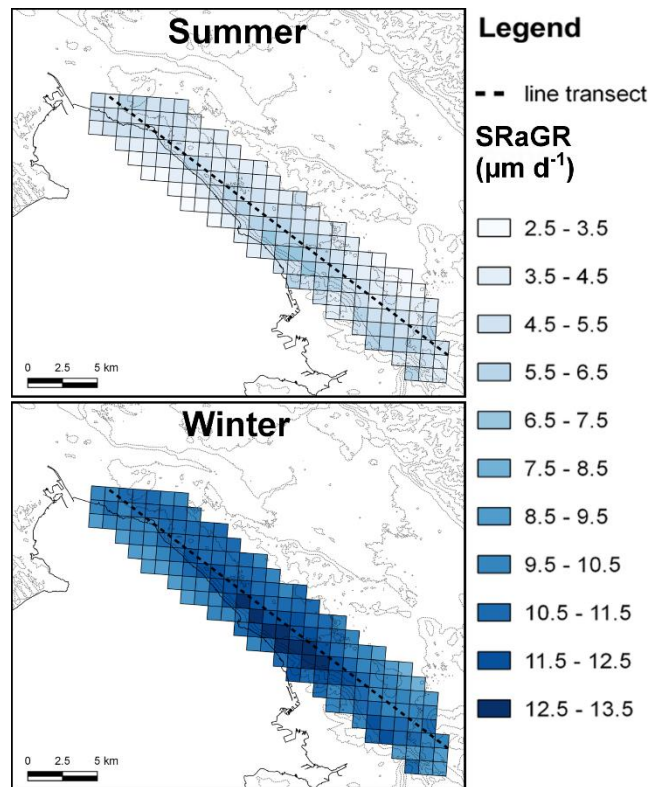
Fig. 6: SRaGR distribution in summer and winter within the spatial domain of 159 km^2.

4. Discussion

The seasonal radial growth of *Xanthoria parietina* increased and decreased accordingly to the seasonal rainfall (Fig. 3; Supplementary Table 1), which was relatively lower in spring and summer 2015 and higher in autumn and winter 2015 and in spring 2016. This is in agreement with the fact that the growth of chlorolichens seems to be affected more by rainfall events than by air humidity (Renhorn et al. 1996; Palmqvist and Sundberg 2000; Palmqvist et al. 2008; Gauslaa 2014). Similar seasonal radial growth patterns were observed in other foliose lichens, such as the epilithic *Melanelixia glabratula* (Armstrong 1975) and the epiphytic *Flavoparmelia caperata*, *Parmelia sulcata* (Fisher and Proctor 1978, Tretiach et al. 2013) and *Pseudocyphellaria berberina* (Caldiz 2004). In the first two studies, as well as in this one, the rainfall events were positively correlated with the seasonal growth rate. The noticeable thalline SRaGR difference observed within sites 3 and 8 between spring and winter 2015 (Fig. 3; Table 1) was well explained by the different precipitation values recorded in those two periods. On the other hand, the homogenous distribution of seasonal precipitations along the transect did not explain the observed differences in site-specific SRaGRs within the same season (e.g. site 1 vs site 8), suggesting that further factors may have affected the

29

lobe lengthening of *X. parietina* at site scale. Since *X. parietina* is a nitrophytic species, it might be argued that its growth rate is conditioned by nitrogen availability. However, in order to minimize such potential confounding factor, the study area was purposely selected because it is not impacted by agricultural activities, and NO_x pollution load is relatively low and homogeneously distributed (Regione FVG). Furthermore, there are evidences that in *X. parietina* the specific thallus mass (i.e. the ratio between dry weight and thallus area) is not correlated with nitrogen contributions at site-specific scale (Gaio-Oliveira et al. 2004a). This means that possible differences in site-specific differences in nitrogen supply are not supposed to affect the growth of *X. parietina*, as it was conversely observed in tripartite lichens (Sundberg et al. 2001; Dahlman et al. 2002). However, our data revealed that SRaGR was negatively correlated with T, DP, SD and the frequency of rainless days with mean daily values of $SD_{max} > 2kPA$ (r = -0.49; p < 0.001). Hence, the pronounced SRaGR differences between site 1 and site 8 (Fig. 3) could be explained by the site-specific air temperature, since it positively affects the environmental evaporative demand by increasing both air saturation vapour pressure (Körner 2007) and dew point (Wallace and Hobbs 2006). This means that thalli occurring in the coastal sites were subjected to a relative higher air saturation deficit, which could rapidly reduce their water content (Kershaw 1985) and thus the time span in which lichens are photosynthetically active (Lange et al. 1986; Jonsson Čabrajić 2010). In addition, hydrated thalli exposed to high temperature increase the so-called resaturation respiration, with a further reduction of the net carbon gain (Green and Lange 1995; Sundberg et al. 1999).

In the study area, a further limiting factor for the growth of *X. parietina* is certainly the frequent dry ENE winds. The Bora, an adiabatic, continental wind, has a noteworthy drying effect on the vegetation of the Classical Karst (Poldini 1989), increasing the rate of thallus water loss from lichens (Kershaw et al. 1975). At the same time, this wind also limits the pre-dawn dew formation, which is the pivotal factor for the re-activation of lichen photosynthesis in absence of rain (Lange et al. 2003). Due to the geo-morphological conformation of the area, the sites of the transect are not uniformly exposed to the bora wind. For instance, this is certainly more intense and frequent at sites 10 and 11 than at sites 6 and 8, as testified by the anemometric records of the four meteorological stations of Fig. 1 (available upon request).

In summary, our data highlighted that in the study area the radial growth of *X. parietina* is negatively affected during the year by the protracted absence of rain. Differences among sites during the same season

are mostly due to the different evaporative demand of some sites, which depends on topological differences in air temperatures and wind frequency and/or intensity.

A final remark concerns the low thalline SRaGR observed at site 1, the driest one. This is certainly caused by a shorter positive CO_2 gain caused by the more arid conditions (which also allows the local persistence of an extra-zonal Mediterranean maquis, see Tretiach et al. 1997). However, the reduced growth might also be due to an organic carbon investment different from that at the other sites. In order to increase water retention, thus prolonging CO_2 uptake, lichens can modify their morphology, e.g. forming multi-layered thalli, or increasing their rhizinae (Tretiach and Brown 1995; Gauslaa and Solhaug 1998). Also, the increase in thallus thickness observed in many species, mostly at medullary level, efficaciously contrasts the evaporative demand (Snelgar and Green 1981; Valladares et al. 1993, 1998). Therefore, we cannot exclude that the thalli of *X. parietina* occurring at site 1 differ in specific thallus mass and/or in thallus thickness with respect to those occurring at the other sites: this should be the subject of further investigation.

4.1   GRDM

Most of the recent studies concerning lichen growth modelling has been carried out in areas with oceanic (Gaio Oliveira et al. 2004b) and boreal climates (Gauslaa et al. 2006, Bidussi et al. 2013b), mostly with *Lobaria pulmonaria* as target species (Larson et al. 2012; Bidussi et al 2013a; Eaton and Ellis 2013). On the other hand, there are only few studies concerning the radial or relative growth rate of *X. parietina* (Richardson 1967; Moxham 1981; Honegger 1996b), and none of them has been carried out in Mediterranean or sub-Mediterranean environments.

With GRDM we tested the effects of altitude, distance from the sea and the climatic variables - the latter summarised up by the first two PCs - on *X. parietina* lobe lengthening along the thermometric gradient (Table 3). In particular, the GRDM outputs indicated that thalli occurring at lower altitude, in proximity of the coast had lower SRaGR (Fig. 5), likely due to the high evaporative demand (see previous section). Concerning altitude, our results are in contrast with those of Bidussi et al (2013b), who did not observe a significant effect of altitude on the area growth rate of *Hypogymnia physodes* and *L. pulmonaria* along an altitudinal gradient of 1100 m on the western slope of Battle Mountain, British Columbia. One possible explanation for this lack of congruence is that the adiabatic lapse rate could affect the specific thallus mass

more in the Mediterranean than in the Boreal zone. Merinero et al. (2015) actually observed that thalli of *L. pulmonaria* from the Mediterranean zone have thicker thalli than those from the Boreal zone.

The coefficients of climatic predictors (i.e. PC1 and PC2; Table 3) were negatively correlated with the predicted SRaGR values. In particular, PC1 was positively correlated with T, DP, and SD, negatively correlated with RH and PSI, whereas PC2 was negatively correlated with seasonal cumulative precipitations. These relationships confirmed once again that *X. parietina* SRaGR is higher in areas with low evaporative demand, especially when humid conditions are prevalent, as in winter (Fig. 5).

In summary, the site-specific climatic variables selected in this study allowed to predict SRaGR with an overestimation ranging between 12 and 22 % for site 3, and between 7 and 26 %, for site 10. For site 1 the overestimation was considerably higher (between 42 and 73 %), probably because we assumed that lobe growth was linearly distributed across the five STI. This assumption could be the main factor explaining the high overestimation of GRDM for sites 8 and 10, especially for summer, when the lobe radial growth is low or at least drastically reduced.

4.2   *Long term radial growth and implication for biomonitoring surveys*

In six sites (i.e. sites 2, 3, 6, 8, 10, 11) LTRaG rates were relatively similar, although the prolonged humid conditions occurred in winter and spring 2016 induced higher $LTRaG_2$s at sites 3 and 8 than at sites 2, 6, 10 and 11. With the exclusion of site 1, anomalous for the unusually high evaporative demand, the average annual growth of *X. parietina* along the transect can be estimated in 2.6 ± 0.3 mm y^{-1}. This estimation is consistent with the value reported by Moxham et al. (1981) (2.7 mm y^{-1}) for thalli occurring on concrete pavers in Bath, UK and with those of Richardson (1967), who observed an increase of the thalline radius between 3.5 and 6.7 mm over a period of 18 months in Oxford, UK. On the contrary, our annual estimation significantly differs from that of Honegger et al. (1996b) (6-7 mm y^{-1}) for thalli occurring on sandstone in sub-montane environments (Switzerland).

Nimis and Bargagli (1998) proposed a methodological framework for the use of epiphytic lichens as a biomonitors of airborne trace elements, which was later adopted by national agencies (e.g. ANPA 1999) and professional associations and widely used in several European countries (Brunialti and Frati 2007; Stamenković et al. 2013; Agnan et al. 2015). The protocol of Nimis and Bargagli (1998), as modified by

Bargagli and Nimis (2002), recommends to measure element concentrations in the outermost portions of thalli. For *X. parietina* it is recommended to analyse the last 2 mm from the lobe tips, which would correspond, in the intention of the authors, to the last year of growth. By strictly applying this provision of the protocol, the lichen material collected in site 1 would be much older (c. 14 ± 2 months), whereas the material collected in the other sites of the transect would be much younger (c. 9.5 ± 2 months) (Fig. 6), due to the different yearly growth rate. In light of these considerations, the biomonitoring surveys based on autochthonous lichens should be limited to climatically homogeneous areas, in order to minimize differences in the growth rates of thalli and ensure comparable exposure periods. This is of primary importance when the aim is to test the predictability of pollutant dispersion models (Fortuna et al. *in prep*.). It is worth-noting that much more work is badly needed on the growth of epiphytic lichens used in biomonitoring surveys, because data are missing for the majority of species, and several growth-related issues must be clarified.

References

Ahmadjian, V., 2001. Trebouxia: reflections on a perplexing and controversial lichen photobiont. In: Seckbach J. (eds) Symbiosis. Cellular origin, life in extreme habitats and astrobiology.Springer, Dordrecht

Agnan, Y., 2013. Bioaccumulation et bioindication par les lichens de la pollution atmosphérique actuelle et passée en métaux et en azote en France: sources, mécanismes et facteurs d'influence (Doctoral dissertation).

Agnan, Y., Séjalon-Delmas, N., Claustres, A., Probst, A., 2015. Investigation of spatial and temporal metal atmospheric deposition in France through lichen and moss bioaccumulation over one century. Sci Total Environ, 529, 285-296.

Armstrong, R.A., 1975. The influence of aspect on the pattern of seasonal growth in the lichen *Parmelia glabratula* ssp. *fuliginosa* (Fr. ex Duby) Laund. New Phytol, 75, 245-251.

Armstrong, R.A., Bradwell, T., 2011. Growth of foliose lichens: a review. Symbiosis, 53, 1-16.

Augusto, S., Sierra, J., Nadal, M., Schuhmacher, M., 2015. Tracking polycyclic aromatic hydrocarbons in lichens: It's all about the algae. Environ Pollut, 207, 441-445.

Bargagli, R., 1998. Trace Elements in Terrestrial Plants. An ecophysiological approach to biomonitoring and biorecovery. Springer, Berlin.

Bargagli, R., Nimis, P.L., 2002. Guidelines for the use of epiphytic lichens as biomonitors of atmospheric deposition of trace elements. In: Nimis, P. L., Scheidegger, C., Wolseley P. A. (eds.), Monitoring with Lichens – Monitoring Lichens. NATO Science Series, IV. Earth and Environmental Sciences, Vol. 7. Kluwer, Dordrecht, pp. 295-299.

Bertuzzi, S., Davies, L., Power, S.A., Tretiach, M., 2013. Why lichens are bad biomonitors of ozone pollution? Ecol Indic, 34, 391-397.

Bertuzzi, S., Pellegrini, E., Carniel, F.C., Incerti, G., Lorenzini, G., Nali, C., Tretiach, M., 2017. Ozone and desiccation tolerance in chlorolichens are intimately connected: a case study based on two species with different ecology. Environ Sci Pollut Res, 24, 1-15.

Bidussi, M., Gauslaa, Y., Solhaug, K.A., 2013a. Prolonging the hydration and active metabolism from light periods into nights substantially enhances lichen growth. Planta, 237, 1359-1366.

Bidussi, M., Goward, T., Gauslaa, Y., 2013b. Growth and secondary compound investments in the epiphytic lichens *Lobaria pulmonaria* and *Hypogymnia occidentalis* transplanted along an altitudinal gradient in British Columbia. Botany, 91, 621-630.

Brandt, A., de Vera, J.P., Onofri, S., Ott, S., 2015. Viability of the lichen *Xanthoria elegans* and its symbionts after 18 months of space exposure and simulated Mars conditions on the ISS. Int J Astrobiol, 14, 411-425.

Branquinho, C., Gaio-Oliveira, G., Augusto, S., Pinho, P., Máguas, C., Correia, O., 2008. Biomonitoring spatial and temporal impact of atmospheric dust from a cement industry. Environ Pollut, 151, 292-299.

Brunialti, G., Frati, L., 2007. Biomonitoring of nine elements by the lichen *Xanthoria parietina* in Adriatic Italy: a retrospective study over a 7-year time span. Sci Total Environ, 387, 289-300.

Brodo, I.M., Lewis, C., Craig, B., 2007. *Xanthoria parietina*, a coastal lichen, rediscovered in Ontario. Northeast Nat, 14, 300-306.

Bubrick, P., Galun, M., 1986. Spore to spore resynthesis of *Xanthoria parietina*. Lichenologist, 18, 47-49.

Büdel, B., Lange, O.L., 1991. Water status of green and blue-green phycobionts in lichen thalli after hydration by water vapor uptake: do they become turgid? Bot Acta, 104, 361-366.

Caldiz, M.S., 2004. Seasonal growth pattern in the lichen *Pseudocyphellaria berberina* in north-western Patagonia. Lichenologist, 36, 435-444.

Crabtree, D., Ellis, C.J., 2010. Species interaction and response to wind speed alter the impact of projected temperature change in a montane ecosystem. J Veg Sci, 21: 744-760.

Cuny, D., Davranche, L., Thomas, P., Kempa, M., Van Haluwyn, C., 2004. Spatial and temporal variations of trace element contents in *Xanthoria parietina* thalli collected in a highly industrialized area in northern France as an element for a future epidemiological study. J Atmos Chem, 49, 391-401.

Dahlman, L., Näsholm, T., Palmqvist, K., 2002. Growth, nitrogen uptake, and resource allocation in the two tripartite lichens *Nephroma arcticum* and *Peltigera aphthosa* during nitrogen stress. New Phytol, 153, 307-315.

Del Prado, R., Sancho, L.G., 2007. Dew as a key factor for the distribution pattern of the lichen species *Teloschistes lacunosus* in the Tabernas Desert (Spain). Flora, 202, 417-428.

Demiray, A.D., Yolcubal, I., Akyol, N.H., Çobanoğlu, G., 2012. Biomonitoring of airborne metals using the lichen *Xanthoria parietina* in Kocaeli Province, Turkey. Ecol Indic, 18, 632-643.

Domínguez-Morueco, N., Augusto, S., Trabalón, L., Pocurull, E., Borrull, F., Schuhmacher, M., Domingo, J.L., Nadal, M., 2017. Monitoring PAHs in the petrochemical area of Tarragona County, Spain: comparing passive air samplers with lichen transplants. Environ Sci Pollut Res, 24, 11890-11900.

Eaton, S., Ellis, C.J., 2012. Local experimental growth rates respond to macroclimate for the lichen epiphyte *Lobaria pulmonaria*. Plant Ecol Divers, 5, 365-372.

Fiechter, E., 1990. Thallusdifferenzierung und intrathalline Sekundärstoffverteilung bei Parmeliaceae: (Lecanorales, lichenisierte Ascomyceten) (Doctoral dissertation).

Fisher, P.J., Proctor, M.C.F., 1978. Observations on a season's growth in *Parmelia caperata* and *P. sulcata* in South Devon. Lichenologist, 10, 81-89.

Frati, L., Santoni, S., Nicolardi, V., Gaggi, C., Brunialti, G., Guttova, A., Gaudino, S., Pati, A., Pirintsos S.A., Loppi, S., 2007. Lichen biomonitoring of ammonia emission and nitrogen deposition around a pig stockfarm. Environ Pollut, 146, 311-316.

Gaio-Oliveira, G., Dahlman, L., Palmqvist, K., Maguas, C., 2004a. Ammonium uptake in the nitrophytic lichen *Xanthoria parietina* and its effects on vitality and balance between symbionts. Lichenologist, 36, 75-86.

Gaio - Oliveira, G., Dahlman, L., Máguas, C., Palmqvist, K., 2004b. Growth in relation to microclimatic conditions and physiological characteristics of four *Lobaria pulmonaria* populations in two contrasting habitats. Ecography, 27, 13-28.

Gauslaa, Y., Solhaug, K. A., 1998. The significance of thallus size for the water economy of the cyanobacterial old-forest lichen *Degelia plumbea*. Oecologia, 116, 76-84.

Gauslaa, Y., Lie, M., Solhaug, K. A., Ohlson, M., 2006. Growth and ecophysiological acclimation of the foliose lichen *Lobaria pulmonaria* in forests with contrasting light climates. Oecologia, 147, 406-416.

Gauslaa, Y., Palmqvist, K., Solhaug, K. A., Holien, H., Hilmo, O., Nybakken, L., Myhre L.C., Ohlson, M., 2007. Growth of epiphytic old forest lichens across climatic and successional gradients. Can J Forest Res, 37, 1832-1845.

Gauslaa, Y., Coxson, D., 2011. Interspecific and intraspecific variations in water storage in epiphytic old forest foliose lichens. Botany, 89, 787-798.

Gauslaa, Y. (2014). Rain, dew, and humid air as drivers of morphology, function and spatial distribution in epiphytic lichens. Lichenologist, 46, 1-16.

Green, T.G.A., Lange, O.L. 1995. Photosynthesis in poikilohydric plants: a comparison of lichens and bryophytes. In: Schulze, E.D. and Caldwell, M.M. (eds.), Ecophysiology of Photosynthesis. Springer, Berlin, Heidelberg, pp. 319-341.

Hill, D.J., 1985. Changes in photobiont dimensions and numbers during co-development of lichen symbionts. In: Brown, D.H. (ed.), Lichen Physiology and Cell Biology. Plenum, New York, 303-317.

Hill, D.J., 1989. The control of the cell cycle in microbial symbionts. New Phytol, 112, 175-184.

Honegger, R., 1993. Developmental biology of lichens. New Phytol, 125, 659-677.

Honegger, R., 1996a. Experimental studies of growth and regenerative capacity in the foliose lichen *Xanthoria parietina*. New Phytol, 133, 573-581.

Honegger, R., Conconiy, S., Kutasi, V., 1996b. Field studies on growth and regenerative capacity in the foliose macrolichen *Xanthoria parietina* (Teloschistales, Ascomycotina). Plant Biol, 109, 187-193.

Honegger, R., 1998. The lichen symbiosis—what is so spectacular about it? Lichenologist, 30, 193-212.

Honegger, R., 2003. The impact of different long-term storage conditions on the viability of lichen-forming ascomycetes and their green algal photobiont, *Trebouxia* spp. Plant Biol, 5, 324-330.

Honegger, R., Zippler, U., Gansner, H., Scherrer, S., 2004. Mating systems in the genus *Xanthoria* (lichen-forming ascomycetes). Mycol Res, 108, 480-488.

Itten, B., Honegger, R., 2010. Population genetics in the homothallic lichen-forming ascomycete *Xanthoria parietina*. Lichenologist, 42, 751-761.

Jonsson Čabrajić, A.V., Lidén, M., Lundmark, T., Ottosson-Lofvenius, M. Palmqvist, K., 2010. Modelling hydration and photosystem II activation in relation to in situ rain and humidity patterns: a tool to compare performance of rare and generalist epiphytic lichens. Plant Cell Environ, 33, 840-850.

Kershaw, K.A., 1975. Studies on lichen-dominated systems. XII. The ecological significance of thallus color. Can J Botany, 53, 660-667.

Kershaw, K.A., 1985. Physiological Ecology of Lichens. Cambridge University Press, Cambridge.

Körner, C., 2007. The use of 'altitude' in ecological research. Trends Ecol Evol, 22(11), 569-574.

Kodnik, D., Candotto Carniel, F., Licen, S., Tolloi A., Barbieri P., Tretiach M., 2015. Seasonal variations of PAHs content and distribution patterns in a mixed land use area: a case study with the transplanted lichen *Pseudevernia furfuracea*. Atmos Environ, 113: 255-263.

Kottek, M., Grieser, J., Beck, C., Rudolf, B., Rubel, F. 2006. World map of the Köppen-Geiger climate classification updated. Meteorologische Zeitschrift, 15, 259-263.

Lange, O.L., Kilian, E., Ziegler, H., 1986. Water vapour uptake and photosynthesis of lichens: performance differences in species with green and blue-green algae as phycobionts. Oecologia, 71, 104-110.

Lange, O.L., 2003. Photosynthetic productivity of the epilithic lichen *Lecanora muralis*: long-term field monitoring of CO_2 exchange and its physiological interpretation: II. Diel and seasonal patterns of net photosynthesis and respiration. Flora, 198, 55-70.

Lange, O.L., Green, T.A., 2008. Diel and seasonal courses of ambient carbon dioxide concentration and their effect on productivity of the epilithic lichen *Lecanora muralis* in a temperate, suburban habitat. Lichenologist, 40, 449-462.

Larsson, P., Solhaug, K.A., Gauslaa, Y., 2012. Seasonal partitioning of growth into biomass and area expansion in a cephalolichen and a cyanolichen of the old forest genus *Lobaria*. New Phytol, 194, 991-1000.

Loppi, S., Nelli, L., Ancora, S., Bargagli, R., 1997. Accumulation of trace elements in the peripheral and central parts of a foliose lichen thallus. Bryologist, 100, 251-253.

Merinero, S., Martínez, I., Rubio-Salcedo, M., Gauslaa, Y., 2015. Epiphytic lichen growth in Mediterranean forests: Effects of proximity to the ground and reproductive stage. Basic Appl Ecol, 16, 220-230.

Moxham, T.H., 1981. Growth rates of *Xanthoria parietina* and their relationhsip to substrate texture. Cryptogamie Bryol Lichénol, 2, 171-180.

Muggia, L., Fleischhacker, A., Kopun, T., Grube, M., 2016. Extremotolerant fungi from alpine rock lichens and their phylogenetic relationships. Fungal Divers, 76, 119-142.

Munzi, S., Cruz, C., Maia, R., Máguas, C., Perestrello-Ramos, M.M., Branquinho, C., 2017. Intra-and inter-specific variations in chitin in lichens along a N-deposition gradient. Environ Sci Pollut Res, 24, 1-7.

Nimis, P.L., Andreussi, S., Pittao, E., 2001. The performance of two lichen species as bioaccumulators of trace metals. Sci Total Environ, 275, 43-51.

Nimis, P.L., Bargagli, R., 1998. Linee-guida per l'utilizzo di licheni epifiti come bioaccumulatori di metalli in traccia. In: atti del workshop: "Biomonitoraggio della qualità dell'aria sul territorio nazionale", Roma, pp. 26-27.

Olsen, H.B., Berthelsen, K., Andersen, H.V., Søchting, U., 2010. *Xanthoria parietina* as a monitor of ground-level ambient ammonia concentrations. Environ Pollut, 158, 455-461.

Palmqvist, K., 2000. Tansley review No. 117 Carbon economy in lichens. New Phytol, 148, 11-36.

Palmqvist, K., Sundberg, B., 2000. Light use efficiency of dry matter gain in five macro‐lichens: relative impact of microclimate conditions and species-specific traits. Plant Cell Environ, 23, 1-14.

Palmqvist, K., Dahlman, L., Jonsson, A., Nash, T.H., 2008. The carbon economy of lichens. In: Nash ,T. H. III (ed.), Lichen Biology, Cambridge University Press, Cambridge, pp 182-215.

Piccotto, M., Bidussi, M., Tretiach, M., 2011. Effects of the urban environmental conditions on the chlorophyll a fluorescence emission in transplants of three ecologically distinct lichens. Environ Exp Bot, 73, 102-107.

Poldini, L., 1989. La Vegetazione del Carso triestino ed isontino. Lint, Trieste.

Richardson, D.H.S., 1967. The transplantation of lichen thalli to solve some taxonomic problems in *Xanthoria parietina* (L.) Th. Fr. Lichenologist, 3, 386-391.

Richardson, D.H.S., 1988. Understanding the pollution sensitivity of lichens. Bot J Linn Soc, 96, 31-43.

Renhorn, K.E., Esseen, P.A., Palmqvist, K., Sundberg, B., 1996. Growth and vitality of epiphytic lichens. Oecologia, 109, 1-9.

Scherrer, S., Zippler, U., Honegger, R., 2005. Characterisation of the mating-type locus in the genus *Xanthoria* (lichen-forming ascomycetes, Lecanoromycetes). Fungal Genet Biol, 42, 976-988.

Sloof, J.E., 1995. Lichens as quantitative biomonitors for atmospheric trace-element deposition, using transplants. Atmos Environ, 29, 11-20.

Snelgar, W.P., Green, T.G.A., 1981. Ecologically-linked variation in morphology, acetylene reduction, and water relation in *Pseudocyphellaria dissimilis*. New Phytol, 87, 403-411.

Stamenković, S.S., Mitrović, T.L., Cvetković, V.J., Krstić, N.S., Baošić, R.M., Marković, M.S., Cvijan, M.V., 2013. Biological indication of heavy metal pollution in the areas of Donje Vlase and Cerje (southeastern Serbia) using epiphytic lichens. Arch Biol Sci, 65, 151-159.

Sundberg, B., Ekblad, A., Näsholm, T., Palmqvist, K., 1999. Lichen respiration in relation to active time, temperature, nitrogen and ergosterol concentrations. Funct Ecol, 13, 119-125.

Sundberg, B., Näsholm, T., Palmqvist, K., 2001. The effect of nitrogen on growth and key thallus components in the two tripartite lichens, *Nephroma arcticum* and *Peltigera aphthosa*. Plant Cell Environ, 24, 517-527.

Tretiach, M., Brown, D.H., 1995. Morphological and physiological differences between epilithic and epiphytic populations of the lichen *Parmelia pastillifera*. Ann Bot, 75, 627-632.

Tretiach, M., Bolognini, G., Rondi, A., 1997. Photosynthetic activity of *Quercus ilex* at the extremes of a transect between Mediterranean and submediterranean vegetation (Trieste-NE Italy). Flora, 192, 369-378.

Tretiach, M., Bertuzzi, S., Carniel, F.C., Virgilio, D., 2013. Seasonal acclimation in the epiphytic lichen *Parmelia sulcata* is influenced by change in photobiont population density. Oecologia, 173, 649-663.

Valladares, F., Wierzchos, J., Ascaso, C., 1993. Porosimetric study of the lichen family Umbilicariaceae: anatomical interpretation and implications for water storage capacity of the thallus. Am J Bot, 80, 263-272.

Valladares, F., Sancho, L.G., Ascaso, C., 1998. Water storage in the lichen family Umbilicariaceae. Plant Biol, 111, 99-107.

Wallace, J.M., Hobbs, P.V., 2006. Atmospheric science: an introductory survey. Academic Press, New York.

Williamson, B.J., Mikhailova, I., Purvis, O.W., Udachin, V., 2004. SEM-EDX analysis in the source apportionment of particulate matter on *Hypogymnia physodes* lichen transplants around the Cu smelter and former mining town of Karabash, South Urals, Russia. Sci Total Environ 322, 139–154.

Yenisoy-Karakaş, S., Tuncel, S.G., 2004. Geographic patterns of elemental deposition in the Aegean region of Turkey indicated by the lichen, *Xanthoria parietina* (L.) Th. Fr. Sci Total Environ, 329, 43-60.

Web References

Regione FVG: http://www.regione.fvg.it/rafvg/export/sites/default/RAFVG/ambiente-

territorio/allegati/DGR913ALL1.pdf

Osmer FVG: www.osmer.fvg.it

Radial growth variability in the lichen biomonitor *Xanthoria parietina*:
a field study along an altitudinal transect with data modelling

Fortuna Lorenzo, Tretiach Mauro*

Department of Life Sciences, University of Trieste,

Via L. Giorgieri 10, I-34127 Trieste, Italy

Corresponding author:

Prof. Mauro Tretiach

email: tretiach@units.it

Phone: +39 040 558 8822

Supplementary Table 1: Values of the 18 site-specific variables measured in the four sites (2, 6, 8 and 11; Fig. 1) equipped with thermo-hygrometric sensors. Below the values the frequencies of rainless days with an average daily value of RH >90%; DP <0°C; SD >2kPA and Ψ_{WV} >-14.2MPa are reported in italic bold. dfs: distance from the sea; STI: seasonal time interval; Pc: cumulative precipitation; T: temperature; RH: relative humidity; DP: dew point; SD: saturation deficit; Ψ_{wv}: air water potential.

Site	Altitude m asl	dfs m	STI	P mm	T °C min	ave	max	RH min	ave	max	DP °C min	ave	max	SD kPa min	ave	max	Ψwv Mpa min	ave	max
2	15	955	1	140	7.6	14.7	23.1	40.90 *-*	65.30 *-*	88.20 *42.9*	3.8 *28.6*	7.3 *9.5*	11.1 *-*	0.128 *-*	0.721 *-*	1.767 *42.9*	-132.34 *-*	-65.69 *-*	-16.79 *45.2*
			2	357	17.1	24.6	32.8	40.20 *-*	64.00 *-*	88.00 *35.5*	13.3 *-*	16.4 *-*	19.9 *-*	0.271 *-*	1.424 *26.3*	3.173 *94.7*	-134.44 *-*	-69.06 *-*	-17.80 *34.2*
			3	405	10.6	15.5	22.7	54.70 *1.6*	74.70 *4.8*	88.10 *53.2*	7.6 *17.7*	10.4 *6.5*	13.5 *-*	0.176 *-*	0.565 *30.6*	1.429 *53.2*	-89.85 *1.6*	-44.04 *4.8*	-18.12 *53.2*
			4	412	3.3	7.6	14.6	61.60 *3.8*	81.90 *11.5*	93.10 *71.2*	1.3 *42.3*	4.3 *23.1*	7.8 *11.5*	0.061 *-*	0.228 *-*	0.716 *1.9*	-72.67 *3.8*	-29.76 *11.5*	-9.77 *71.2*
			5	364	10.6	17.4	26.6	45.30 *-*	71.30 *-*	91.20 *65.6*	8.2 *10.9*	11.5 *1.6*	15.0 *-*	0.121 *-*	0.720 *-*	2.045 *59.4*	-113.75 *-*	-50.74 *-*	-12.56 *65.6*
6	202	957	1	163	7.5	13.5	21.7	40.70 *-*	64.00 *-*	84.30 *12.5*	2.6 *42.5*	5.9 *15.0*	9.6 *2.5*	0.170 *-*	0.675 *-*	1.643 *47.5*	-135.03 *-*	-68.05 *-*	-23.02 *15.0*
			2	364	17.2	23.3	31.1	41.50 *-*	62.70 *-*	82.40 *2.8*	12.2 *-*	14.9 *-*	18.1 *-*	0.402 *-*	1.315 *27.8*	2.860 *86.1*	-130.98 *-*	-70.68 *-*	-27.23 *2.8*
			3	413	9.9	14.0	19.8	60.40 *-*	76.30 *5.9*	87.60 *25.5*	6.8 *19.6*	9.5 *11.8*	12.5 *3.9*	0.171 *-*	0.468 *-*	1.049 *19.6*	-74.83 *-*	-39.93 *5.9*	-18.49 *25.5*
			4	454	2.8	6.4	13.0	64.70 *-*	82.90 *9.5*	92.50 *50.0*	0.6 *54.8*	3.4 *28.6*	6.8 *14.3*	0.057 *-*	0.189 *-*	0.587 *-*	-65.07 *2.4*	-27.45 *9.5*	-10.50 *54.8*
			5	333	10.4	16.1	24.2	47.20 *-*	70.90 *-*	88.60 *28.3*	7.2 *16.7*	10.2 *5.0*	13.6 *-*	0.154 *-*	0.647 *-*	1.699 *43.3*	-107.77 *-*	-50.69 *-*	-16.45 *28.3*
8	310	2121	1	168	6.5	12.8	21.3	40.60 *-*	65.40 *-*	86.60 *29.3*	2.3 *46.3*	5.5 *14.6*	8.9 *4.9*	0.134 *-*	0.630 *-*	1.628 *43.9*	-133.86 *-*	-64.53 *-*	-19.39 *29.3*
			2	409	16.3	22.9	31.0	40.30 *-*	63.20 *-*	85.60 *11.4*	11.9 *-*	14.6 *-*	17.7 *-*	0.306 *-*	1.286 *21.4*	2.876 *90.0*	-133.53 *-*	-70.02 *-*	-21.77 *11.4*
			3	420	9.1	13.7	21.7	54.50 *-*	76.40 *3.3*	89.00 *54.1*	6.4 *19.7*	9.1 *11.5*	12.2 *-*	0.147 *-*	0.481 *-*	1.426 *37.7*	-91.01 *-*	-39.94 *3.3*	-16.08 *52.5*
			4	496	2.2	5.9	12.4	65.20 *3.4*	83.60 *23.7*	93.90 *78.0*	0.5 *50.8*	3.2 *25.4*	6.5 *11.9*	0.047 *-*	0.174 *-*	0.589 *1.7*	-63.63 *5.1*	-24.52 *25.4*	-8.57 *79.7*
			5	350	9.7	15.5	22.7	48.80 *-*	71.00 *-*	88.60 *45.2*	6.6 *14.5*	9.8 *4.8*	13.2 *-*	0.164 *-*	0.623 *-*	1.492 *22.6*	-102.09 *-*	-49.75 *-*	-16.21 *45.2*
11	481	6933	1	164	6.3	11.4	17.9	45.10 *-*	64.50 *-*	83.60 *31.1*	1.1 *53.3*	4.3 *22.2*	7.7 *4.4*	0.163 *-*	0.550 *-*	1.168 *6.7*	-115.72 *-*	-63.99 *-*	-23.87 *31.1*
			2	410	15.6	21.1	27.1	48.09 *-*	65.70 *-*	83.90 *23.1*	11.0 *-*	13.8 *-*	16.8 *-*	0.334 *-*	1.041 *9.0*	2.011 *61.5*	-106.56 *-*	-62.05 *-*	-24.56 *21.8*
			3	310	8.9	12.7	18.6	58.10 *-*	74.50 *4.5*	86.60 *34.8*	5.3 *18.2*	7.9 *10.6*	10.6 *-*	0.169 *-*	0.448 *-*	1.013 *15.2*	-79.43 *-*	-42.50 *4.5*	-19.69 *33.3*
			4	447	1.5	4.9	10.6	64.50 *5.9*	81.80 *17.6*	92.70 *55.9*	-1.0 *57.4*	1.8 *30.9*	5.0 *11.8*	0.052 *-*	0.178 *-*	0.507 *-*	-63.81 *19.1*	-28.71 *30.9*	-9.98 *72.1*
			5	391	8.9	13.9	20.3	53.90 *-*	72.90 *-*	88.70 *29.2*	5.8 *21.5*	8.8 *9.2*	12.0 *-*	0.140 *-*	0.505 *-*	1.142 *4.6*	-86.85 *-*	-45.24 *-*	-16.18 *29.2*

Supplementary Table 2: Summary of the LSD's post hoc test results, which evaluate the significant differences among site-specific SRaGR average values. Sites are ordered according to their altitude, from 1 (15 m a.s.l.) to 11 (500 m a.s.l.).Values ($\mu m\ d^{-1}$) are reported as mean ± standard deviation. Different letters indicate statistical significant difference for p-value < 0.05.

Site	Spring	Summer	Autumn	Winter	Spring 2016
1	4.70 ± 2.59 [abcde]	3.44 ± 0.49 [a]	4.81 ± 0.67 [abcde]	6.07 ± 1.07 [bcdefghi]	4.40 ± 0.90 [abc]
2	6.79 ± 0.76 [defghij]	5.36 ± 1.74 [abcdefg]	6.75 ± 0.76 [defghij]	8.01 ± 1.72 [ijkl]	7.46 ± 0.62 [fghijkl]
3	5.66 ± 1.32 [bcdefgh]	5.09 ± 1.46 [abcdef]	9.37 ± 2.02 [klm]	12.17 ± 2.15 [n]	8.43 ± 1.04 [jkl]
6	6.36 ± 0.71 [bcdefghij]	3.82 ± 1.60 [ab]	5.45 ± 1.07 [abcdefghi]	9.66 ± 2.68 [klm]	5.22 ± 1.85 [abcdefghi]
8	5.09 ± 1.18 [abcde]	6.38 ± 1.93 [cdefghi]	9.06 ± 1.76 [kl]	14.82 ± 2.10 [o]	11.26 ± 3.22 [mn]
10	5.18 ± 0.58 [abcdef]	7.50 ± 1.13 [ghijk]	6.86 ± 1.02 [efghij]	8.84 ± 0.88 [jkl]	6.87 ± 1.24 [efghij]
11	5.82 ± 3.35 [abcdefghi]	4.65 ± 1.53 [abcd]	5.31 ± 1.48 [abcdefg]	9.9 ± 1.56 [lm]	7.84 ± 1.87 [hijkl]

Supplementary Table 3: Summary of the LSD's post hoc test results, which evaluate the significant differences among site-specific LtRaG average values. Sites are ordered according to their altitude, from 1 (15 m a.s.l.) to 11 (500 m a.s.l.).Values (mm) are reported as mean ± standard deviation. Different letters indicate significant statistical difference for p-value < 0.05.

Site	LTRaG$_1$	LTRaG$_2$
1	1.27 ± 0.46 [a]	1.79 ± 0.57 [ab]
2	2.58 ± 0.89 [bcd]	3.20 ± 0.70 [de]
3	3.00 ± 0.82 [cd]	3.88 ± 0.78 [ef]
6	2.54 ± 0.28 [bcd]	3.03 ± 0.80 [cde]
8	3.19 ± 0.38 [de]	4.44 ± 0.47 [f]
10	2.67 ± 0.52 [cd]	3.38 ± 0.53 [de]
11	2.16 ± 0.82 [abc]	2.86 ± 0.93 [cd]
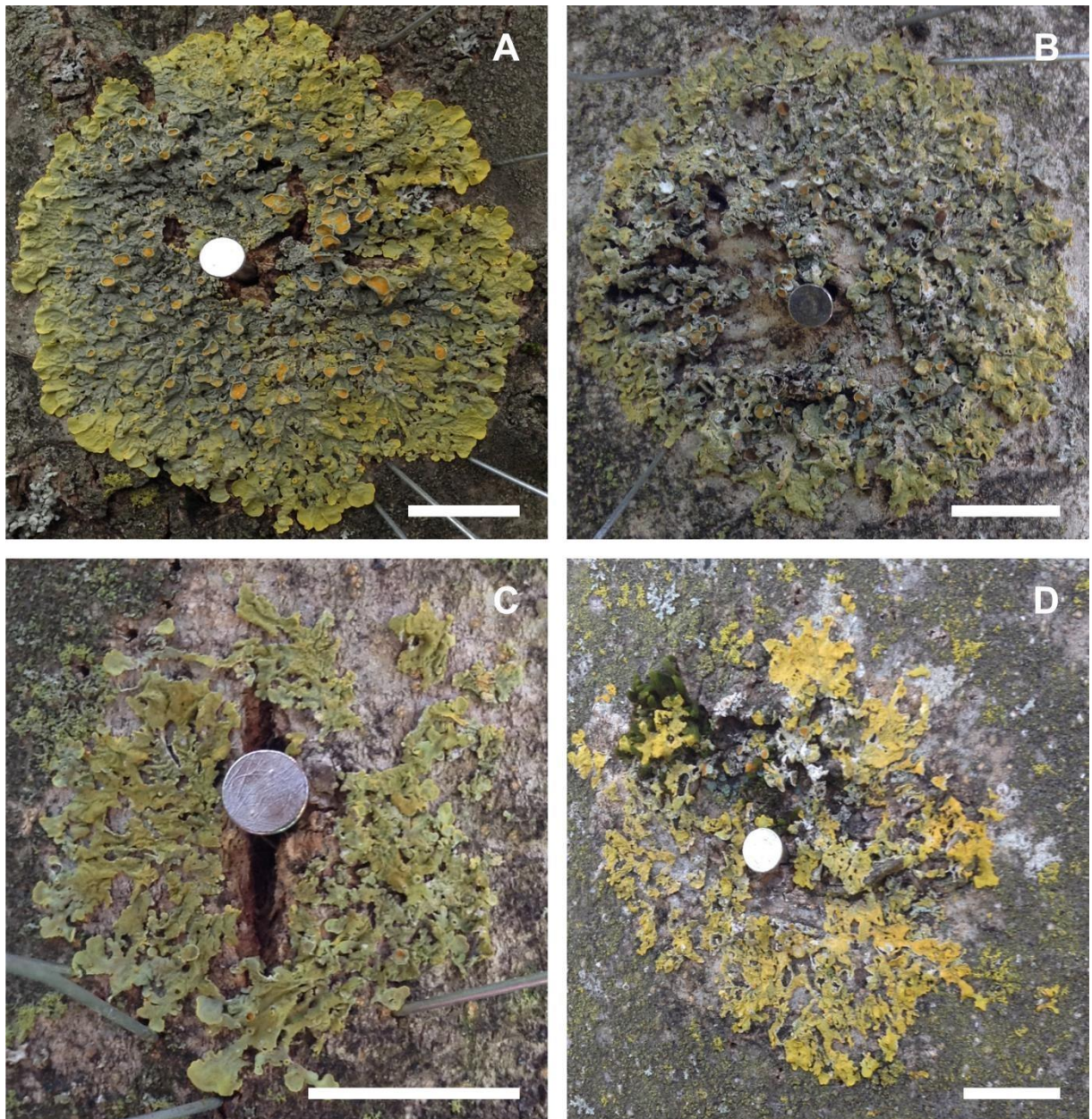
Supplementary Figure 1: An example of a healthy thallus at time t_4. Thalli at time t_2 showing thallus decolouration (B), deep cracks (C) or which have been entirely grazen (D). Bars indicate 10 mm.
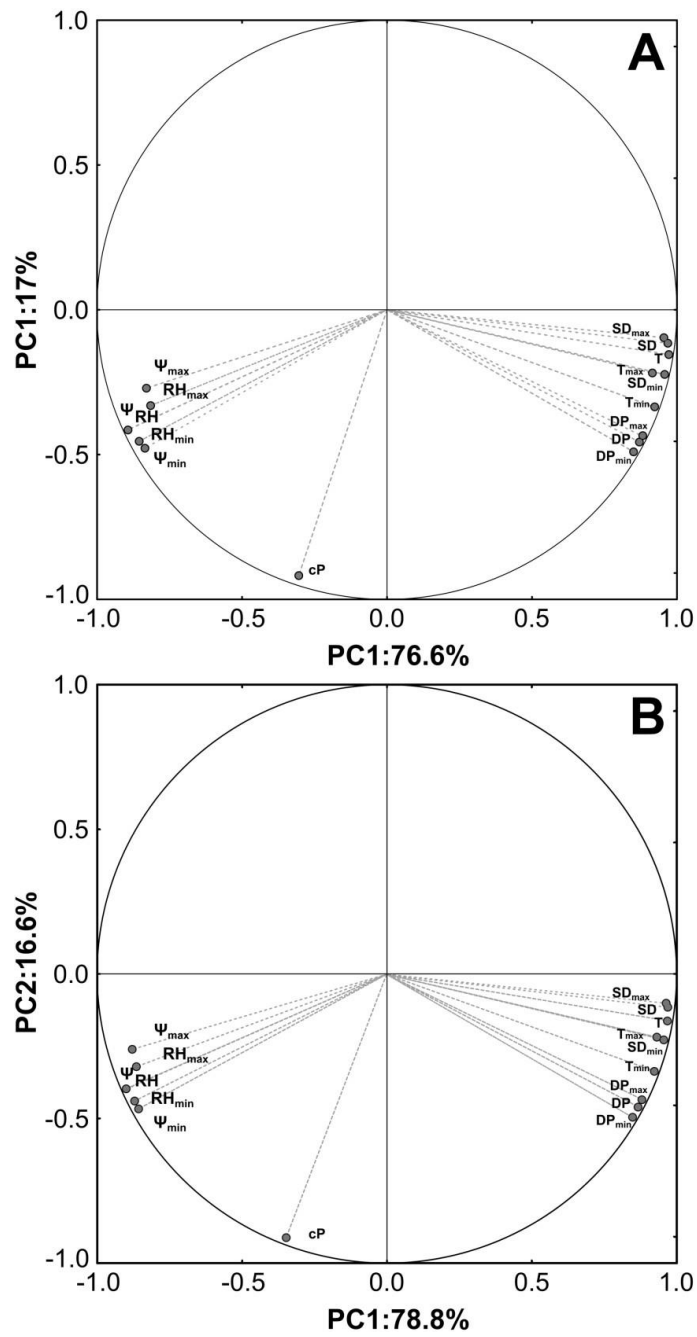
Supplementary Figure 2: projection on the factor plane of the 16 sites-climatic variable measured in the

4 sites equipped with thermo-hygrometric sensors (A) and in the 159 OGUs (B)

Lichen as point receptors for the validation of Atmospheric Dispersion Modelling (ADM):

a case study in NE Italy

Lorenzo Fortuna[1], Guido Incerti[2],

Daniele Da Re[3], Mauro Tretiach[1]*

[1]Department of Life Sciences, University of Trieste,

Via Licio Giorgieri, 10, 34127, Trieste

[2]Department of Agri-Food, Animal and Environmental Sciences (DI4A),

University of Udine, Italy

[3]Earth and Life Institute (ELI), Université catholique de Louvain (UCL),

Louvain-la-Neuve, Belgium.

Abstract

Atmospheric dispersion models (ADMs) are increasingly used as a management tool to simulate transport, transformation and deposition of air pollutants. Their reliability depends on the quality of input emission rates, meteorological fields, chemical-physical properties of air pollutants, and topography. However, the validation of ADM simulations require relatively expensive and spatially coarse ground-based observations from air pollution monitoring networks. Biomonitoring survey with lichens has been often used as an effective tool for air pollution assessment and thus it represents a less expensive alternative for ADM validation.

In this study, the results of a biomonitoring survey of airborne trace element based on two native lichens (*Flavoparmelia caperata* and *Xanthoria parietina*) were used as validation dataset for two ADM simulations of the Total Suspended Particulate (TSP) emitted by a coal-fired power plant. The two ADM simulation were respectively run for two reference time periods: the whole year 2005, selected as representative of the local average meteorological conditions (Mod 05); the six-month period preceding lichen sample collection (Mod 14) at 40 locations within a 176 km^2 area, highly heterogeneous in terms of soil types and land use classes. Results clearly showed that trace element content in lichen samples were more correlated with Mod 14 and in lesser extent with Mod 05, suggesting that the reference period is a key factor for reliable modelling of air pollution dispersion. In particular, the content of Cr in lichen samples showed a unimodal pattern along the main wind direction at increasing distance from the source. The evidence that Cr content in lichen samples was related to the plant emissions was confirmed by the results of an air particulate matter sampling carried out during both operational and non-operational state of the plant.

Key-words: biomonitoring; air pollution; lichens; model validation

Introduction

Nowadays, increasing concern is given to air pollution effects on human health (Kampa and Castanas 2008), biodiversity (Barker and Tingey 2012) and ecosystem services (Paoletti et al. 2010), especially in urban environment (Le Terte et al. 2002). The European Union has adopted restrictive air pollution regulation policies with set maximum atmospheric concentration for specific pollutants (2008/50/CE: Air Quality Directive). The compliance to air pollutant limit values is ensured by complementary regulatory instruments, which, on one side, force the industrial companies to implement the Best Available Technologies for reduce pollutant emission and, on the other, provide a co-ordinate program for air pollution monitoring and assessment, which is usually manged by local environmental protection agencies (Wolterbeek et al. 2002). Recently, the so-called atmospheric dispersion models (ADMs) have been introduced as a new regulatory instrument for air pollution control (2008/50/CE Air Quality Directive). These models simulate pollutant dispersion scenarios in a given area depending on meteorological and geomorphological input dataset, chemical-physical properties of air pollutants and the pollutant emission rates from point or non-point source pollution (Holmes and Morawska 2006). However, the validation of ADM simulations requires relatively expensive and spatially coarse ground-based observations from air pollution monitoring networks (Ham 1992). A less expensive alternative, which provides punctual measurements of air pollutant time-integrated concentrations is given by other well-known and established monitoring techniques, such as the biomonitoring surveys with lichens as biomonitor of airborne pollutants (Nimis et al. 2000; Demiray et al. 2012; Kodnik et al.2015, Augusto et al. 2007).

Lichens are a stable mutualistic symbiotic relationship between a fungus, mainly an ascomycete (the so-called mycobiont), and one or more populations of unicellular photosynthetic organisms (the so-called photobiont), such as green algae, cyanobacteria or both (Honegger 1998). Since lichens lack root and waxy cuticle, they predominantly acquired inorganic nutrients from dry and wet depositions (Van Dobben et al. 2001) making them excellent biomonitors of airborne trace elements. In fact, their element content has found to be correlated with that of site-specific bulk deposition (Sloff et al. 1995) and positively affected by the thalli age (Nimis et al. 2001). Foliose epiphytic lichens growth radially by extending their outermost part (lobes), few millimetres per year (Armstrong 2011). Consequently, the inner parts of foliose thalli have higher elemental content because they are older and were exposed for a longer time in the environment

(Loppi et al. 1997). Hence, protocols in biomonitoring with foliose lichens highly recommend that only the last millimetres from the tip of juvenile, peripheral lobes should be sample and analysed (Bargagli and Nimis 2002). In this manner, the occurrence of biased data related to lichen material with different age would be minimized (Nimis et al. 2001) and, on the parallel, the element content of lichen sample would reflect better that of the immediate past environment (Seaward 1980). This straight relationship between the elemental content and the exposure time of the lobes encourage the implementation of lichens as alternative point receptors for the validation of ADM simulations (Sloof et al. 1991). To date, several authors validate the outcomes of ADM simulation of several air pollutants (e.g. PAH, PM_{10} and trace elements) with lichen and mosses at both high (Sloof et al. 1991) and small (De Nicola et al. 2013) geographical scale. Yet, the coupled use of biomonitoring survey and ADM simulation has been seldom implemented in monitoring trace element emissions from a point source pollution (Abril et al 2014).

In this study, we used the results of a biomonitoring survey with lichens to test two Total Suspend Particulate (TSP) dispersion simulations run for two reference time periods: the whole year 2005, selected as representative of the local average meteorological conditions (Mod 05); the six-month period preceding the collection (Mod 14) of two native lichens at 40 locations within a 176 km^2 area, highly heterogeneous in terms of soil types and land use classes.

2. Material and methods

2.1. Study Area

The study area is located in the north east of Italy (45°47'47.83"N; 13°32'44.02"E) between the eastern end of Padanian floodplain and the limestone region of the Classical Karst (Fig. 1). Its surface was 176 km^2 and was defined depending on the distribution of the Total Suspended Particulate (TSP) concentrations as predicted by two ADM simulations (see section 2.5), which modelled the emissions of a coal-fired power plant (herein the source). Here, the climate is fully humid temperate with a mean yearly temperature of 13.4 °C and annual average precipitations of 1135 mm y^{-1} (Osmer FVGa). The yearly anemometric regime show a strong seasonality. During winter, cold, dry, intense ENE wind gusts are frequent, whereas in summer the SW sea breezes increase their frequencies (Osmer FVGb). Due to its peculiar geographical position, the study area was highly heterogeneous in terms of geomorphology (0-251 m asl), pedology (Fig. 1b;

Michelutti et al. 2006) and land cover classes (Fig. 1a; see Bossard et al. 2000). In the north-eastern karstic environment the main land cover classes were broad-leaved forest associations partially mixed with coniferous ones, both developed on paleosoils *Rendzic leptosols* (E soil). On the contrary, the floodplain was composed by sedimentary soils such as *Calcari-fluvic-Cambisols* (C soil) and *Gleyi-fluvic-Cambisols* (D soil) covered by urban-industrial, agricultural, and mixed land cover classes, which were respectively concentrated in the central, southern and western portions of the study area (Fig. 1a-b).

2.2. *Lichen biomonitoring survey*

The study area was divided in 44 Primary Sampling Units (PSUs) of 4 km^2 each, according to the systematic sampling design proposed by ANPA (2001). Then, in each PSU was defined 16 Secondary Sampling Units (SSUs) with an area of 0.05 km^2 each (Figure 1c). Lichen sampling was carried out between the 12th and the 14th of February 2014 following the method described by Nimis and Bargagli (1998). In each PSU, one to three lichen samples of *Flavoparmelia caperata* (L.) Hale or *Xanthoria parietina* Th. Fr. were collected by sampling the outermost part of five to ten thalli growing on straight, healthy trees placed in one or more SSUs. Lichen material was sampled using a ceramic knife and immediately stored in a sterile petri dish. The geographic location of lichen-hosting trees were measured using a mobile device (Samsung SM-J530; accuracy ±15 m). At the laboratory, lichen samples were air dried for 24 h and cleaned from bark debris and senescence or damaged portion under a stereomicroscope. Therefore, a thorough sample preparation was performed by selecting only the last marginal portion from lobe tips, i.e. 3-3.5 mm for *F. caperata* and 2-2.5 mm for *X. parietina*. Lichen material of both species were never mixed among them. Finally, samples were grinded with liquid nitrogen (20 ml) in an agate mortar, dried at 40°C overnight and stored until chemical analyses.

2.3 *Soil sampling*

Soil sampling surveys has often been coupled to biomonitoring with lichens (Bargagli et al. 1998), since the soil elemental content allow to discern whether the elemental content of lichen samples is mainly related to the effect of soil dust resuspension rather than to that of trace element airborne depositions. Therefore, in order to assess the effects of soil contribution on lichen samples, the elemental composition of the three

pedological classes (Fig. 1b) were measured by analysing two reference soil samples for each of the pedological class. In particular, reference C soil samples were collected in the PSUs B3 and D5, whereas those of D and E soils were collected in the PSUs A7 and F3, respectively. At each sampling site, four subsamples of the first 15-30 cm of soil were collected within a 10 m^2 plot, mixed among them and stored in a glass flasks of 10 L until chemical analyses.

2.4.   Chemical analysis

Both lichen and soil samples (100-250mg$_{dw}$ each) were individually mineralised in Teflon bombs with an acid solution of 7 ml of HNO_3, 3 ml of H_2O_2 and 0.2 of HF following a four-step heating program in a microwave oven (Ethos 1 – MILESTONE). The concentration of 16 (Al, As, Ba, Be, Ca, Co, Cd, Cr, Cu, Fe, Hg, Mn, Pb, Tl, V and Zn) and 15 elements (the previous elements except Ca) were respectively measured in mineralized lichen and soil samples by a mass spectrophotometer (Perkin-Elmer DRCII) following UNI EN ISO 17294-1/2007 and UNI EN ISO 17294-2/2005. The reliability of the analytical results was checked by analysing nine samples of certified reference material CRM 482 (Quevauviller et al. 1996).

2.5.   ADM simulations and airborne particulate matter sampling

The outcomes of ADM simulations (herein Mod 05 and Mod14) were provided by the local environmental protection agency (ARPA FVG) as GIS shapefile georeferenced in EPSG:3004 reference system with the following attributes: latitude, longitude and TSP concentration values expressed as $\mu g \ m^{-3}$. The outcome of the two ADM simulations represent two different source emission scenarios because they were run with different meteorological input dataset and assumed different source emission conditions. Indeed, Mod 05 simulated the average distribution of TSP concentration values over one-year period, by assuming a constant rate emission (4.8 g s^{-1}) of an inert pollutant (TSP) from the source. The meteorological input dataset used for Mod 05 was that of the year 2005, selected by the authorities as reference meteorological period for ADM simulations. On the other hand, Mod 14 assumed a variable TSP emission rate depending on the duration of both operational and non-operational state of the source during the six months preceding

lichen sampling collection (September 2013 – February 2014). The climatic data observed during lichen sample pre-collection period were used as meteorological input dataset in Mod 14 simulation.

The airborne particulate matter (PM) sampling were performed during both operational and non–operational state of the source by using four air pollution-monitoring stations over the whole year 2014. For both source operational state, the concentration of As, Cd, Cr, Cu, Fe, Mn, Ni, Pb, Sb, V and Zn were measured in PM_{10} samples. The result of this study are available on the web site of the ARPA FVG (ARPA FVG 2014).

2.6. Data analyses

Descriptive statistics were calculated to give information about the differences among element concentrations between species. Lichen sample element concentrations were compared with the naturality-alteration scale of Nimis and Bargagli (1998) to describe the degree of deviation from background conditions within the 44 PSU as total charge index (Minganti et al. 2003).

Then, the element enrichment factors (EFs) was computed as proposed by Bargagli (1998). The element concentrations of each lichen sample was standardised as a function of the elemental composition of the reference soil samples of the pdeological class occurring within the lichen sampling site. In order to evaluate whether the elemental composition of lichen samples were related to the ADM simulation outcomes, the geographic coordinates of lichen-hosting trees, predicted TSP concentration values by both ADM simulations and the spatial distribution of the three pedological classes were georeferenced in EPSG:3004 reference system using QGIS (version 2.6.). Then, both element concentrations (L dataset) and element EFs (EF dataset) of lichen samples were geographically related to the ADM simulation values at tree scale and averaged as function of lichen species and site of collection (PSU). Consequently, both L and EF datasets were submitted to a Principal Component Analyses (PCA) using the pedological soil classes and the species as supplementary variables whereas the values of ADM simulations as continuous predictors. In the PCA analysis performed on EF dataset also the Al concentration in lichen samples were used as continuous predictor. Linear correlations between TSP concentration values and L and EF dataset were analysed using Pearson's correlation coefficient (r). Finally, the trends of the enrichment factors of those elements significantly correlated with ADM simulation outcomes were analysed along two transects following TSP

concentration gradients, which occurred along the PSUs A6, B6, C6, D6, E6, F6 and G6 (transect T1) and the PSUs C8, C7, C6, D6, E6 and G6 (transect T2), respectively. Results of air matter particulate sampling will be limited used to discuss the main results of this study.

Results

Element concentrations in lichen samples

The co-occurrence of the floodplain and the karstic environment within the study area affected the species-specific distribution of *F. caperata* and *X. parietina*, pointing out their allopatric relationship. *F. caperata* occurred more frequently in the north eastern Classical Karst, whereas *X. parietina* was bound to the agricultural environment occurring in the western study area. Overall, 40 out of 44 selected PSUs were sampled by collecting 54 samples of *F. caperata* and 26 of *X. parietina*. Samples of both species were limited collected in seven PSUs (i.e. A4, B3, C3, C6, D4, D5 and G1). The descriptive statistics of elemental content of both species are summarised in Tab. 1. The element mean concentrations measured in 85% of lichen samples were close to the background values as defined by the naturality/alteration scale of Nimis and Bargalgli (1998), highlighting that, within the study area, the load of trace element emissions were relatively low. The total charge index showed relatively higher trace element contents in lichen samples from those PSU placed within or in the surroundings of urban and industrial areas (Fig 2a).

AMD simulations

The maximum TSP concentration values predicted by the two ADM simulations had different magnitude and spatial distribution within the study area. The highest yearly average TSP concentration values predicted by Mod 05 were distributed in both north eastern and south western study area (Fig. 2b) with a maximum of 0.038 µg m^{-3}. On the other hand, the maximum values predicted by Mod 14 during lichen sample pre-collection period, were higher than those of Mod 05 and were limited concentrated in the south western study area with a maximum of 0.095 µg m^{-3} (Fig. 2c). The predictions of the distribution of the TSP concentration values of both models accorded well with the anemometric data observed by respective meteorological input data sets (Supplementary Figure 1). Although both anemograms showed high

frequency of NEN and ENE winds, that relating to the six month preceding lichen collection (September 2013 – February 2014) had significant lower frequencies of WSW winds.

PCA of L dataset

The results of the PCA performed on L dataset revealed that the elements segregated in two distinct clusters (Fig. 3a) depending on the element composition of lichen species. *F. caperata* samples had on average higher Ba, Ca, Co, Pb and Zn concentrations with respect to *X. parietina* ones, whereas for Al, As, Be, Cr and Fe it is observed the opposite (Tab. 1). These two groups of elements were, respectively, negatively and positively correlated with the second principal factors of the PCA, in good accordance with the arrangement of *F. caperata* and *X. parietina* supplementary variables in Fig. 3a. Mn, Cd, Cu, Hg and Tl were little related with both first two principal components indicating that they were weakly correlated with the remaining elements. V was unrelated to the species, soils and ADM simulations but it was highly and negatively correlated with the first principal factor. The arrangement of E and C soil supplementary variables reflected the relative abundance of *F. caperata* and *X. parietina* samples collected within the karstic environment and the floodplain, respectively. On the contrary, D soil were unrelated to both species since here an equal number of *F. caperata* and *X. parietina* samples were collected (n=4; Fig. 3a). The predicted TSP concentration values of Mod 05 and Mod 14 were unrelated with the first two principal components of the PCA and to the majority of selected elements. However, the matrix correlation of Tab. 2 reports low significant Pearson's correlation coefficient ($r < 0.4$) between Mod 05 predictions and Ba, Cd, Cr and Zn concentrations in lichen samples. Nevertheless, high TSP concentration values predicted by Mod 05 were related to low concentrations of Ba, Cd, Cr and Zn as well, making these correlations weaker in comparison with that observed between Cr concentrations in lichen samples and Mod 14, especially when only *F. caperata* samples were considered (Tab. 2).

PCA of EF dataset

The EF values submitted to PCA revealed two distinct and well-defined cluster of element EFs, one of which were more related to the supplementary variables of ADM simulations and in a lesser extent with those of lichen species (Fig. 3b). The first cluster included all those elements (As, Ba, Be, Cd, Co, Cu, Fe,

Hg, Mn, Tl and Zn) whose high EF values were observed in *F. caperata* samples from karstic environment. On the other hand, the second cluster identified three elements: Cr, Pb and V, whose high EF values were observed for those lichen samples from western PSU downwind from the source (i.e. PSUs C7, C6, D6 and E6). At the same time, these three elements were highly correlated with the TSP concentration values of Mod 14 and in a lesser extent with those of Mod 05 (Tab. 2). It should be noted that also in this case, the Person's correlation coefficient increased when only *F. caperata* samples were selected to calculate the correlation between Cr, Pb and V EFs and ADM simulation values (r > 0.65).

Trends of Cr, Pb and V EFs along TSP concentrations gradient.

The multivariate analyses of Fig. 3b as well as the Person's r of Tab. 2 highlighted a strict relationship between Mod 14 outcomes and Cr, Pb and V EFs, especially when only *F. caperata* samples were considered. T1 was extended from western to eastern PSUs (i.e. A6, B6, C6, D6, E6, F6 and G6) in which samples of one or another lichen species were collected. Here, the EF values of Cr fitted well with Mod 14 outcomes (Fig. 4). On the other hand, T2 was extended across those PSUs in which only *F. caperata* samples were collected (i.e. PSUs C8, C7, C6, D6, E6 and G6). In this case, the trends of Cr EFs and Mod 14 predictions fitted even better than that observed along T1 (Fig 4).

Along both T1 and T2, the maximum values of Pb and V EFs did not coincide with the highest TSP concentrations values predicted by both ADM simulations. Nevertheless, both element EFs were more closely related to Mod 14 rather than Mod 05 (Fig 4; Tab. 2).

Discussion

The outcomes of lichen biomonitoring survey expressed as total charge index (Fig. 2a) indicated relatively high concentrations of As, Ba, Be, Co, Cr, Cu, Fe, Mn, and V in lichen samples from urban (PSUs D5 and E5) and industrial (PSUs E6 and F6) areas. These elements could be indicative of mechanical component abrasion related to vehicular traffic (Adamo et al. 2011) as well as to other industrial processes such as coal combustion (Querol et al. 1995; Xu et al. 2004), galvanization (Van Caneghem et al. 2010) and oxy-fuel welding and cutting (Topham et al. 2011). Lichen samples collected in two PSUs (D7 and G6) had the

maximum content of Al, suggesting that their elemental composition may been affected by high soil contributions (e.g. earth handling activities or soil dust resuspension).

Despite the occurrence of these point and non-point source pollutions, the distribution pattern of Cr content in lichen samples was found to be highly correlated with the emission of the coal-fired power plant. This result has been achieved by integrating the outcomes of lichen biomonitoring survey expressed as element EFs with those of an ADM simulation, i.e. Mod 14, and the results of the air matter particulate sampling, which was carried out during both operational and non-operational state of the source (see section 2.5; ARPA FVG 2014).

By computing the element EFs, the elemental composition of the three pedological classes was used as a proxy of the average elemental contribution of C, D and E soils within the respective 40 lichen sampling sites. On average, *X. parietina* had very low element EFs for most of the investigated elements and in some extent, also when it was collected together with *F. caperata* (PSUs A4, B3, C3, C6, D5, D4 and G1). This because *X. parietina* is ecologically bound to communities with strong accumulation of dust (Barkman 1958) and thus it tend to accumulate higher concentration of Al and Fe with respect to *F. caperata* (Tab. 1; see also Nimis et al. 2001). According to EF equation (Bargagli 1998), this means low element EFs, which made it difficult to discern whether or not the elemental content of lichen samples has been affected by local soil contribution rather than to an atmospheric deposition (Bergamaschi et al. 2002; Kłos et al. 2011). Then, for the purposes of this research, it was preferred to improve the statistical analysis using the element EFs of *F. caperata* samples only.

Results clearly revealed that the EFs of Cr, Pb and V in *F. caperata* samples were highly correlated with the TSP concentration values predicted by Mod 14 and in a lesser extent also with those predicted by Mod 05 (Fig. 3b; Tab. 2). The key factor in explaining this result was the time span during which the lichen material were exposed to trace element pollution before lichen sample collection, i.e. the exposure time. The annual radial growth rate of *F. caperata* is 4.78 mm y^{-1} (Fisher and proctor 1978). Therefore, according to sample preparation (see section 2.2), the element concentrations in *F. caperata* samples were measured in lichen material grew in the last 7-9 months before lichen sample collection (August 2013 – February 2014). This time span was approximately the same of the meteorological input dataset used for run Mod 14 (September 2013 – February 2014), whereas it differed from that selected for Mod 05 (yearly

meteorological reference period (see section 2.5). The fact that both Mod 14 simulation and the exposure time of *F. caperata* samples were referred to the same period, it made possible to use the Cr, Pb and V EFs of *F. caperata* samples as point receptor values for the validation of Mod 14 simulation along two TSP concentrations gradients.

Nevertheless, consideration should be given to the fact that up until the lichen sample collection, the source was equipped with the best devices for the abatement of particulate emissions such as an electrostatic precipitator (ESP) and a wet scrubber flue gas desulphurization (FGD) system. Despite the high efficiency (>99.9%), the ESP system is not able in removing particle with a size included between 0.5–1.5 µm, whereas the FGD system may actually increase As, Cd, Pb and Zn concentrations downstream to the particulate abatement systems (Vejahati et al. 2010). Overall, the load of particulate emissions related to the source activity can be considered as negligible, because it stayed within the limit defined by Italian regulation concerning the environmental pollution prevention (ARPA FVG 2014). Yet, the distribution pattern of Cr, Pb and V EFs in *F. caperata* samples accorded well with the TSP concentration gradients as predicted by Mod 14, especially along the PSUs downwind from the source, i.e. the transect T1 and T2 (Fig. 4).

Therefore, it can be possible to assume that ESP and FGD system could not entrap a part of particulate emission from the source, especially the finest one. On the other hand, further consideration has to be given to the fact that lichen sample collection was carried out during wet season (fall-winter 2014), when the performance of Cr, Pb and V accumulation of lichens could be enhanced by prolonged wet periods (Adamo et al. 2003). This could explain why, although the low load of particulate emission, relatively high Cr, Pb and V EFs in lichen samples where highly correlated with the TSP concentration values predicted by Mod 14 along T1 and T2. Along T1, the trends of Cr, Pb and V EFs were based on lichen samples of both species. As previously discussed, the coupled used of two biomonitor species could provide contrasting results in terms of element EF magnitude. This was true for Pb and in a much lesser extent for V and Cr (Fig. 4). Along T2, where only *F. caperata* samples were collected, the trends of Cr EF fitted even better with the predictions of Mod 14. On the contrary, as far as is concerned for Pb and V, their maximum EFs did not coincide with the maximum TSP concentration values predicted by Mod14. This suggest that other source pollution such as a fastener factory and a shipyard (both occurring next to the source) could interfered with

Pb and V atmospheric contribution along T1 and T2. This could be true for V, since it is also indicative of shipyard activity (Moldanovà et al. 2009) and commercial shipping (Viana et al. 2009).

A final important remark is given to the results of the air particulate matter sampling carried out during both operational and non-operational state of the source (ARPA FVG 2014). In that study was showed that Cr concentration in atmospheric PM_{10} significantly increase when the coal burning groups were active, whereas those of Pb and V did not vary between operational and non-operational state of the source (ARPA FVG 2014). Although the authors interpreted the increasing Cr concentration as an instrumental anomaly, on the other hand, it should be taken into account that the same result supports the highly significant correlation observed between the EF of Cr in *F. caperata* samples and the TSP concentration values of Mod 14. Therefore, further studies should be carried out in order to investigate deeply the relationship between Cr content in lichen samples and the trace element emissions within the study area.

In conclusion, for the first time the outcomes of a biomonitoring survey with native lichens were related to the activity of a point source pollution even though this was in large, environmentally complex area characterised by a low diffuse pollution due to other urban and industrial activities. This result was achieved by coupling the outcomes of biomonitoring survey with those of an ADM simulation and the results of an air particulate matter sampling. Moreover, it was demonstrated that the exposure time of lichen material and the time span considered in meteorological input dataset of ADM simulations are key factors when lichen biomonitors are employed as point receptor for ADM validation.
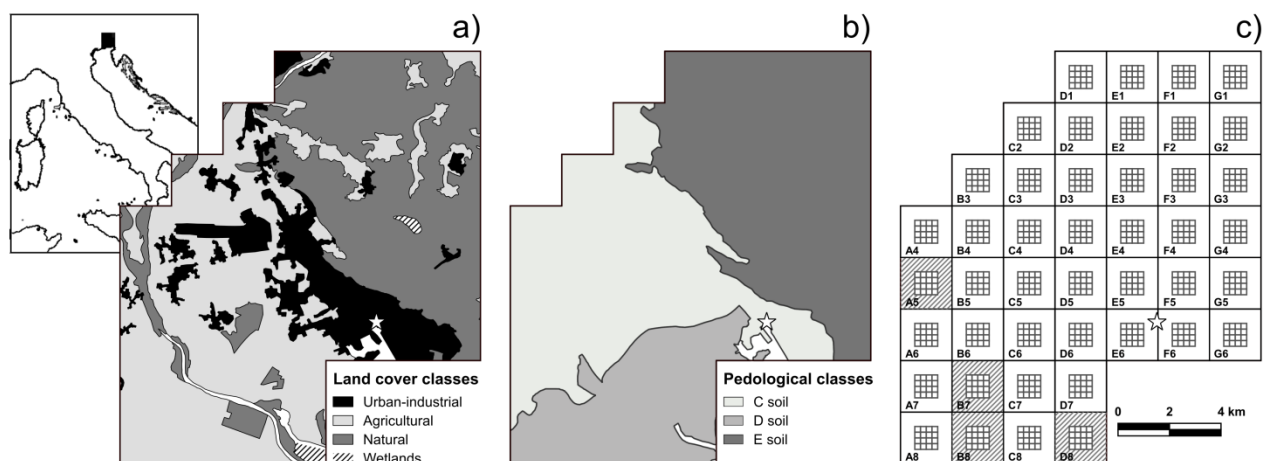
Fig. 1: The upper left insert depicted the geographical location of the study area. a) and b) show the distribution of land cover and soil pedological classes within the study area, respectively. c): study area divided in 44 primary sampling units (PSUs) according to ANPA 2001. In c), dashed PSUs (A5, B7, B8 and D8) were not sampled during lichen biomonitoring survey.
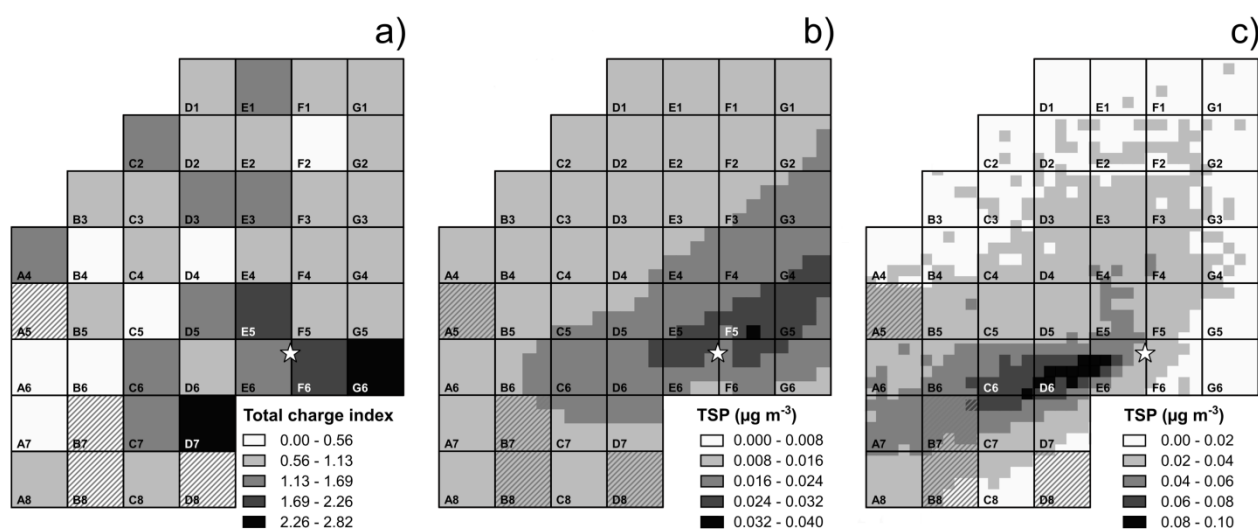

Fig. 2: a) Total charge index calculated for each PSU as proposed by Nimis et al. 1999. b) and c): distribution of TSP concentration values as predicted by Mod 05 (yearly reference period) and Mod 14 (lichen sampling pre-collection period), respectively.
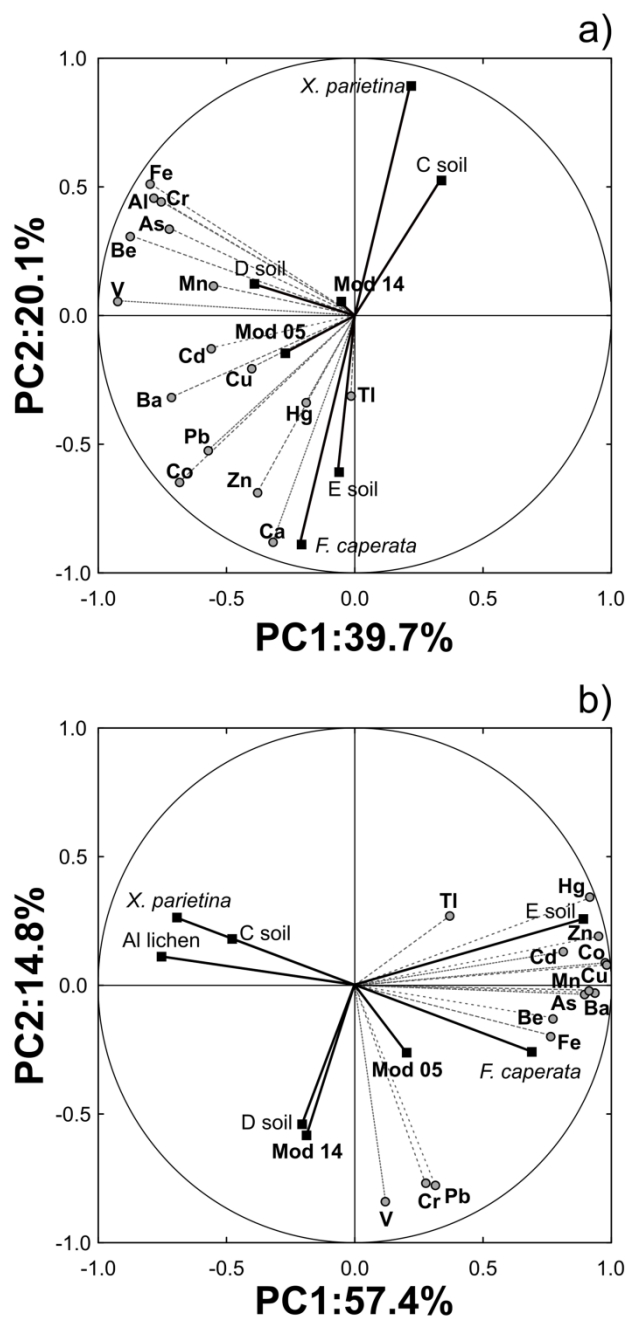
Fig. 3: a) and b): results of the PCA performed on L and EF dataset, respectively. Grey dashed vectors represent variables as element concentration in a) and element EFs in b). Black vectors represent supplementary variables such as species, pedological classes (C, D and E soil) or continuous predictors: Mod 05 and Mod14: TSP concentration values predicted for yearly reference conditions or for the lichen sampling pre-collection period, respectively; Al lichen: Al concentration in lichen samples.
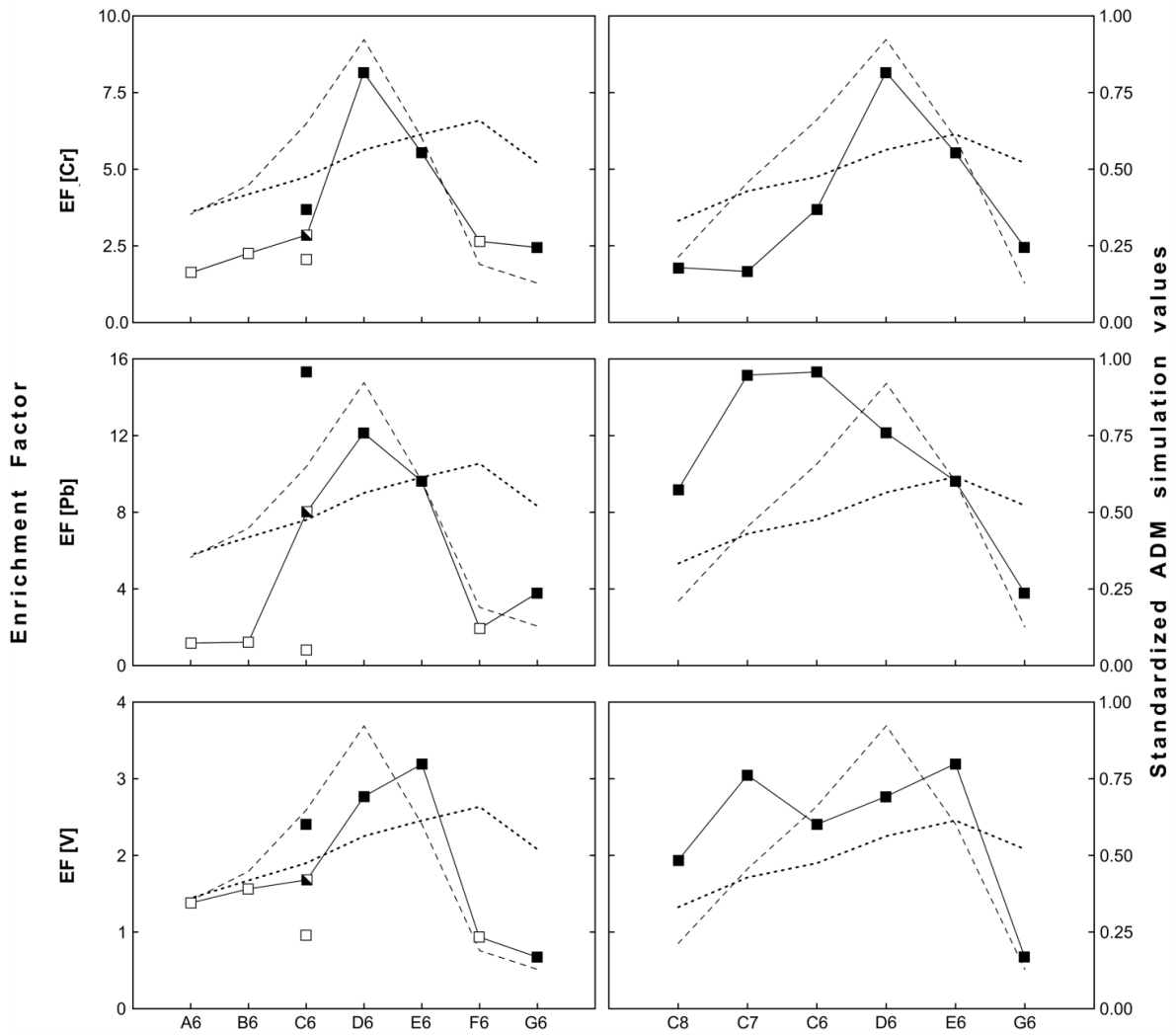
Fig. 4: trends of Cr, Pb and V EFs along two TSP concentration gradients occurring across PSUs A6, B6, C6, D6 ,E6, F6, G6 (left panels; transect T1) and C8, C7, C6, D6, E6, G6 (right panels; transect T2). Note that along T1, element EFs of one or another species were considered: Filled squares: *F. caperata*; empty squares *X. parietina*; half-filled squares: average values between *F. caperata* and *X. parietina* element EFs. Dashed and dotted lines represent respectively the TSP concentrations values as predicted by Mod 14 and Mod 05. Note that predicted values of both ADM simulations were reported as standardized values included between 0 and 1.

TABLES

Tab. 1: Descriptive statistics of element concentrations (mg kg^{-1}) measured in *F. caperata* and *X. parietina* samples collected in 40 out of the 44 selected PSUs. Min and Max: minimum and maximum values, respectively; SD: standard deviation; CV: coefficient of variation expressed as percentage

	Al	As	Ba	Be	Ca	Cd	Co	Cr	Cu	Fe	Hg	Mn	Pb	Tl	V	Zn
F.caperata																
Min	110	0.14	1.5	0.002	7200	0.11	0.16	0.36	4.9	94	0	8.3	0.98	0.030	0.34	22
Max	1600	0.67	13.0	0.027	37000	0.67	0.75	5.80	9.9	1100	0.200	26	11.0	0.180	3.70	80
Mean	303	0.27	4.9	0.008	20707	0.24	0.31	1.27	6.7	232	0.073	16	2.7	0.016	1.25	44
Median	255	0.24	4.4	0.007	21000	0.21	0.30	0.89	6.4	195	0.068	15	2.3	0.007	1.10	41
SD	218	0.11	2.5	0.005	6584	0.12	0.10	1.05	1.2	155	0.033	5	1.9	0.027	0.63	13
CV	71.9	40.5	50.1	55.4	31.8	49.3	32.7	82.8	17.8	66.9	45.7	28.3	71.2	169.0	50.8	30.9
X. parietina																
Min	150	0.12	1.6	0.003	520	0.04	0.04	0.69	3.2	140	0	9.2	0.36	0.004	0.51	13
Max	1300	1.00	6.8	0.029	1400	0.75	0.37	5.10	15.0	1600	0.290	37	2.6	0.019	4.10	56
Mean	453	0.28	3.3	0.009	866	0.14	0.11	1.64	5.6	360	0.047	16	0.9	0.008	1.05	23
Median	380	0.25	2.9	0.008	850	0.09	0.10	1.45	4.6	285	0.038	15	0.7	0.006	0.90	21
SD	234	0.20	1.4	0.005	218	0.17	0.07	0.92	2.7	287	0.053	6	0.5	0.004	0.70	10
CV	51.7	70.6	41.1	55.8	25.2	120.3	62.8	55.9	47.6	79.9	114.6	38.3	59.1	48.6	66.2	42.2

Tab. 2: Pearson's correlation coefficient (r) calculated among TSP concentration values of both Mod 05 and Mod 14 simulations and the element concentrations (L dataset) or element EFs (EF dataset) by considering lichen samples of both species (F+X) or solely those of *Flavoparmelia caperata* (F) or *Xanthoria parietina* (X). Significant correlation for p-value <0.05 are reported in bold. - : not calculated.

	Al	As	Ba	Be	Ca	Cd	Co	Cr	Cu	Fe	Hg	Mn	Pb	Tl	V	Zn
L dataset																
F + X																
Mod 05	0.06	0.16	**0.34**	0.13	0.16	**0.31**	0.19	**0.30**	0.12	0.16	-0.01	0.00	0.22	0.02	0.23	**0.39**
Mod 14	-0.11	0.10	0.07	-0.01	-0.02	0.15	-0.01	**0.30**	-0.07	0.00	0.05	-0.10	0.01	-0.05	0.16	-0.09
F																
Mod 05	0.14	**0.44**	0.36	0.26	-0.08	**0.37**	0.08	**0.42**	0.13	0.24	-0.02	-0.03	0.14	-0.03	0.29	0.35
Mod 14	-0.13	0.36	0.18	0.06	0.01	0.03	0.08	**0.54**	0.00	0.07	0.15	0.00	0.09	-0.04	0.30	-0.10
X																
Mod 05	0.12	0.01	0.03	-0.03	-0.03	0.22	0.00	0.24	0.07	0.31	-0.17	0.05	0.12	-0.01	0.10	0.37
Mod 14	-0.12	-0.15	-0.30	-0.13	**-0.56**	0.39	-0.16	-0.23	-0.16	-0.08	-0.07	-0.28	-0.44	-0.16	-0.06	-0.08
EF dataset																
F + X																
Mod 05	-	0.21	0.21	0.16	-	**0.30**	0.12	0.28	0.09	0.27	0.17	0.05	0.23	0.03	0.27	0.22
Mod 14	-	-0.16	-0.08	-0.10	-	-0.07	-0.25	**0.38**	**-0.30**	-0.15	-0.28	-0.24	**0.39**	0.00	**0.57**	-0.22
F																
Mod 05	-	0.18	0.15	0.16	-	0.24	-0.03	**0.38**	-0.03	0.12	0.08	-0.06	0.16	0.00	0.25	0.14
Mod 14	-	-0.20	-0.06	-0.08	-	-0.15	-0.35	**0.65**	**-0.37**	-0.15	-0.36	-0.28	**0.64**	0.00	**0.67**	-0.30
X																
Mod 05	-	-0.03	-0.13	-0.33	-	0.27	-0.20	0.01	-0.08	0.40	-0.21	-0.10	0.01	-0.15	0.10	0.08
Mod 14	-	-0.08	-0.26	-0.17	-	**0.63**	-0.32	-0.28	-0.23	-0.16	-0.14	-0.23	-0.33	0.22	0.35	-0.10

Reference

Abril GA, Wannaz ED, Mateos AC, Pignata ML (2014) Biomonitoring of airborne particulate matter emitted from a cement plant and comparison with dispersion modelling results. Atmos Environ, 82:154-163.

Adamo P, Giordano S, Vingiani S, Cobianchi RC, Violante P (2003) Trace element accumulation by moss and lichen exposed in bags in the city of Naples (Italy). Environ Pollut, 122:91-103.

Adamo P, Giordano S, Sforza A, Bargagli R (2011) Implementation of airborne trace element monitoring with devitalised transplants of *Hypnum cupressiforme* Hedw.: assessment of temporal trends and element contribution by vehicular traffic in Naples city. Environ Pollut, 159:1620-1628.

ANPA (2001) I.B.L. Indice di Biodiversità Lichenica: Manuale. ANPA, Agenzia Nazionale per la Protezione dell'Ambiente, Roma.

Armstrong RA, Bradwell T, (2011) Growth of foliose lichens: a review. Symbiosis, 53:1-16.

Augusto S, Pereira MJ, Soares A, Branquinho C (2007) The contribution of environmental biomonitoring with lichens to assess human exposure to dioxins. Int J Hyg Envir Heal, 210:433-438.

Bargagli R (1998) Trace Elements in Terrestrial Plants. An ecophysiological approach to biomonitoring and biorecovery. Springer, Berlin.

Bargagli R, Nimis PL, (2002) Guidelines for the use of epiphytic lichens as biomonitors of atmospheric deposition of trace elements. In: Nimis PL, Scheidegger C, Wolseley PA (eds.), Monitoring with Lichens – Monitoring Lichens. NATO Science Series, IV. Earth and Environmental Sciences, Vol. 7. Kluwer, Dordrecht, pp. 295-299.

Bergamaschi L, Rizzio E, Valcuvia MG, Verza G, Profumo A, Gallorini M (2002) Determination of trace elements and evaluation of their enrichment factors in Himalayan lichens. Environ Pollut, 120:137-144.

Barker JR, Tingey DT (2012) Air pollution effects on biodiversity. Springer Science & Business Media, New York.

Barkman JJ (1958). Phytosociology and ecology of cryptogamic epiphytes. Assen, Van Gorcum

Bossard M, Feranec J, Otahel J. (2000) CORINE land cover technical guide: Addendum 2000. Technical report 40. European Environment Agency, Copenhagen.

De Nicola F, Murena F, Costagliola MA, Alfani A, Baldantoni D, Prati MV, Giordano S (2013) A multi-approach monitoring of particulate matter, metals and PAHs in an urban street canyon. Environ Sci Pollut R, 20:4969-4979.

Domínguez-Morueco N, Augusto S, Trabalón L, Pocurull E, Borrull F, Schuhmacher M, Domingo JL, Nadal M (2017) Monitoring PAHs in the petrochemical area of Tarragona County, Spain: comparing passive air samplers with lichen transplants. Environ Sci Pollut R, 24:11890-11900

Fisher PJ, Proctor MCF (1978) Observations on a season's growth in *Parmelia caperata* and *P. sulcata* in South Devon. Lichenologist, 10:81-89.

Ham J (1992) Discussion about the national model for dispersion of air pollution. Lucht 9:84-85.

Honegger R (1998) The lichen symbiosis—what is so spectacular about it? Lichenologist, 30:193-212.

Holmes NS, Morawska L (2006) A review of dispersion modelling and its application to the dispersion of particles: an overview of different dispersion models available. Atmos Environ, 40:5902-5928.

Kampa M, Castanas E (2008) Human health effects of air pollution. Environ Pollut, 151:362-367.

Kłos A, Rajfur M, Wacławek M (2011) Application of enrichment factor (EF) to the interpretation of results from the biomonitoring studies. Ecol. Chem. Eng. S, 18:171-183.

Kodnik D, Carniel FC, Licen S, Tolloi A, Barbieri P, Tretiach M (2015) Seasonal variations of PAHs content and distribution patterns in a mixed land use area: A case study in NE Italy with the transplanted lichen *Pseudevernia furfuracea*. Atmos Environ, 113:255-263.

Le Tertre A, Medina S, Samoli E, Forsberg B, Michelozzi P, Boumghar A, Sunyer J (2002) Short-term effects of particulate air pollution on cardiovascular diseases in eight European cities. J Epidemiol Commun H, 56:773-779.

Loppi S, Nelli L, Ancora S, Bargagli R (1997) Accumulation of trace elements in the peripheral and central parts of a foliose lichen thallus. Bryologist, 100:251-253.

Michelutti G, Barbieri S, Bianco D, Zanolla S, Casagrande G (2006) Suoli e paesaggi del Friuli Venezia Giulia-2. Province di Gorizia e Trieste. Note illustrative. Agenzia regionale per lo sviluppo rurale-Servizio della sperimentazione agraria-Ufficio del suolo, Udine.

Minganti V, Capelli R, Drava G, De Pellegrini R, Brunialti G, Giordani P, Modenesi P (2003) Biomonitoring of trace metals by different species of lichens (*Parmelia*) in north-west Italy. J Atmos Chem, 45:219-229.

Moldanová J, Fridell E, Popovicheva O, Demirdjian B, Tishkova V, Faccinetto A, Focsa C (2009) Characterisation of particulate matter and gaseous emissions from a large ship diesel engine. Atmos Environ, 43:2632-2641.

Nimis PL, Bargagli R, (1998) Linee-guida per l'utilizzo di licheni epifiti come bioaccumulatori di metalli in traccia. In: atti del workshop: Biomonitoraggio della qualità dell'aria sul territorio nazionale, Roma, pp. 26-27.

Nimis PL, Lazzarin G, Lazzarin A, Skert N (2000) Biomonitoring of trace elements with lichens in Veneto (NE Italy). Sci Total Environ, 255:97-111.

Nimis PL, Andreussi S, Pittao E (2001) The performance of two lichen species as bioaccumulators of trace metals. Sci Total Environ, 275:43-51.

Paoletti E, Schaub M, Matyssek R, Wieser G, Augustaitis A, Bastrup-Birk AM, Serengil Y (2010) Advances of air pollution science: from forest decline to multiple-stress effects on forest ecosystem services. Environ Pollut, 158:1986-1989.

Querol X, Fernández-Turiel J, López-Soler A (1995) Trace elements in coal and their behaviour during combustion in a large power station. Fuel, 74:331-343.

Quevauviller P, Herzig R, Muntau H (1996) Certified reference material of lichen (CRM 482) for the quality control of trace element biomonitoring. Sci Total Environ, 187:143-152.

Seaward MRD (1980) The use and abuse of heavy metal bioassays of lichens from environmental monitoring. In: Spaleny J (ed.) Proceedings Third International Conference Bioindicatores Deteriorisationis Regionis. Akademia, Praha, pp. 375-384.

Sloof JE, Wolterbeek HT (1991) National trace-element air pollution monitoring survey using epiphytic lichens. Lichenologist, 23:139-165.

Sloof JE, (1995) Lichens as quantitative biomonitors for atmospheric trace-element deposition, using transplants. Atmos Environ, 29:11-20.

Topham N, Wang J, Kalivoda M, Huang J, Yu KM, Hsu YM, Paulson K (2011) Control of Cr^{6+} emissions from gas metal arc welding using a silica precursor as a shielding gas additive. Ann Occup Hyg, 56:233-241.

Van Caneghem J, Block C, Cramm P, Mortier R, Vandecasteele C (2010) Improving eco-efficiency in the steel industry: the ArcelorMittal Gent case. J Clean Prod, 18:807-814.

Van Dobben HF, Wolterbeek HT, Wamelink GWW, Ter Braak CJF (2001) Relationship between epiphytic lichens, trace elements and gaseous atmospheric pollutants. Environ Pollut, 112:163-169.

Viana M, Amato F, Alastuey A, Querol X, Moreno T, Dos Santos SG, Fernández-Patier R (2009) Chemical tracers of particulate emissions from commercial shipping. Environ Sci Technol, 43:7472-7477.

Vejahati F, Xu Z, Gupta R (2010) Trace elements in coal: Associations with coal and minerals and their behavior during coal utilization–A review. Fuel, 89:904-911.

Wolterbeek B (2002) Biomonitoring of trace element air pollution: principles, possibilities and perspectives. Environ Pollut, 120:11-21.

Xu M, Yan R, Zheng C, Qiao Y, Han J, Sheng C (2004) Status of trace element emission in a coal combustion process: a review. Fuel Process Technol, 85:215-237.

Web reference

Osmer FVGa http://www.meteo.fvg.it/clima/clima_fvg/schede/T/CLIMA-FVG-VIAVAS_SCHEDA18_T-Costa.pdf

Osmer FVGb http://www.meteo.fvg.it/clima/clima_fvg/schede/V/CLIMA-FVG-VIAVAS_SCHEDA24_V-Costa_Laguna_e_Monfalcone.pdf
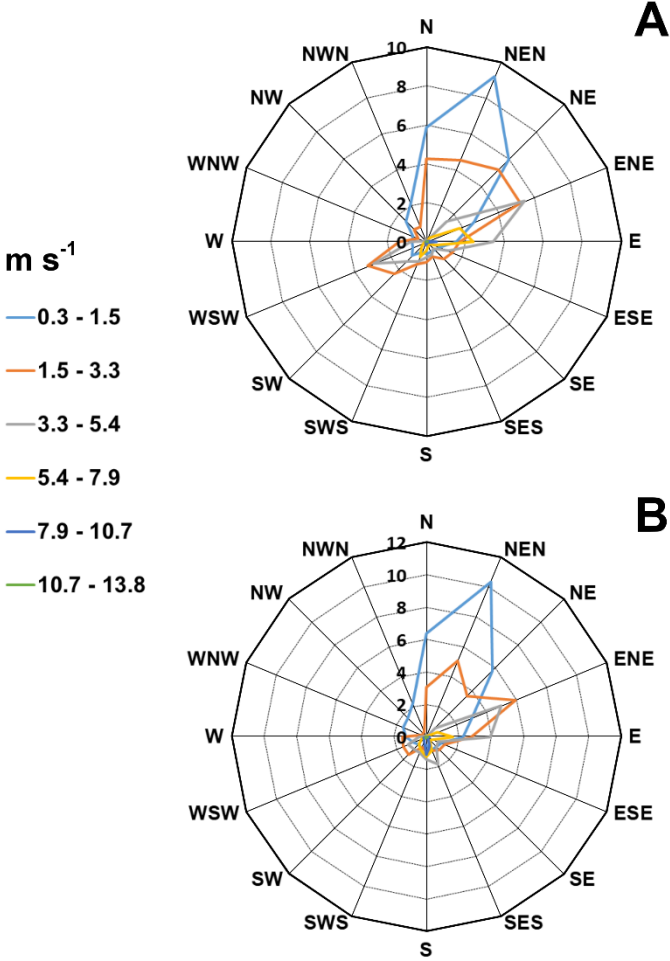
Supplementary Figure 1: Frequency of wind speed (m s^{-1}) and wind direction observed during the reference meteorological periods used as input dataset in Mod 05 (A) and Mod 14 (B) simulations. Lines with different colours correspond to different wind speed classes as reported in legend.

Melanization affects the content of selected elements in parmelioid lichens

Lorenzo Fortuna [1], Elena Baracchini [2],

Gianpiero Adami [2], Mauro Tretiach [1,*]

[1] *Department of Life Sciences, University of Trieste,*

Via L. Giorgieri 10, I-34127 Trieste, Italy

[2] *Department of Chemical and Pharmaceutical Sciences, University of Trieste*

Via L. Giorgieri 1, I-34127 Trieste, Italy

e-mail: tretiach@units.it

Phone: +39 040 558 8822

Abstract Lichens belonging to Parmeliaceae are highly diversified, but most of them share an extremely conserved morpho-chemical trait: the lower cortex is heavily melanized. The adaptive value of this character is still uncertain. Melanins are ubiquitous compounds found in most organisms since they fulfil several biological functions including defense against UV radiation, oxidizing agents, microbial stress, and metal complexation. This work aims to establish whether melanization can affect the elemental content of lichen thalli. The relative abundance of macro- (Ca, K and S) and micro- (Fe, Mn and Zn) nutrients in melanized and non-melanized pseudotissues of nine species was first evaluated by a non-destructive micro-X-ray fluorescence elemental analysis on either the upper and lower cortex, and on the internal medulla, which was artificially exposed to the mechanical removal of the lower cortex. Afterwards, the total concentration of the same elements was measured in composite samples by inductively coupled plasma atomic emission spectroscopy after acidic digestion. In order to verify whether Fe and Zn are chemically bound to the melanized pseudotissues, a sequential elution experiment was performed on two species: the two-side heavily melanized *Melanelixia glabratula* and the one-side lightly melanized *Punctelia subrudecta*. The content of Fe and Zn was higher in the melanized species than in the non-melanized ones. Species deprived of their melanized lower cortex showed a sharp decrease in Fe but not in Zn, suggesting that the melanized lower cortex is involved in Fe complexation, whereas Zn is homogeneously distributed throughout the thallus.

Key Words Bioaccumulation, fungi, melanins, homeostasis, iron, zinc.

Introduction

Lichens are a stable, extracellular symbiosis between a fungus, mostly an ascomycete (the so-called mycobiont), and one or more populations of algae and/or cyanobacteria (the so-called photobionts). Since lichens lack roots and waxy cuticle, they acquire inorganic nutrients from dry and wet atmospheric depositions (Williamson et al. 2004). Selective processes led mycobionts to evolve a multi-stratified thallus, which is dorsiventral in foliose lichens, with distinct upper and lower cortices (Nash 2008): the upper cortex ensures a favourable, variable light radiance to the photobiont (Honegger 1993), whereas the lower cortex provides the attachment to the substratum. Lichen-forming ascomycetes biosynthesize in their cortices a wide spectrum of secondary metabolites of different chemical nature (Huneck and Yoshimura 1996). This varied range of secondary metabolites provides antiherbivore defense (Asplund and Gauslaa 2008; Benesperi and Tretiach 2004), protection against excess light (Gauslaa and McEvoy 2005; Solhaug and Gauslaa 1996), and/or contribute to macro- and micronutrients uptake (Hauck and Huneck 2007). The capability of certain lichen substances in over-accumulating inorganic nutrients could significantly contribute even to ecosystem functioning by providing to other organisms the needed micro-nutrient supply (Knops et al. 1996).

Most of the foliose macrolichens belonging to a highly evolved and diversified group, e.g. the family Parmeliaceae, share a common, highly conserved phenotypic trait: a well-developed lower cortex which is brown to black due to the heavy deposition of melanin-like pigments on the mycobiont cell wall (Rikkinen 1995). This trait is often present in other taxonomic groups as well, e.g. in Physciaceae and Peltigerales, but in this case species with a highly melanized lower cortex are closely related to a white, non-melanized lower cortex. The adaptive value of the melanization of the lower cortex is still unclear.

Melanins are found in most organisms of all biological kingdoms and can fulfil different functions; from the most obvious and well-known, i.e. UV-screening (Mafole et al. 2017; Matee et al. 2016; Solhaug et al. 2003), to defense against oxidising agents (Eisenman and Casadevall 2012) and biochemical threats (Pilas et al. 1988). Melanogenesis in non-lichenised ascomycetes has been related to the polyketide synthase (PKS) genes, which control the intracellular biosynthesis of the melanin monomer, 1,8-dihydroxynaphtalene (DHN) (Bell & Wheeler 1986; Muggia and Grube 2010). Opanowicz et al. (2005) detected the PKS1 paralog in both Parmeliaceae and non-lichenized ascomycetes, pointing out that some

genera of Parmeliaceae form a sister clade with non-lichenized genera. The authors cautiously argued that PKS1 paralog could be involved in the production of DHN-derived melanin also in Parmeliaceae.

In non-lichenized ascomycetes, melanin monomers are extruded within the cell wall or in the extracellular medium, where their polymerization may be promoted by oxidase enzymes (Butler and Day 1998). Alternatively, polymerization is triggered by an increase in the pH, which allows autoxidation of monomers. Some authors refer to these melanins as "heterogeneous melanin" or "fungal humic acids" (Schnitzer and Neyroud 1975), since their structure is a mixture of phenols and amino acids, carbohydrates, proteins and lipids, all of which can be partially derived from other organisms (e.g. plants, bacteria, other non-lichenized fungi). Hence, fungal DHN-derived melanin structure contains a plurality of functional groups and chemical moieties (quinone, hydroquinone and semiquinone moieties), which provide many potential binding sites for metal ions (Fogarty and Tobin 1996). Whilst saprotrophic fungal DHN-derived melanins were widely studied as Cd^{2+}, Cu^{2+} and Zn^{2+} adsorbants (Fomina and Gadd 2003; Gadd and Rome 1988;), only a few studies have been focused on melanins of lichenized fungi (McLean et al. 1998; Purvis et al. 2004). Considering that (*i*) the melanized lower cortex is a highly conserved character, (*ii*) the lower cortex is not exposed to direct sun radiation, (*iii*) several metals show high chemical affinity for fungal melanins, and (*iv*) lichen-forming fungi have to provide inorganic nutrients to their photobionts in order to get the organic carbon they need (Clark et al. 2001; Palmqvist 2000), it is plausible to suppose that the melanization process of the lower cortex might be involved in the mineral uptake of lichen thalli. This hypothesis is tested here based on a thorough investigation of the relative abundance of macro- (Ca, K and S) and micro- (Fe, Mn and Zn) nutrients in melanized and non-melanized pseudotissues of nine lichens, which have been characterized by energy dispersive micro-X-ray fluorescence (ED-µXRF) and inductively coupled plasma atomic emission spectroscopy (ICP-AES), and thanks to a sequential elution experiment performed on two species with high vs. low degree of melanization.

Methods and material

Sample Collection and Preparation

Thalli of nine foliose lichens (Table 1) were collected with a ceramic knife in four sampling sites of the Classical Karst plateau (Trieste, NE Italy). The thalli were immediately transported to the laboratory and left to rehydrate overnight by equilibration above distilled H_2O [close to 100% relative humidity (RH)] inside sealed plastic jars, at 20 °C, and then each thallus was carefully removed from the substratum under a stereomicroscope using wooden toothpicks and plastic tweezers. Debris, possibly present and dead bryophytes or damaged portions of the thalli were carefully removed. The cleaned samples were left to dry out in a protected environment in dim light.

Table 1: List of species, subdivided between Parmeliaceae and Teloschistales, ordered according to the degree of melanisation of their thallus layers.

Taxon[#]	Degree of melanisation	Species	U	M		L	Datasets
Parmeliaceae							
	Two-side melanised						
		Melanelixia glabratula	++	-		++	B
		Xanthoparmelia loxodes	++	-	nd	++	A
	One-side heavily melanised						
		Flavoparmelia caperata	-	-		++	B
		Hypogymnia physodes	-	-		++	B
		Punctelia borreri	-	-		++	B
	One-side lightly melanised						
		Punctelia subrudecta	-	-		+	B
Teloschistales							
	One-side heavily melanised						
		Physconia distorta	-	-	nd	++	A
	One-side lightly melanised						
		Physconia grisea	-	-	nd	+	A
	Non-melanised						
		Xantoria parietina	-	-	nd	-	A

U, Upper cortex; M, Medulla; L, Lower cortex. Species are referred to datasets a, b depending on which thalline surface was analysed by ED-µXRF. A: Analysis limited to external thalline layers (U, L); B: Analysis performed on internal and external thalline layers (U, M, L), Parmeliaceae species only. ++: Heavily melanized; +: Lightly melanized; −: Non-melanized; nd: Not analysed

[#]Nomenclature according to Nimis (2016)

ED-µXRF Analyses

In order to evaluate the relative abundance of macro- and micro-nutrients in melanised and non-melanised thalline cortical surfaces, non-destructive ED-µXRF analysis was performed on nine lobes (i.e. the outermost, lobate part of a foliose thallus) of each species (Table 1). The measurements were directly taken on the upper surface of 3 lobes (herein, the U samples), on the lower surface of further 3 lobes (herein, the L samples), and, in five species (*F. caperata, H. physodes, M. glabratula, P. borreri and P. subrudecta*), on the internal aerenchymatic layer, the so-called medulla, of the last 3 lobes (herein, the M samples), which had been subjected to the mechanical removal of the lower cortex with a ceramic blade precision cutter under a stereomicroscope (for examples, see Online Resource 1). In order to flatten the surfaces, all the lobes were humidified for 24 hours before dehydration between two layers of filter paper (APTACA, Canelli, Italy) under a load of about 1 kg. ED-µXRF measurements were conducted on a single focal spot of 1.2×0.1 mm^2 on each lobe using an ARTAX 200 micro-X-ray fluorescence spectrometer (Bruker Nano GmbH, Karlsruhe, Germany). The instrument was set up with the following test parameters: X-ray tube, Mo target U= 50 kV, I= 700 µA, acquisition time: 120 s (live time), collimator: 650 µm (air environment). The examined elements were: Ca (line: Kα1 3.6923 keV), K (line: Kα1 3.3138 keV), Fe (line: Kα1 6.4052 keV), Mn (line: Kα1 5.9003 keV), S (line: Kα1 2.3095 keV) and Zn (line: Kα1 8.6372 keV). The ED-µXRF spectra (n=78) were processed with ARTAX ® software to calculate by integration the area of elemental peaks (Ap) and that of the spectrum included between 2 and 10 keV (At). The relative abundance of Ca, K, Fe, Mn, S and Zn detected in each sample was then expressed as a percentage ratio between Ap and At.

In order to verify if a moiety of the investigated elements was associated to the soluble fraction, nine samples of *F. caperata* were prepared as described before, after washing them separately four times for 20, 15, 10 and 5 min respectively in 10 ml of distilled water.

ICP-AES Analyses.

Total elemental compositions were assessed by ICP-AES with a PerkinElmer Optima 8000 equipped with autosampler S10 in composite samples of the single species respectively formed by the intact lobes (U plus L samples: herein, the U+L samples) and the lower-cortex-deprived M samples (herein, the M' samples). This material was digested in polypropylene flasks containing 1 mL HNO_3 69% (Trace Select, Fluka

Analytical), 100µL H₂O₂ 30% (Trace Select, Sigma Aldrich) and 25 µL HF 48% (Trace Select, Sigma Aldrich) following a three-step heating program in "bain-marie" up to 70° C in a digestion block (PerkinElmer SPB 100-12). After mineralization, 100 µL of 6% boric acid solution (Trace Select, Sigma Aldrich) was added and then the solutions were diluted to a final volume of 10 mL with MilliQ water.

Element concentrations were measured using a calibration curve, obtained by dilution of Ca, K, Fe, Mn and Zn standard solutions (SPECTRASCAN ®, Teknolab) for ICP-AES analyses. The limit of detection (LOD) at the operative wavelength for each element was: 0.050 mg/L for Ca at 317.933 nm and K at 766.490 nm, 0.030 mg/L for Fe at 238.204 nm, 0.020 mg/L for Mn at 257.610 nm and Zn at 206.200 nm. The repeatability of the measurements as relative standard deviation (RSD%) was always lower than 5%.

Sequential Elution Technique (SET)

In order to evaluate whether Fe and Zn are bound to the melanized hyphae, a SET experiment was carried out on two species: the two-side heavily melanized *M. glabratula* and the one-side lightly melanized *P. subrudecta*, selected for their uniform cell wall chemistry (Blanco et al. 2004; Krog 1982; Smith et al. 2009). SET protocols call for the use of a well-defined chemical compound to extract the extracellular fraction of a specific element. Several studies provide detailed information regarding Zn extraction by NiCl, EDTA or Na₂-EDTA whereas Fe extraction was discussed in fewer studies, based on the use of EDTA or Na₂-EDTA (Pérez-Llamazares et al. 2011). Since EDTA can cause the efflux of intracellular elements by cell membrane damage, in this work the less reactive Na₂-EDTA was chosen as extractant for both Fe and Zn.

Five samples (about 100 mg dry mass each) of *M. glabratula* and *P. subrudecta*, taken from the same thalli analysed by ED-µXRF and ICP-AES, were processed. After selection, the material was stored at 98% RH (as above) to re-establish the permeability membrane integrity (Buck and Brown 1979) and treated following Branquinho and Brown (1994) with the modifications proposed by Pérez-Llamazares et al. (2011). The intercellular fraction was removed by shaking the samples twice in 10 mL of double distilled water for 30 and 40 min, respectively. Afterwards, the samples were shaken in 10 mL of 20 mM Na₂-EDTA (Sigma Aldrich) for 40 min, then the solution was replaced and the samples were incubated at room temperature for 30 min. The two Na₂-EDTA solutions were combined for analysis to obtain the elemental

content of the extracellular fraction. The intracellular fractions were extracted by shaking the samples in 10 mL of 1 M HNO_3 (Carlo Erba) for 2 h at about. 15 °C. The samples were then dried at 45 °C for 36 h and weighed to calculate the mass of the cell walls.

In order to evaluate the residual fraction, the samples were digested with a mixture of 2.63 mL of 69% HNO_3, 380 µL of 30% H_2O_2 and 75 µL of 48% HF in Teflon pressure vessels by means of a microwave-assisted digestion system (Multiwave PRO, Anton Paar) following a heating program in accordance with the standard procedure EPA-3052. After mineralization, 380 µL of 6% boric acid solution was added and the solutions were heated again and diluted to a final volume of 15 mL with MilliQ water. After each treatment, about 10 mL of the elution was sampled, filtered with a 0.45 µm pre-filter (GHP Acrodisc, Pall Corporation) and analyzed by ICP-AES to measure the concentration of K, Fe and Zn. Five untreated samples of both species were ground in an agate mortar with 20 mL of liquid nitrogen and then mineralized as described above. The total concentrations of K, Fe and Zn measured in these samples were compared with the sum of the four fractions.

Statistical Analyses

The ED-µXRF data were organized in two datasets, namely A and B, the former comprised of the nine species analysed at the cortical level, and the latter including only the five species that could also be analysed at the medullary level (see Table 1). Dataset A was implemented to compare the differences in terms of elemental relative abundance between upper and lower cortex (i.e. U and L samples) with the *Mann-Whitney U test for unpaired samples.* Dataset B was submitted to *Principal Component Analysis* (PCA) in order to investigate specific relations among groups of elements, external and internal layers (i.e. U, L and M samples), and degree of melanization. Furthermore, the specific relations among the abundance of the elements were evaluated by Pearson's *r* for each thalline layer, and *one-way ANOVA* and *LSD's post-hoc* test were used to evaluate the statistical differences in terms of relative abundance of elements among thalline layers.

The ED-µXRF data of Parmeliaceae (see Table 1) were correlated to the respective ICP-AES data. For example, the U and L samples were coupled with the respective U+L samples, and the M samples were

coupled with the respective M' samples. These comparisons were repeated using the average value of each thalline surface as well as the average value obtained from all the measurements.

The element concentrations measured in the SET experiment were compared by *factorial ANOVA* considering species and fractions as categorical factors. The statistical differences among the fractions of each species and between the same fraction of the two species were evaluated by *LSD's post-hoc* test.

Results

ED-µXRF Analyses.

In all the species the relative abundance of Ca, K and Fe (Table 2) was on average one to two order of magnitude higher than that of Mn, S and Zn. The species belonging to the Parmeliaceae showed on average a lower abundance of K and Zn than those belonging to the order Teloschistales (*Xanthoria parietina* at first, then *Ph. grisea* and *Ph. distorta*). On the other hand, the spectra of Parmeliaceae were characterised by a Ca peak corresponding up to 85% of the whole spectrum area. Therefore, the relative abundance of other elements was highly and negatively correlated with that of Ca (Table 3). Despite this, the PCA based on dataset B reveals a clear relationship among groups of elements, thalline surfaces and degree of melanization (Figure 1): K and S were strictly associated with the upper cortex, Ca with the medulla and Fe with the melanized lower cortex; conversely, Mn and Zn were associated with both the upper and the lower cortex. The outcomes of *one-way ANOVAs* analyses (Table 2; *F-statistic* are reported in Online Resource 2) show that on average the upper cortex of all the species contained more K, Mn and S than the other thalline surfaces. In particular, the U samples of *F. caperata*, *P. subrudecta* and *M. glabratula* were characterised by a significant high relative abundance of K and S, K, and Mn and S, respectively. All species showed an enrichment of Ca

in M samples; these samples were statistically different from U samples of *F. caperata* and *P. subrudecta*. On the contrary, Zn did not differ among the U, M and L samples of all these species. When melanised, the lower surfaces and – to a lesser extent – the upper ones contained Fe for the most part (Figure 2). In fact, the removal of the melanised lower cortex caused a sharp decrease of Fe, as confirmed by the statistical differences between the M and L samples of *F. caperata*, *H. physodes* and *P. subrudecta* (Table 2).

Table 2: Average relative abundances of Ca, Fe, K, Mn, S and Zn measured by ED-µXRF on the thalline layers of U, M and L samples

Taxon	Sample	Ca	Fe	K	Mn	S	Zn
Parmeliaceae							
M. glabratula							
	U	0.618±0.012	0.048±0.042	0.141±0.044	0.008±0.002 *b*	0.015±0.004 *b*	0.021±0.003
	M	0.685±0.064	0.039±0.022	0.092±0.030	0.005±0.001 *a*	0.010±0.003 *ab*	0.020±0.006
	L	0.646±0.051	0.093±0.039	0.087±0.015	0.005±0.002 *a*	0.007±0.001 *a*	0.021±0.004
X. loxodes							
	U	0.636±0.110	0.147±0.097 *	0.045±0.009	0.002±0.0005 *	0.003±0.001	0.013±0.004
	M	nd	nd	nd	nd	nd	nd
	L	0.749±0.012 *	0.070±0.011	0.032±0.007	0.002±0.0002	0.002±0.001	0.008±0.003
F. caperata							
	U	0.725±0.011 *a*	0.021±0.008 *ab*	0.108±0.004 *c*	0.003±0.001	0.006±0.001 *b*	0.009±0.002
	M	0.779±0.026 *b*	0.006±0.004 *a*	0.075±0.021 *b*	0.002±0.001	0.005±0.002 *b*	0.008±0.004
	L	0.783±0.022 *b*	0.041±0.016 *b*	0.035±0.007 *a*	0.003±0.002	0.002±0.0004 *a*	0.005±0.002
F. caperata (w)							
	U	0.583±0.137 *a*	0.021±0.011 *ab*	0.231±0.111 *b*	0.006±0.001 *c*	0.015±0.007 *b*	0.020±0.014
	M	0.766±0.043 *b*	0.007±0.001 *a*	0.071±0.022 *a*	0.002±0.001 *a*	0.007±0.004 *ab*	0.014±0.005
	L	0.756±0.019 *b*	0.044±0.011 *b*	0.051±0.011 *a*	0.003±0.0002 *b*	0.004±0.001 *a*	0.011±0.002
H. physodes							
	U	0.675±0.097	0.046±0.008 *ab*	0.090±0.065	0.006±0.003	0.008±0.007	0.021±0.010
	M	0.817±0.022	0.009±0.001 *a*	0.029±0.018	0.003±0.002	0.002±0.001	0.009±0.004
	L	0.534±0.242	0.229±0.159 *b*	0.060±0.059	0.005±0.002	0.005±0.005	0.020±0.019
P. borreri							
	U	0.676±0.019	0.044±0.022	0.124±0.010	0.004±0.001	0.007±0.001	0.009±0.003
	M	0.736±0.059	0.015±0.008	0.108±0.045	0.002±0.002	0.009±0.006	0.005±0.003
	L	0.691±0.096	0.057±0.039	0.099±0.044	0.004±0.003	0.005±0.003	0.006±0.003
P. subrudecta							
	U	0.697±0.084 *a*	0.019±0.005 *b*	0.121±0.061 *b*	0.006±0.002	0.004±0.004	0.005±0.002
	M	0.841±0.003 *b*	0.003±0.002 *a*	0.026±0.004 *a*	0.003±0.0002	0.001±0.0002	0.003±0.0003
	L	0.770±0.034 *ab*	0.020±0.009 *b*	0.061±0.027 *ab*	0.005±0.004	0.002±0.001	0.004±0.002
Teloschistales							
Ph. distorta							
	U	0.645±0.180	0.033±0.027	0.140±0.111	0.003±0.003	0.004±0.004	0.043±0.034
	M	nd	nd	nd	nd	nd	nd
	L	0.526±0.093	0.122±0.146	0.161±0.080	0.007±0.004	0.005±0.001	0.035±0.013
Ph. grisea							
	U	0.733±0.013 *	0.037±0.010	0.091±0.021	0.002±0.001	0.003±0.001	0.010±0.004
	M	nd	nd	nd	nd	nd	nd
	L	0.458±0.113	0.122±0.030 *	0.224±0.074 *	0.004±0.003	0.009±0.005 *	0.029±0.009 *
X. parietina							
	U	0.204±0.014	0.085±0.067	0.438±0.067	0.010±0.004	0.080±0.010	0.025±0.008
	M	nd	nd	nd	nd	nd	nd
	L	0.227±0.034	0.108±0.056	0.372±0.022	0.014±0.001	0.075±0.022	0.037±0.009

Species ordered as in Table 1. nd, Not analyzed; W, Water-washed

Different letters indicate significant differences as calculated by *one-way ANOVA* and *LSD*'s post-hoc tests ($P < 0.05$) for the species B of Table 1 (*F* values are reported in Online Resource 2). *: significant differences ($P < 0.05$) between U and L samples as calculated by *Mann-Whitney* U test for the species A of Table 1. Values are reported as mean ± standard deviation; n = 3

The washing of *F. caperata* samples in distilled water did not affect the intra-thalline element distribution (Table 2).

Table 3 Pearson's correlation coefficients (R) calculated among relative abundances of elements measured by ED-µXRF in each thalline layer (U, M and L samples) for the species B of Table 1

		Ca	K	Fe	S	Mn	Zn
U							
	Ca						
	K	-0.814***					
	Fe	-0.150	-0.407				
	S	-0.850***	0.849***	-0.220			
	Mn	-0.561*	0.416	-0.103	0.670**		
	Zn	-0.819***	0.563*	0.216	0.809***	0.558*	
M							
	Ca						
	K	-0.873***					
	Fe	-0.837***	0.537*				
	S	-0.929***	0.917***	0.630**			
	Mn	-0.571*	0.341	0.661**	0.457		
	Zn	-0.693**	0.353	0.704**	0.562*	0.543*	
L							
	Ca						
	K	-0.600**					
	Fe	-0.939***	0.297				
	S	-0.697**	0.817***	0.471**			
	Mn	-0.548**	0.538**	0.426	0.327		
	Zn	-0.824***	0.525*	0.727**	0.788***	0.372	

Levels of significance: *** for $P \leq 0.001$; ** for $0.001 < P \leq 0.01$; * for $0.01 < P \leq 0.05$

The comparisons made by *Mann-Whitney U test for unpaired samples* between U and L samples of those species whose medulla could not be analyzed (dataset B, see Table 1) revealed a significantly higher relative abundance of Ca in the upper surface of *Ph. distorta* and in the lower surface of *X. loxodes*. The upper melanized surface of *X. loxodes* was significantly enriched with both Fe and Mn whereas the lower melanized surface of *Ph. grisea* was significantly enriched with K, Fe, S and Zn (Table 2).
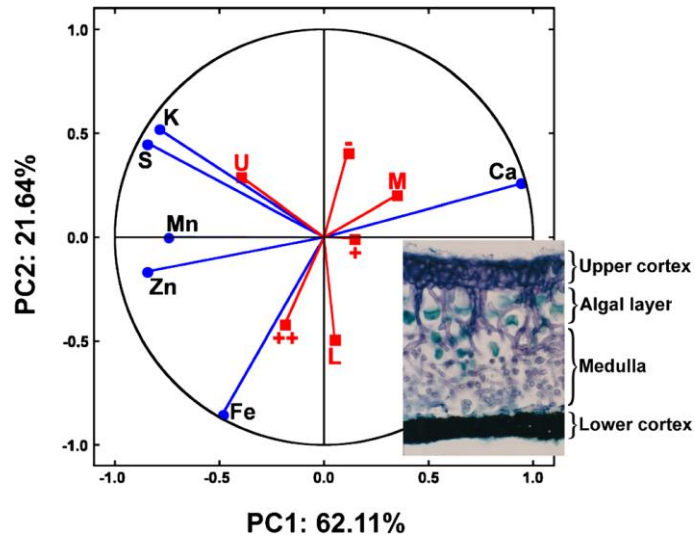
Fig. 1 The projection of the variables on the factor-plane for the relative abundance of Ca, K, Fe, Mn, S and Zn measured by ED-µXRF in U, M and L samples of species B in Table 1. The thalline surfaces and their degree of melanization (see Table 1) were treated as supplementary variables. U: upper cortex; M: medulla; L: lower cortex. ++: heavily melanised surfaces; +: lightly melanized surfaces; −: non-melanised surfaces. The frame on the right shows a transversal section of a thallus of *Punctelia borreri* after staining with Toluidine blue O 0.05% in acetate buffer pH 4.4 as a metachromatic stain.
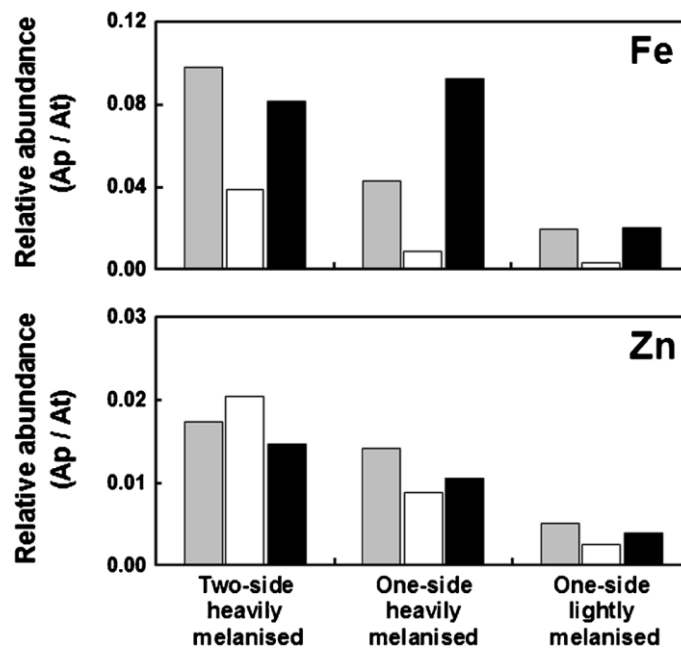
Fig. 2 The average of Fe and Zn relative abundances (upper and lower panel, respectively) measured by ED-µXRF in U (grey bars), M (white bars), L (black bars) samples of two-side and one-side heavily melanized and one-side lightly melanized Parmeliaceae species. The vertical axis reports the ratio between the area of element peak (Ap) and that of the ED-µXRF spectrum between 2 and 10 keV (At). See Table 1 for species description

ICP-AES Analyses and Reliability of ED-µXRF Measurements

The quantitative ICP-AES analyses showed that Fe and Zn were the highest in the Parmeliaceae species classified as two-side heavily melanized and one-side heavily melanized whereas the lowest concentrations were observed in the one-side lightly melanized species (Figure 3). The samples U+L and M' had similar concentrations of Ca, K, Mn and Zn, except for Fe, as the removal of the lower cortex heavily affected the concentration of this element (Table 4).
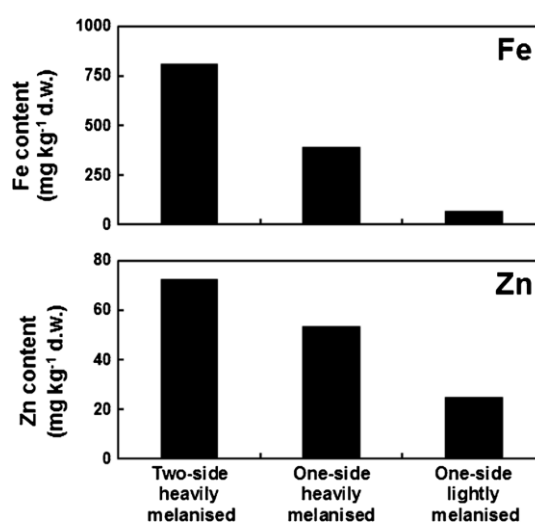
Fig. 3 The average concentrations of Fe and Zn (upper and lower panel, respectively) measured by ICP-AES in U + L samples of two-side and one-side heavily melanized and one-side lightly melanized Parmeliaceae species. See Table 1 for species description

The elemental composition measured in U+L samples of Parmeliaceae and Teloschistales differ significantly, because on average the former had higher contents of Ca, Fe, Mn and Zn. Based on these results, the comparison between ICP-AES and ED-µXRF data were restricted to Parmaliaceae only (Table 5). The total concentrations of K and Mn measured in U+L and M' samples by ICP-AES were not correlated with their respective ED-µXRF measurements or with the average values. As far as Ca is concerned, only the ED-µXRF measurements performed on the medulla were significantly correlated with total concentrations measured in the same samples (M'; $P < 0.01$). On the contrary, the total concentrations of Zn measured in U+L and M' samples were highly correlated with the respective ED-µXRF data (Table 5). As for Fe the correlations between ED-µXRF and ICP-AES data were significant

Tab. 4: Total concentration (mg/kg) of Ca, K, Fe, Mn and Zn measured by ICP-AES on composite samples of intact lobes (U + L) and lower-cortexdeprived lobes (M')

Taxon	Ca U+L	Ca M'	K U+L	K M'	Fe U+L	Fe M'	Mn U+L	Mn M'	Zn U+L	Zn M'
Parmeliaceae										
M. glabratula	16442	21059	3105	2925	409.8	151.2	21.2	20.0	64.0	72.3
X. loxodes	59566	nd	4634	nd	1212.2	nd	34.1	nd	79.6	nd
F. caperata	30605	23563	4732	5082	306.5	11.6	15.3	15.0	40.4	44.5
F. caperata (w)	30234	23083	4955	3839	322.6	< LOD	16.6	11.3	65.7	70.2
H. physodes	34436	32110	3373	2981	687.5	114.5	24.8	19.8	69.1	73.8
P. borreri	22157	28840	4552	4336	244.4	63.9	17.5	13.0	32.2	25.7
P. subrudecta	23204	46803	4292	4335	183.0	65.9	37.4	42.0	29.1	24.7
Teloschistales										
Ph. distorta	25999	nd	6209	nd	152.5	nd	12.9	nd	76.5	nd
Ph. grisea	9733	nd	5688	nd	222.9	nd	12.6	nd	30.3	nd
X. parietina	2371	nd	3772	nd	183.0	nd	8.9	nd	36.9	nd

Species are ordered as in Table 1. nd Not analyzed; W, Water-washed; LOD, Limit of detection

for both U vs U+L samples and for M vs M' samples (Table 5). Although the L samples had on average a high relative abundance of Fe with respect to both U and M samples, the correlation between L and U+L samples was significant only when the data of *X. loxodes* were excluded. In fact, Fe relative abundance evaluated by ED-µXRF on the lower surface of *X. loxodes* was highly underestimated in comparison to the total Fe concentration measured by ICP-AES (Figure 4).

Tab. 5: Pearson's r calculated between ED-µXRF and ICP-AES data of Parmeliaceae species

	Single values a	Single values b	Single values c	Average for each surface d	Average for each surface e	Average for each surface f	Average of U, M and L samples g	Average of U, M and L samples h
Ca	-0.061	0.641**	0.101	-0.111	0.772°	0.143	0.206	0.518
Fe	0.712***	0.610**	0.300	0.972***	0.729	0.386	0.947**	0.686
K	0.193	0.116	-0.308	0.255	0.142	-0.451	0.286	-0.039
Mn	-0.065	0.187	0.070	-0.084	0.242	0.113	0.449	0.424
Zn	0.560**	0.702**	0.440*	0.787*	0.808°	0.599	0.920**	0.925**

Levels of significance: *** for $P \leq 0.001$; ** for $0.001 < P \leq 0.01$; * for $0.01 < P \leq 0.05$; ° for $0.05 < P \leq 0.1$
a: U VS U + L samples; b: M VS M' samples; c: LVS U + L samples; d: average values of U vs U + L samples; e: average values of M samples VS M'; f: average of L samples vs U + L; g: average of U, L and M samples vs U + L samples; h: average of U, L and M samples vs M' samples
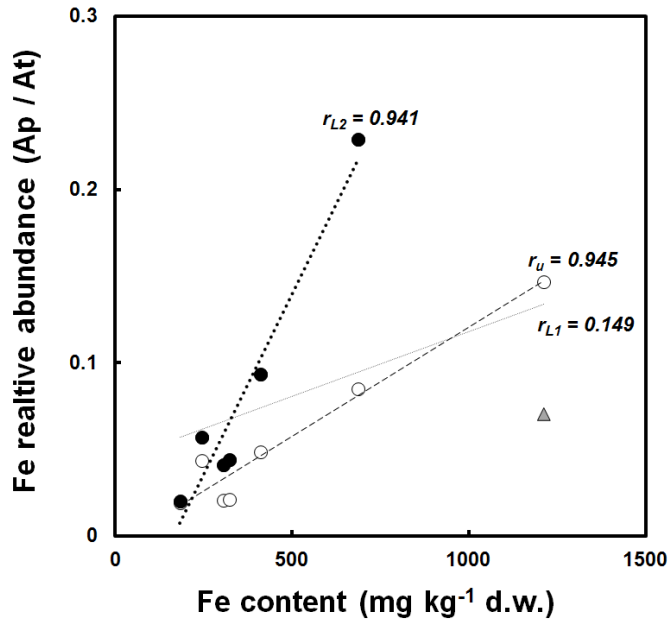
Fig. 4: The correlations among Fe content measured by ICP-AES in U + L samples and average Fe relative abundance detected by ED-µXRF in U (white dots) and L (black dots plus grey triangle) samples of Parmeliaceae species. rL1, rL2 and rU: Person's r respectively calculated for L samples, L samples excluding *X. loxodes* samples (grey triangle) and U samples

Sequential Elution Technique (SET)

The K, Fe and Zn content measured in the intercellular, extracellular, intracellular and residual fraction of *M. glabratula* and *P. subrudecta* are given as average values in Figure 5. The trends of the concentrations of Fe and Zn measured in the four fractions were similar in both species showing an intercellular content of Fe and Zn lower than their limit of detection. The highest contents of Fe and Zn were respectively observed in the residual and intracellular fraction of both species. In the mutual comparison, the highly two-side heavily melanised *M. glabratula* contained more Fe and Zn than the one-side lightly melanized *P. subrudecta.*
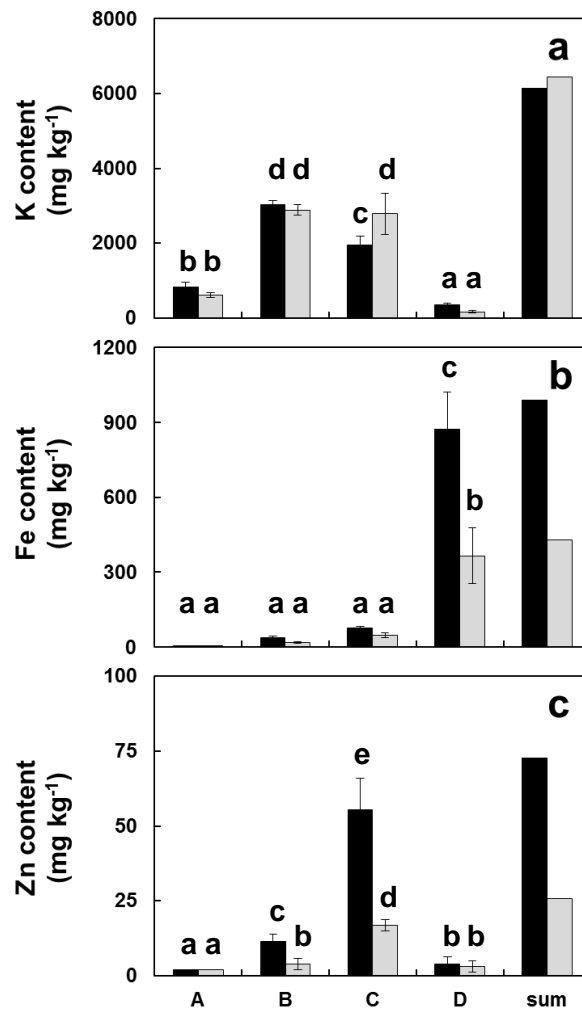
Fig. 5 The average concentrations of K, Fe and Zn (upper, middle and lower panel, respectively) measured in the intercellular (A), extracellular (B), intracellular (C) and residual fraction (D) of *Melanelixia glabratula* (black bars) and *Punctelia subrudecta* (grey bars) samples. Sum: sum of the 4 fractions. Different letters refer to statistical differences among fractions of both species for each element (*LSD*'s Fisher post-hoc; $P < 0.05$), n = 5.

Discussion

Richardson et al. (1995) and Aslan et al. (2006) have already employed X-ray fluorescence techniques with the aim of estimating the elemental composition of lichens, but in those studies the samples were manipulated as fine powders or pellets. Whilst the pulverization of lichen material ensures high accuracy, it does not allow to discern possible differences in the elemental content of thalline layers. In order to verify the accuracy of our ED-µXRF analyses on intact thalline surfaces, we selected a set of elements (Ca, K, Mn and S) that have well known intrathalline distribution patterns. K, Mn and S are concentrated in the upper cortex and in the algal layer, mostly in the intracellular fraction (Godinho et al. 2009, Paul et al. 2003). Although the relative abundance of both K and Mn was higher in U samples than in the other thalline layers,

it was not related to the total concentrations measured by ICP-AES on composite samples (i.e. U+L and M' samples; see Table 5). The lack of congruence between the two analytical techniques suggests that ED-μXRF data acquired from intact lobes cannot be used in the estimation of the total concentration of K and Mn. Nevertheless, comparing the *one-way ANOVAs* results (Table 2) with those of the SET experiment (Figure 5), also considering the significant correlation with S (Table 3), our ED-μXRF data confirm that both elements are mainly stored in the upper portion of lichen thalli, in accordance with the results of the above-mentioned studies.

Data on Ca can be used to verify the ED-μXRF data, because many lichens form Ca-oxalates deposits in the medulla, in the upper cortex or both, up to 6% of their dry mass (Giordani et al. 2003). In our case, Ca contents measured by ED-μXRF and ICP-AES on the same samples of Parmeliaceae were significantly correlated ($P < 0.01$), highlighting a more than satisfactory accuracy of the ED-μXRF analyses when performed on M samples. Similarly, the U samples of *Physconia* species revealed an enrichment of Ca in comparison to the L samples (Table 2) because the upper cortex is covered by Ca-oxalate crystals, forming the so-called *pruina* (Wadsten and Moberg 1985). At the same time, we also observed agreement between ED-μXRF and ICP-AES data concerning the content of Fe and Zn (Table 5). Therefore, it is possible to assert that the ED-μXRF technique provided reliable data, particularly for those elements that mostly occur extracellularly or in the residual fraction (Ca, Zn and Fe), even though the measurements were performed on intact lichen surfaces.

In our study, the removal of melanized lower cortex evidently affected only Fe content whereas the degree of melanization seems to influence the total Zn content (Figure 2; Figure 3). In fact, both the ED-μXRF and ICP-AES analyses clearly showed that the two-side heavily melanized species (*M. glabratula* and *X. loxodes*) have higher Fe and Zn contents than the one-side heavily melanized (*F. caperata*, *H. physodes*, *P. borreri*) and the one-side lightly melanized (*P. subrudecta*) species (Figure 3). Nevertheless, the patterns of intra-thalline distribution of Fe and Zn are different. Zn showed similar relative concentrations in the three thalline surfaces (Figure 2) investigated by ED-μXRF, whereas Fe was mainly concentrated in the external thalline surfaces, especially in the lower cortex (Figure 2). In all the species, the removal of the lower cortex did not affect the total concentration of Zn. The similar concentrations between U+L and M' samples is consistent with the observation that Zn species are highly water-soluble and thus they can spread

through the thallus, especially during wet periods. Through SET, Zn was found to be mainly associated to the intracellular fraction, which was significantly higher in the two-side heavily melanized *M. glabratula* than in the one-side lightly melanized *P. subrudecta* (Figure 5). These results agree with previous work showing that Zn is mainly stored in the intracellular fraction (Mikhailova and Sharunova 2008) and can be translocated within the thallus (Goyal and Seaward 1982). This leads us to suppose that melanins could effectively improve Zn retention in the extracellular fraction of the melanized thalline surface(s), thus increasing the intracellular fraction, not only of the cells close to the melanized cortical layers but of the whole thallus. On the other hand, all species showed a significant decrease in Fe when the samples were deprived of their lower surface, based on measurements with either ED-µXRF or ICP-AES. Interestingly, this result is confirmed by an unpublished work by Andreussi (personal communication) carried out by synchrotron radiation X-Ray fluorescence spectrometry, which claims that the highest relative concentration (79.2%) of Fe along the vertical thalline profile of *F. caperata* actually occurs in the lower cortex.

In terrestrial environment, Fe mostly occurs as ferric-(oxy)hydroxides rather than as the free cation (Fe^{3+} and Fe^{2+}). Our samples were collected in the Classical Karst, an environment characterised by dry, shallow (xero-)rendzina soils (Poldini 1989) that are highly enriched with several species of Al and Fe-(oxy)hydroxide (e.g. bauxite, goethite, hematite, limonite), the so-called "Terra Rossa". The major supply of Fe for epiphytic lichens collected in the Classical Karst is related to terrigenous particulate matter (PM) (Nimis et al. 2001). Terrigenous PM is mainly accumulated on the external surfaces and to a lesser extent in the medulla (Bargagli and Mikhailova 2002), where it can remain entrapped for long periods while it is dissolved by organic acids (Adamo et al. 1997), causing the release of metal ions and even inducing the neoformation and precipitation of several minerals (e.g. Garty and Garty-Spitz 2011). Hence, the considerable accumulation of terrigenous PM in the lower surfaces might explain the dramatic decrease of Fe content for those samples whose lower cortex was removed. Moreover, Fe content measured by both techniques in washed vs. unwashed samples of *F. caperata* was similar (Table 2; Table 4), confirming that this element is not available in a soluble form, and is unlikely to be removed by solubilization.

Although the relationship between melanized surfaces and Fe content seems to stem from the accumulation of terrigenous PM on the external thalline surfaces, other authors observed a strong chemical affinity of Fe

for melanins of free-living and lichenized fungi, based on electron spin resonance (Saiz-Jimenez and Shafizadeh 1984; Senesi et al. 1987), electron microprobe analysis (Purvis et al. 2004) and colorimetric method (Rinino et al. 2005).

As already described for saprotrophic ascomycetes, lichenized ascomycetes could synthesize DHN-derived melanins in extracellular medium (Chowdhury et al. 2017; Purvis and Pawlik-Skowrońska 2008). During this process, either organic molecules produced by the surrounding epiphytic community and airborne materials can be included in the three-dimensional melanin structure. The structure of melanins is found to be highly heterogeneous but quite similar to that of humic-like substances, since both have high concentration of carboxyl, phenolic, hydroxyl, and amine groups that provide many potential binding sites for metal ions (Felix et al. 1978; Tian et al. 2003). Considering that in terrestrial environment Fe is not available as a free cation, it is possible to assume that melanin directly entraps Fe-(oxy)hydroxides rather than Fe^{3+}. According to this hypothesis, Schwertmann (1966) demonstrated that the anionic groups of organic matter have an inhibitory effect on the crystallization of amorphous Fe-hydroxides. Moreover, Cesco et al. (2000) showed that water–extractable humic substances are able to increase the amount of Fe present in the soil solution, possibly by forming mobile complexes with the micronutrient.

Regarding the role of melanins in Fe intracellular accumulation, De Luca and Wood (2000) suggested that fungal melanins can stimulate the reduction of Fe^{3+} to Fe^{2+} through a passive process of electron exchange so as to regulate the intracellular Fe uptake by a Fe^{2+} specific trans-membrane carrier. Although our ED-μXRF and ICP-AES data could be in agreement with this, the results of our SET experiment pointed out that in both species almost all Fe content was in the residual fraction rather than in the intracellular fraction or chemically bound to the melanised cell wall as an exchangeable cation. However, since the difference between the intracellular fraction of *M. glabratula* and *P. subrudecta* was very low (3%), and the relative abundance of Fe in their lower surface (heavily vs lightly melanized) is different (respectively, 0.09 vs. 0.02), it can be assumed that the degree of melanization does not influence the intracellular Fe content.

Although Fe was not extractable by Na_2-EDTA treatment, there is evidence that both two-sided and one-sided highly melanized species are more Fe-enriched than the one-side lightly melanized species. This leads us tp propose that melanins could improve soil particulate retention when the soil is rich in Fe-(oxy)hydroxides. Therefore, melanizsed thalline surfaces might act as a reservoir pool of Fe to be

assimilated by the mycobiont at a later stage. In addition, this Fe reservoir pool might be important not only for lichen nourishment but also for the surrounding epiphytic community, since, as it is well-known, lichens are involved in forest nutrient cycling at the canopy level (Knops et al. 1991). In forest ecosystems, Fe is five times more concentrated in lichen thalli than in the canopy leaves (Loppi et al. 1997) and is 1000 times more concentrated in the stemflow (Hauck et al. 2002). This means that, especially when melanized, lichens could influence the forest Fe cycle between canopy and soil by retaining Fe-rich dry depositions (e.g. dust and soil particulate).

Although our findings suggested that melanins promote the Fe species retention, he biological mechanisms involved in the provision of bioavailable Fe species from the Fe-(oxy)hydroxides-melanin system remains unknown. It is known that the dissolution of pedogenetic Fe-hydroxides is promoted either by fungal and bacterial siderophores. To date, siderophore production has never been investigated in Parmeliaceae or in other lichen-forming fungi (Haselwandter and Winkelmann 2007). However, Swamy et al. (2016) have recently isolated lichen-inhabiting bacteria belonging to genus *Enterobacter*, which can produce siderophores.

In conclusion, our study provides analytical evidence to support the hypothesis that in parmelioid lichens the external melanized thalline surfaces influence the thallus content of Zn and are enriched in Fe. Considering the strong affinity of Fe for fungal melanins and the low bioavailability of Fe cations in terrestrial environment, the Fe(oxy)hydroxides-melanin complexes that may be present in the melanized pseudotissues might serve as a Fe reservoir pool for the provision of this essential micronutrient to the cells of both symbionts. However, alternative biological functions of melanins, only hinted at in the introduction of this work, should also be thoroughly tested.

Acknowledgments

References

Adamo P, Colombo C, Violante P (1997) Iron oxides and hydroxides in the weathering interface between *Stereocaulon vesuvianum* and volcanic rock. Clay Miner 32:453-461.

Aslan A, Budak G, Tıraşoğlu E, Karabulut A (2006) Determination of elements in some lichens growing in Giresun and Ordu province (Turkey) using energy dispersive X-ray fluorescence spectrometry. J Quant Spectrosc Radiat Transf 97:10-19.

Asplund J, Gauslaa Y (2008) Mollusc grazing limits growth and early development of the old forest lichen *Lobaria pulmonaria* in broadleaved deciduous forests. Oecologia 155:93-99.

Bargagli R, Mikhailova I (2002) Accumulation of inorganic contaminants. In: Nimis PL, Scheidegger C, Wolseley P (eds) Monitoring with lichens - monitoring lichens. Springer Science and Business Media, Dordrecht, pp 65-84

Bell AA, Wheeler MH (1986) Biosynthesis and functions of fungal melanins. Annu Rev Phytopathol 24:411-451.

Benesperi R, Tretiach M (2004) Differential land snail damage to selected species of the lichen genus *Peltigera*. Biochem Syst Ecol 32:127-138.

Blanco O, Crespo A, Divakar PK, Esslinger TL, Hawksworth DL, Lumbsch HT (2004) *Melanelixia* and *Melanohalea*, two new genera segregated from *Melanelia* (Parmeliaceae) based on molecular and morphological data. Mycol Res 108:873-884.

Branquinho C, Brown DH (1994) A method for studying the cellular location of lead in lichens. Lichenologist 26:83-90.

Buck GW, Brown DH (1979) The effect of desiccation on cation location in lichens. Ann Bot 44:265-277.

Butler MJ, Day AW (1998) Fungal melanins: a review. Can J Microbiol 44:1115-1136.

Cesco S, Römheld V, Varanini Z, Pinton R (2000) Solubilization of iron by water extractable humic substances. J Plant Nutr Soil Sc 163:285-290.

Chowdhury DP, Solhaug KA, Gauslaa Y (2017) Ultraviolet radiation reduces lichen growth rates. Symbiosis 73:27-34.

Clark BM, Clair LLS, Mangelson NF, Rees LB, Grant PG, Bench GS (2001) Characterization of mycobiont adaptations in the foliose lichen *Xanthoparmelia chlorochroa* (Parmeliaceae). Am J Bot 88:1742-1749.

De Luca NG, Wood PM (2000) Iron uptake by fungi: contrasted mechanisms with internal or external reduction. Adv Microb Physiol 43:39-74.

Eisenman HC, Casadevall A (2012) Synthesis and assembly of fungal melanin. Appl Microbiol Biotechnol 93:931-940.

Felix CC, Hyde JS, Sarna T, Sealy RC (1978) Interactions of melanin with metal ions. Electron spin resonance evidence for chelate complexes of metal ions with free radicals. J Am Chem Soc 100:3922-3926.

Fogarty RV, Tobin JM (1996) Fungal melanins and their interactions with metals. Enzyme Microb Technol 19:311-317.

Fomina M, Gadd GM (2003) Metal sorption by biomass of melanin producing fungi grown in clay containing medium. J Chem Technol Biotechnol 78:23-34.

Gadd GM, Rome L (1988) Biosorption of copper by fungal melanin. Appl Microbiol Biotechnol 29:610-617.

Garty J, Garty-Spitz RL (2011) Neutralization and neoformation: analogous processes in the atmosphere and in lichen thalli—a review. Environ Exp Bot 70:67-79.

Gauslaa Y, McEvoy M (2005) Seasonal changes in solar radiation drive acclimation of the sun-screening compound parietin in the lichen *Xanthoria parietina*. Basic Appl Ecol 6:75-82.

Giordani P, Modenesi P, Tretiach M (2003) Determinant factors for the formation of the calcium oxalate minerals, weddellite and whewellite, on the surface of foliose lichens. Lichenologist 35:255-270.

Godinho RM, Wolterbeek HT, Pinheiro MT, Alves LC, Verburg TG, Freitas MC (2009) Micro-scale elemental distribution in the thallus of *Flavoparmelia caperata* transplanted to polluted site. J Radioanal Nucl Ch 281:205-210.

Goyal R, Seaward MRD (1982) Metal uptake in terricolous lichens. III. Translocation in the thallus of *Peltigera canina*. New Phytol 90:85-98.

Haselwandter K, Winkelmann G (2007) Siderophores of symbiotic fungi. In: Varma A, Chincholkar SB (eds) Microbial siderophores, Soil biololgy, 12. Springer Berlin Heidelberg, pp 91-103.

Hauck M, Huneck S (2007) Lichen substances affect metal adsorption in *Hypogymnia physodes*. J Chem Ecol 33:219-223.

Hauck M, Runge M (2002) Stemflow chemistry and epiphytic lichen diversity in dieback-affected spruce forest of the Harz Mountains, Germany. Flora 197:250-261.

Honegger R (1993) Developmental biology of lichens. New Phytol 125:659-677.

Huneck S, Yoshimura I (1996) Identification of lichen substances. Springer, Berlin Heidelberg.

Knops JMH, Nash TH, Boucher VL, Schlesinger WH (1991) Mineral cycling and epiphytic lichens: implications at the ecosystem level. Lichenologist 23:309-321.

Knops JM, Nash TH, Schlesinger WH (1996) The influence of epiphytic lichens on the nutrient cycling of an oak woodland. Ecol Monogr 66:159-179.

Krog H (1982) *Punctelia*, a new lichen genus in the Parmeliaceae. Nord J Bot 2:287-292.

Loppi S, Nelli L, Ancora S, Bargagli R (1997) Passive monitoring of trace elements by means of tree leaves, epiphytic lichens and bark substrate. Environ Monit Assess 45:81-88.

Mafole TC, Chiang C, Solhaug KA, Beckett RP (2017). Melanisation in the old forest lichen *Lobaria pulmonaria* reduces the efficiency of photosynthesis. Fungal Ecol 29:103-110.

Matee LP, Beckett RP, Solhaug KA, Minibayeva FV (2016) Characterization and role of tyrosinases in the lichen *Lobaria pulmonaria* (L.) Hoffm. Lichenologist 48:311-322.

McLean J, Purvis OW, Williamson BJ, Bailey EH (1998) Role for lichen melanins in uranium remediation. Nature 391:649-650.

Mikhailova IN, Sharunova IP (2008) Dynamics of heavy metal accumulation in thalli of the epiphytic lichen *Hypogymnia physodes*. Russ J Ecol 39:346-352.

Muggia L, Grube M (2010) Type III polyketide synthases in lichen mycobionts. Fungal Biol 114:379-385.

Nash, 2008 Lichen biology. Cambridge University Press, New York.

Nimis PL (2016) The lichens of Italy. A second annotated catalogue. Edizioni Università di Trieste, Trieste.

Nimis PL, Andreussi S, Pittao E (2001) The performance of two lichen species as bioaccumulators of trace metals. Sci Total Environ 275:43-51.

Opanowicz M, Blaha J, Grube M (2005) Detection of paralogous polyketide synthase genes in Parmeliaceae by specific primers. Lichenologist 38:47-54.

Palmqvist K (2000) Tansley review No. 117 Carbon economy in lichens. New Phytol 148:11-36.

Paul A, Hauck M, Fritz E (2003) Effects of manganese on element distribution and structure in thalli of the epiphytic lichens *Hypogymnia physodes* and *Lecanora conizaeoides*. Environ Exp Bot 50:113-124.

Pérez-Llamazares A, Ángel Fernández J, Carballeira A, Aboal JR (2011) The sequential elution technique applied to cryptogams: a literature review. J Bryol 33:267-278.

Pilas B, Sarna T, Kalyanaraman B, Swartz HM (1988) The effect of melanin on iron associated decomposition of hydrogen peroxide. Free Radical Bio Med 4:285-293.

Poldini L (1989) La vegetazione del Carso isontino e triestino. Lint, Trieste.

Purvis OW, Bailey EH, McLean J, Kasama T, Williamson BJ (2004) Uranium biosorption by the lichen *Trapelia involuta* at a uranium mine. Geomicrobiol J 21:159-167.

Purvis OW, Pawlik-Skowrońska B (2008) Lichens and metals. In: British Mycological Society Symposia Series, Academic Press, Cambridge, pp. 175-200.

Richardson DHS, Shore M, Hartree R, Richardson RM (1995) The use of X-ray fluorescence spectrometry for the analysis of plants, especially lichens, employed in biological monitoring. Sci Total Environ 176:97-105.

Rikkinen JK (1995) What's behind the pretty colours? A study on the photobiology of lichens. Finnish Bryological Society, Helsinki

Rinino S, Bombardi V, Giordani P, Tretiach M, Crisafulli P, Monaci F, Modenesi P (2005) New histochemical techniques for the localization of metal ions in the lichen thallus. Lichenologist 37:463-466.

Saiz-Jimenez C, Shafizadeh F (1984) Iron and copper binding by fungal phenolic polymers: an electron spin resonance study. Curr Microbiol 10:281-285.

Schnitzer M, Neyroud JA (1975) Further investigations on the chemistry of fungal "humic acids". Soil Biol Biochem 7:365-371.

Schwertmann U (1966) Inhibitory effect of soil organic matter on the crystallization of amorphous ferric hydroxide. Nature 212:645-646.

Senesi N, Sposito G, Martin JP (1987) Copper (II) and iron (III) complexation by humic acid-like polymers (melanins) from soil fungi. Sci Total Environ 62:241-252.

Smith CW et al. (2009) The lichens of Great Britain and Ireland. British Lichen Society, London

Solhaug KA, Gauslaa Y (1996) Parietin, a photoprotective secondary product of the lichen *Xanthoria parietina*. Oecologia 108:412-418.

Solhaug KA, Gauslaa Y, Nybakken L, Bilger W (2003) UV-induction of sun-screening pigments in lichens. New Phytol 158:91-100.

Swamy CT, Gayathri D, Devaraja TN, Bandekar M, D'Souza SE, Meena RM, Ramaiah N (2016) Plant growth promoting potential and phylogenetic characteristics of a lichenized nitrogen fixing bacterium, *Enterobacter cloacae*. J Basic Microbiol 56:1369-1379.

U.S. Environmental Protection Agency, EPA-Method 3052. Microwave assisted acid digestion of siliceous and organically based matrices. U.S. Government printing office, Washington DC, 1996.

Tian S, Garcia-Rivera J, Yan B, Casadevall A, Stark RE (2003) Unlocking the molecular structure of fungal melanin using ^{13}C biosynthetic labeling and solid-state NMR. Biochemistry 42:8105-8109.

Wadsten T, Moberg R (1985) Calcium oxalate hydrates on the surface of lichens. Lichenologist 17:239-245.

Williamson BJ, Mikhailova I, Purvis OW, Udachin V (2004) SEM-EDX analysis in the source apportionment of particulate matter on *Hypogymnia physodes* lichen transplants around the Cu smelter and former mining town of Karabash, South Urals, Russia. Sci Total Environ 322:139-154.

Online Resource 1 Examples of lobes samples after cleaning and the removal of lower cortex. The species were ordered from right to left as a function of their degree of melanization. !: sample not prepared. The orange colour in the medulla of M. glabratula is due to extracellular deposits of the pigment rhodophyscine.

Thalline surface	Two-side heavily melanized	One-side heavily melanized	One-side lightly melanized	Non-melanized
	Melanelixia glabratula	*Flavoparmelia caperata*	*Punctelia subrudecta*	*Xanthoria parietina*
U (upper cortex)				
L (lower cortex)				
M (Medulla) Lower cortex removed				

Online resource 2 *F* values from *one-way ANOVAs* calculated among U, M and L samples of each of the five Parmeliaceae species grouped in dataset B

Taxon	Ca	K	Fe	Mn	S	Zn
M. glabratula	1.49	2.62	2.03	4.39	4.62	0.05
F. caperata	7.29	22.96	8.28	11.83	0.62	1.77
F. caperata (w)	4.63	6.55	3.84	4.18	28.23	0.72
H. physodes	2.63	1.07	4.9	1.01	2.24	0.84
P. borreri	0.66	0.34	2.02	0.76	0.84	1.05
P. subrudecta	5.72	4.67	8.14	2.02	1.24	2.38

Conclusion

This PhD project was aimed at improving the protocols currently applied in the biomonitoring of airborne trace elements with native lichens. Particular attention was paid to: *i*) the relationship between the Radial Growth Rate (RaGR) and the exposure time of the lobes of an epiphytic lichen; *ii*) the potential suitability of lichens as point receptors for the validation of ADM simulations and; *iii*) the chemical affinity of Fe and Zn for melanin-like compounds produced by parmelioid lichens.

Specifically, the first study (study 1) contributed at improving the knowledge of both seasonal and long-term RaGRs of a species frequently used in biomonitoring surveys, *X. parietina*. It was highlighted that site-specific differences in terms of water availability andwind frequency, increase the inter-site variability of both seasonal and long-term RaGRs. For this reason, it was concluded that biomonitoring surveys with native lichens should be limited to climatically homogeneous areas, in order to minimize the inter-site variability of RaGRs and ensure a comparable exposure time of all lichen samples.

The importance of the relationship between long term RaGR and exposure time of foliose thalli emerged also from the results of the second study (study 2). Indeed, RaGR of another lichen frequently used in biomonitoring surveys, *F. caperata,* has turned out to be a key factor for the validation of ADM simulations . The high correlation observed between the outcomes of Mod 14 and the content of selected elements in *F. caperata* samples suggests that lichens can be used to validate ADM simulations based on meteorological input dataset corresponding to the estimated exposure time of lichen samples.

Finally, the third study (study 3), demonstrated that in parmelioid lichens the degree of melanisation affects the content of selected elements, namely Fe and Zn. Therefore, one is lead to wonder whether and how the degree of melanisation has to be taken into account when lichens are used as biomonitor of trace elements. In parmelioid lichens the ageing of the thallus generally drives the lichen melanogenesis of the lower surface, with the younger, outermost part of lobes that shows a progressive melanisation, from the lobe tip (light brown) to the base (black). Therefore, in order to exclude any bias related to the different degree of melanisation, the proposal is to compose analytical samples with lichen material characterized by a similar degree of melanisation.